WIND FORCES ON MICROWAVE ANTENNAS, EQUIPMENT AND TOWERS

by

J. E. Cermak[1]
J. A. Peterka[2]
B. Bienkiewicz[3]
and
N. Hosoya[4]

for

Bayar and Associates
Structural Engineers
109 Montgomery Avenue
Scarsdale, NY 10583

Fluid Mechanics and Wind Engineering Program
Fluid Dynamics and Diffusion Laboratory
Department of Civil Engineering
Colorado State University
Fort Collins, CO 80523

CSU Project 2-95380

March 1983

[1]Professor-in-Charge, Fluid Mechanics and Wind Engineering Program

[2]Associate Professor

[3]Assistant Professor

[4]Graduate Research Assistant

TABLE OF CONTENTS

LIST OF FIGURES

Figure		Page

LIST OF TABLES

LIST OF SYMBOLS

A	reference area
A_e	enclosed area of tower section
C_D	drag force coefficient
C_L	lateral force coefficient
C_{MP}	pitching moment coefficient
C_{MR}	rolling moment coefficient
C_{MY}	yawing moment coefficient
F_D	drag force
F_L	lateral force
L	reference length (= 10 ft at full-scale)
L_m	typical length for model
L_p	typical length for prototype
M_P	pitching moment
M_R	rolling moment
M_Y	yawing moment
q	reference dynamic pressure ($= \frac{1}{2} \rho U^2$)
Re_c	critical Reynolds number
U	reference wind speed
y_D	eccentricity of drag force
α	wind direction
β	tilt angle
λ_L	geometric scale
	kinematic viscosity of air
ρ	density of air
ψ	solidity ratio

1. INTRODUCTION

Wind induced loads are important parameters to be evaluated during structural analysis of microwave antennas, equipment and supporting towers. Theoretical prediction of the wind forces exerted on such structures is practically impossible. Consequently, most of the available data are based on an information obtained from wind-tunnel tests.

The present state of knowledge on the wind forces on lattice tower sections was summarized by Sachs (1, 2), and Ghiocel and Lungu (3). Hoerner (4) collected data related to the drag on various bluff bodies. Some of his data can be used to estimate the drag force of single horn antennas.

The wind forces on lattice structures were more recently investigated by Melling (5) who undertook a series of wind-tunnel tests in a smooth flow. Sykes (6) investigated effects of turbulence for a lattice structure. A comparative study, partially based on the data of Melling (5) and Sykes (6), was published by Clow (7). The effects of shielding for multiple frame structures were analyzed by Jacobs (8). Whitbread (9) presented results of a similar study for an array of lattice structures. Wind forces on horn antennas were measured in a wind tunnel by Kamei et al. (10). Full-scale tests on a free-standing latticed steel tower under strong winds were reported by Mackey et al. (11).

The main objective of the wind-tunnel study presented herein was to evaluate time averaged wind loads on various microwave horn antennas and supporting tower sections proposed by American Telephone and Telegraph Company (AT&T). The drag force was of particular interest. Tested were pyramidal horn antennas and three conical horn antennas of different geometries. The effects of several structural elements attached to the horn antennas and to the tower sections were also examined.

2. RELATED CONSIDERATIONS AND DEFINITIONS

2.1 Similarity Requirements

Investigations of wind effects on structures are usually conducted for strong wind conditions, where thermal stratification of the atmosphere is destroyed by intense vertical mixing (12). Such flow conditions were modeled for the wind tunnel study presented in this report. The essential requirements for the physical modeling included geometric similarity and preservation of the Reynolds numbers for model and prototype structures.

Geometric similarity was achieved by an undistorted scaling of the model geometry.

$$\frac{L_m}{L_p} = \lambda_L = \text{constant} \tag{2.1}$$

where L_m and L_p are typical lengths, respectively, for a model and a prototype.

Generally, dynamic similarity of the flow requires equality of the Reynolds numbers for model and prototype fields. However, aerodynamic coefficients for bluff and lattice structures become Reynolds number independent for sufficiently high (higher than critical) Reynolds numbers (1,13). Since the critical Reynolds number is dependent on the model geometry, the Reynolds number independency was examined in the present wind-tunnel study. The following condition should be satisfied in the wind-tunnel testing.

$$\left(\frac{L_m U}{\nu}\right) > Re_c \tag{2.2}$$

where U is the wind speed, ν is the kinematic viscosity of air, and Re_c is the critical Reynolds number, which is experimentally determined.

In addition, flow characteristics of the approach flow must be properly modeled. Turbulence intensity could affect the mean wind loads on a bluff body represented by a microwave horn antenna. On the other hand, Sykes (6) reported no significant effects of turbulence intensity (ranging from 3.5 to 13.5 percent) on the mean wind loads on a lattice structure.

2.2 Definition of Wind Loads - Mean Forces and Moments

Time averaged wind loads on several horn antennas and supporting tower sections were of interest in the present study. Wind tunnel tests were conducted using small-scale rigid models mounted on a platform which was also exposed to the wind. In order to evaluate mean wind loads on the model, the load contribution due to the platform was separately measured and it was subtracted from the measured total loads. The net loads on the horn antenna and the tower section are herein defined by

(the net wind loads on the model)

= (the wind loads on the model and the platform)

- (the wind loads on the platform with the model removed) (2.3)

The above formula is merely an approximation and no attempt was made to account for the induced wind loads due to flow interaction between the model and the platform.

Unless explicitly specified, the time averaged net wind loads defined by Equation (2.3) shall be referred to as wind loads.

2.2.1 Horn Antenna Tests

Wind loads measured in the wind tunnel for pyramidal and various conical horn antennas consisted of two components of forces and three components of moments. They were:

F_D = drag force (lbs),

F_L = lateral force (lbs),

M_R = rolling moment (ft-lbs),

M_P = pitching moment (ft-lbs),

and

M_Y = yawing moment (ft-lbs).

Using a conventional notation, the wind loads at wind direction α are schematically defined in Figure 1.*

Eccentricity of the drag force measured from the upper surface of the platform was then calculated using the following formula

$$y_D = M_P / F_D \quad \text{(ft)} .$$

The wind direction for the horn antenna tests was varied from 0° to 350° at increments of 10° by rotating the wind tunnel turntable.

2.2.2 Tower Section Tests

Two components of wind forces were measured for the tower section model at various wind directions α and tilt angles β. The measured forces were:

F_D = drag force (lbs),

and

F_L = lateral force (lbs).

---

*This convention is slightly different than the convention used in (14), p. 31.

The sketch of the wind loads on the tower section is shown in Figure 2. Note that the wind loads are defined in the frame of reference associated with the tilted tower section.

The wind direction for the tower section tests was varied from -10° to 55° while the tilt angles considered were 0°, 5°, 10° and 15°.

2.3 Data Presentation

It is a common practice to present the wind loads (defined in the preceding sections) in a normalized form. The normalizing formulas for the mean forces and moments are

$$C_D = F_D \,/\, qA \;,$$

$$C_L = F_L \,/\, qA \;,$$

$$C_{MR} = M_R \,/\, qLA \;,$$

$$C_{MP} = M_P \,/\, qLA \;,$$

and

$$C_{MY} = M_Y \,/\, qLA \;, \tag{2.5}$$

where $q = \frac{1}{2} \rho U^2$ (psf) is the reference dynamic pressure, L (ft) is a typical length scale, and A (ft^2) is the reference area. The length L was in this study arbitrarily chosen to be 10 ft for the prototype conditions. The corresponding length for the 1:16 geometric scale horn antenna models was 0.625 ft. The reference area A was defined as follows:

for the horn antenna

A = the area of the antenna and its mountings projected on a plane normal to the wind. The area was updated for each wind direction α.

for the tower section

A = the area occupied by the truss elements projected on a plane normal to the wind. The area evaluated at the wind direction 0° was used for all the wind directions tested. Thus for the tower section

$$A = \psi A_e \tag{2.6}$$

where ψ is the solidity ratio and A_e is the enclosed area of the projection of the tower section. Note that the reference area used for the horn antenna varies with the wind direction whereas the area for the tower section remains constant. The areas for the horn antennas and tower sections used in this study are given in Tables 1 to 8, and 10 to 14.

Among the aerodynamic coefficients defined above, the drag coefficient C_D was of particular interest. Therefore, most of the discussions of the experimental results are devoted to the behavior of the drag coefficient.

3. EXPERIMENTAL APPARATUS

3.1 Wind Tunnel

The experiments described in this report were conducted in the meteorological wind tunnel of the Fluid Dynamics and Diffusion Laboratory at Colorado State University. The wind tunnel is shown in Figure 3. This closed-circuit wind tunnel is characterized by a long (96 ft) slightly diverging test section. The test section is 6 ft 8 in. wide and 6 ft high at the location of the turntable. The ceiling is adjustable for the longitudinal pressure gradient corrections. The facility is driven by a 400 HP variable pitch propeller with wind speed varying continuously from 0.5 fps to 100 fps.

3.2 Flow Simulation

3.2.1 Horn Antenna Tests

Atmospheric conditions suggested by Cermak (12) were simulated in the wind tunnel by means of a biplanar grid placed at inlet to the wind-tunnel test section. The horn antenna models were placed 85 ft downstream of the grid at the location of the wind-tunnel turntable. Vertical profiles of the mean wind speed and the local turbulence intensity are shown in Figure 4. The data show that flow characteristics are quite uniform in the region where the horn antenna models were immersed (25 in. up to 45 in. above the floor). The reference wind speed was monitored in the uniform flow region at a height of 38 in.

3.2.2 Tower Section Tests

A uniform turbulent flow was modeled at the turntable by placing a biplanar grid 30 ft upstream from the turntable. Vertical profiles of the wind speed and the turbulence intensity are shown in Figure 5. A boundary layer 5 in. thick developing over the smooth wind tunnel floor is evident. To minimize the effects of the boundary layer on the wind load measurements, the tower section model was supported 4.5 in. above the turntable. As a result the tower section was located above the boundary layer region.

3.3 Models

3.3.1 Pyramidal Horn Antennas

A 1:16 geometrical scale model of the upper portion of the supporting tower, the platform, and two pyramidal horn antennas were fabricated at the Engineering Research Center Machine Shop, Colorado State University. All the significant geometric details of the prototype structure were preserved. Figure 6 shows the model, the force balance and the supporting tower. The two pyramidal horn antennas were made of lucite. Details of the pyramidal horn antenna models are shown in Figure 7. Technical details for the prototype antennas are enclosed in Appendix B (Fig. B.1).

The upper portion of the supporting tower was made of steel to provide sufficient rigidity desired for accurate wind load measurements.

The platform shown in Figure 8 was made of aluminum. The top view of the platform is a square with the full scale dimensions of 29 ft by 29 ft (see Figure B.2).

Two bottom edge blinders and ice protection canopies were also constructed at a geometrical scale of 1:16. They were used to investigate flow interaction between them and the pyramidal horn antennas. These additional attachments are shown, respectively, in Figures 9 and 10. Technical data for the prototype is presented in Figures B.3 and B.4.

3.3.2 Conical Horn Antennas

Three different conical horn antennas (AFC CH10, ANDREW SHX10, and GABRIEL UHR10 D) were tested. The antennas were modeled at a geometrical scale of 1:16.

Shown in Figure 11 is the model of AFC CH10. This model was supplied by the project sponsor. The models of ANDREW SHX10 and GABRIEL UHR10 D, which were manufactured at Colorado State University, are shown, respectively, in Figures 12 and 13.

A platform for the conical horn antennas was constructed of an aluminum plate with the full scale dimensions of 0.69 ft by 9 ft by 18 ft.

The model of the supporting tower, which was described in the previous section, was also used for the conical horn antenna tests.

Figure 14 is a typical view of the conical horn (GABRIEL UHR10 D) antenna setup.

3.3.3 Tower Sections

Conceptual sketches of the tested antenna tower sections are shown in Figure 15. Two representative sections were selected for the wind tunnel tests. One section consisted of the level A-A through D-D. The other one included the level F-F through J-J. Photographs of the selected tower sections are shown in Figure 16.

The tower sections AA-DD and FF-JJ were modeled at the geometrical scales of, respectively, 1:12 and 1:18. Both the sections were constructed of brass angle members. They were manufactured at the Engineering Research Center Machine Shop, Colorado State University.

The tower section models were modified for a series of the wind-tunnel tests. A heel angle was attached to each leg (see Figure 47), to determine the effects of the increased leg size upon the resulting wind load. The full scale dimensions of the heel angle were 3.5 in. by 3.5 in.

After a series of tests the tower section FF-JJ was cut at the H-H level (see Figure 15b) to permit a wind-tunnel investigation of the lower portion HH-JJ. During wind-tunnel testing, the upper portion was supported in its proper location without contacting the lower portion and served as a guard section, see Figure 41a.

A square aluminum platform with size of 32 in. by 32 in. was attached to the lower part of the tower section to provide rigidity at the bottom end of the tower legs where force balances were mounted. The platform was attached to the wind-tunnel turntable in such a way that testing of the tower section at the tilting angle of 0°, 5°, 10° and 15° was possible.

3.4 Data Acquisition

3.4.1 Flow Measurement

The mean wind velocity and the local turbulence intensity profiles presented in Section 3.2 were measured using a single hot film probe in conjunction with a constant temperature anemometer (TSI Inc. Model 1050). The hot film probe consisted of a 0.001 in. diameter platinum sensing element of 0.02 in. in length. The probe was carried by a vertical traverse to measure the local wind speed and turbulence intensity at different heights above the wind tunnel floor. The data were sampled for 32 seconds at a rate of 260 samples per second. The output from the hot wire anemometer was fed to a data acquisition system consisting of a Hewlett-Packard System 1000 minicomputer. The data were analyzed and stored using appropriate software.

3.4.2 Wind Load Measurement

Mean wind loads on the horn antennas and the tower sections defined in Section 2.2 were measured using strain gage force balances. The data were acquired at a rate of 260 samples per second for 16 seconds, and processed with the data reduction system described above. For each measurement the reference velocity in the approach wind was simultaneously monitored by a pitot-static tube.

A five component force balance manufactured by Inca Engineering Corporation was used for the measurements of wind loads on the horn antennas (see Figure 45). The same force balance was used in the related preceding study (14). Possible experimental error in the system examined in detail by Poreh and Cermak (14) was found to be ±3% for the force measurement and ±5% for the moment measurement.

Four force balances with two-directional sensors were designed and used for the measurements of the loads on the tower sections. One force balance was mounted at each corner of the platform (see Figure 46). The outputs from the force balances were added in the data acquisition system to obtain the resultant forces in two perpendicular directions. Calibration of the force balance system indicated that the possible experimental errors in measurements of the resulting forces should not exceed ±1.5%.

3.5 Flow Visualization

Flow visualization experiments for several typical antenna configurations were conducted in a 3 x 3 ft cross section wind tunnel located at the Fluid Dynamics and Diffusion Laboratory, Colorado State University.

A schematic diagram of the smoke generating system is shown in Figure 17. Compressed air was ducted through a jar containing a mixture of titanium tetrachloride and carbon tetrachloride. A dense white smoke of titanium dioxide was produced as a result of a chemical reaction due to the presence of moisture in the air. The smoke was supplied through flexible Tygon tubing to a brass rake located at the entrance of the wind tunnel. A honeycomb was placed downstream close to the rake to attenuate disturbances present in the streaklines of the generated smoke.

4. RESULTS AND DISCUSSION

4.1 Effects of Wind Speed - Reynolds Number Independence

Figure 18 shows the effects of the wind speed on the total drag coefficient for a conical horn antenna ANDREW SHX10 and the platform, evaluated at several wind directions. The drag coefficient remained constant when the wind speed exceeded 40 fps. Note that the drag coefficient remained constant even when the horn antenna was on the downstream side of the supporting tower (the wind direction $\alpha = 240°$).

Similarly, the effects of the wind speed on the total drag coefficient (the drag force on the platform included) for the tower section AA-DD are shown in Figure 19. It is clear that the drag coefficient is independent of the wind speeds higher than 30 fps.

Based on the above data, the experimental reference wind speeds were determined to be 50 fps for the horn antenna tests and 40 fps for the tower section tests.

4.2 Horn Antenna Tests

4.2.1 Pyramidal Horn Antennas

Figure 20 compares the total drag (drag on the platform included) on a two pyramidal horn cluster measured during the present study (1982) with the data from the preceding study (1976).* Reasonable agreement is seen for the wind direction from 0° to 180°. For the remaining wind directions, where the pyramidal horn antennas were located downstream of the platform, a notable difference is observed. This discrepancy is attributed to the different platform configurations used in the compared studies; a covered platform in the present study and an uncovered platform in the preceding study. This implies that the platform geometry can affect the wind loads on horn antennas when the platform is located upstream of the cluster.

The net drag coefficient defined in Sections 2.2 and 2.3 is shown in Figure 21 for the two pyramidal horn antenna cluster. Comparison of the drag force for the wind directions from 60° to 150°, and from 210°

*In the preceding study, this configuration was referred to as the Condition 3C.

to 300° shows that the drag is lower for the wind direction from 60° to 150°. In these two configurations, the supporting tower is, respectively, downstream and upstream of the horn cluster. It appears that the wind blockage due to the presence of the tower was insignificant. The solidity of the tower was relatively low and the platform size was much larger than the tower width. In addition only the small portion of the pyramidal horn antennas projected below the platform.

Effects of the blinders attached to the pyramidal horn antennas are shown in Figure 22. It is evident that the blinders increase the net drag force approximately by 10% when the wind directly approaches the blinders (wind direction from 180° to 300°).

Figure 23 indicates that the ice protection canopies can also increase the drag force by 10% at most wind directions.

Figures 24 through 26, and Tables 1 through 3 summarize the wind loads for various pyramidal horn antenna configurations. Notice that at each wind direction, the normalized wind loads were obtained by the use of the projected area common for all the configurations.

The data show that for each tested configuration the magnitude of the lateral force is smaller than that of the drag force. There exists, however, a variation of the mean lateral force with the wind direction, especially for the wind direction larger than 180°. The moment coefficients are also found to be sensitive to the wind direction. These variations seem to be due to the complex nature of the wake and bluff body interaction.

4.2.2 Conical Horn Antennas

Figure 27 compares the drag measured on the models of the three single conical horn antennas. Variation of the drag coefficient with the wind direction is similar for the three antennas. The largest drag coefficient at every wind direction corresponds to the GABRIEL UHR10 D antenna. In addition, the drag for GABRIEL UHR10 D deviates remarkably from the drag for the other models for wind direction between 120° and 240°. The deviation suggests a different aerodynamic behavior of the GABRIEL UHR 10 D antenna. Furthermore, the secondary drag induced by the flow interaction in the vicinity of the joint of the antenna and the supporting platform may not be negligible. Attempts to reduce the drag for the GABRIEL UHR10 D antenna are described in Appendix A.

The wind loads on each conical horn antenna are presented in Figures 28 through 30, and Tables 4 through 6.

4.3 Tower Section Tests

4.3.1 Original Geometry

Figures 31 and 32, and Tables 7 and 8 show the drag and lateral forces on the tower sections AA-DD and FF-JJ. Similarity between the two results is evident. The drag at the wind directions of 0° and 45° is compared in Table 9 with the values suggested by the ANSI Standard (15). The suggested values are somewhat higher than the experimental results. It should be noted that the slope of the lateral force curve at the wind direction of 0° is positive for both tower sections.

The drag and lateral forces on the tower section AA-DD for various tilt angles are shown in Figures 33 through 36, and Tables 10 through 12. No significant effect of the tilting is found.

4.3.2 Modified Geometry - Heel Angles Attached

Figures 37 and 38 show effects of the heel angles on the drag coefficient of the tower sections. Addition of the heel angles resulted in an increase of the drag on the tower sections for the range of wind directions tested.

The lateral force shown in Figures 39 and 40 was significantly affected by the presence of the heel angles. The force changed sign for most of the tested wind directions. This unexpected sign reversal should be further investigated.

The wind loads on the tower sections with heel angles are summarized in Tables 13 and 14.

4.3.3 Wind Loads on Tower Half Section - Section HH-JJ

The drag on the tower section HH-JJ (the lower half of the section FF-JJ) at the wind direction of 0° is given in Figure 41. In addition, data for the sections FF-JJ and FF-HH are presented. The tower sections have similar geometry. There seems to be, see Figure 41a, a linear relation between the drag and the solidity ratio. The two quantities appear to be inversely proportional. Empirical formulas describing this relation could be stated if the data were available for a wider range of the solidity ratio. It should be noted that the presence of the guard section FF-HH affects the results of measurements of the drag force on the section HH-JJ (compare Figures 41a and 41b).

4.4 Flow Visualization

Figures 42 to 43 show visualized streamlines around pyramidal horn antenna cluster at different configurations. It is observed that the ice protection canopies cause a larger and more unsteady wake--the source of the increased drag. The elevation views (Figures 42a and 43a) show that the flow is deflected as it approaches the horn antennas, and the platform creates a wake underneath. The implication of this is that the effects of the platform vary with the wind direction and as a result the net drag on the horn antenna investigated in this study is only an estimate.

Figure 44 shows a flow around the conical horn antenna, GABRIEL UHR10 D. In Figure 44b, the position of the flow stagnation point can be clearly distinguished. At the wind direction of 0°, shown in this figure, a large portion of the approach flow is diverted toward the joint of the horn antenna and the platform. Hence, considerations of aerodynamically efficient geometry for the mounting of the antenna are desirable.

5. CONCLUSIONS AND RECOMMENDATIONS

5.1 Conclusions

A. Reasonable agreement between the results of the present and preceding (14) studies was obtained for the drag on the two pyramidal horn antenna cluster.

B. The bottom edge blinders and ice protection canopies increased the drag force of the pyramidal horn antenna cluster. The increase reached maximum value of approximately 10% for some wind directions.

C. The conical horn antenna, GABRIEL UHR10 D, exhibited larger drag than the other conical antennas tested (AFC CH10 and ANDREW SHX10).

D. The effects of the platform on the forces on the horn antennas may not be negligible. Further investigation of this interaction is desirable.

E. The data for the tower sections AA-DD and FF-JJ exhibited similarity.

F. The heel angles increased the drag of the tower sections. In addition, they significantly modified the lateral forces.

G. The effects of tilting of the tower sections upon the mean drag and the lateral forces were negligible.

H. Small modifications of the geometry of the horn antenna mounting significantly changed the aerodynamic behavior of the antenna. Dynamic wind-tunnel study of such changes is desirable.

5.2 Recommendations

5.2.1 Reliability of Test Results

The estimated error in drag force measurements for these tests is less than ±10%. Therefore, the results presented herein are more representative of wind loads to be experienced by towers having the geometry tested than can be obtained from reference to standards such as Ref. 15 in which nominal drag coefficients are given without consideration of geometrical details for specific towers. Based upon these considerations, the recommended wind loads for design of tower geometries tested in this study are those presented in this report.

5.2.2 Future Investigations

It is recommended that additional wind-tunnel tests be performed to address problems which were not fully investigated in the present study.

The future investigation of the microwave antennas and equipment should include evaluation of:

A. Interaction between horn antennas and the supporting platform.

B. The effects of different antenna mountings upon the static and dynamic wind forces on the antennas.

C. Dynamic response and aerodynamic stability of the antennas which exhibit highly unsteady wind forces.

The present study provided the preliminary data on wind loads on typical sections of towers used to support the microwave antennas and equipment. The future related study should:

A. Provide data on the static wind loads on tower sections for different values of the solidity ratio. The present study resulted in two data points on the drag force-solidity ratio curve. More data are needed to define the relation between the drag force and the solidity ratio. The new relation (based on the experimental data) could then be used in the design of towers, replacing presently used more conservative formulas suggested by the ANSI Standard (15). Substantial financial savings might result from such modification.

B. Undertake wind-tunnel studies of the dynamic response of towers due to wind loading. More conservative design of towers requires refined analysis of the tower dynamics. Evaluation of the response to the wind forces is an important part of such an analysis.

C. Evaluate gust load factor for typical towers based on wind-tunnel data. Recent developments of the wind-tunnel instrumentation allow precise measurement of integrated dynamic and static wind loads on various structures, including latticed towers. The experimentally obtained gust load factors could be very useful in assessing validity of the present techniques used to account for the dynamic response of towers to wind loading.

REFERENCES

1. Sachs, P., "Wind Forces in Engineering," (1978), 2nd Ed., Pergamon Press, pp. 78-81.

2. Sachs, P., "Determination of Wind Forces Acting on Antenna Structures," in "Mechanical Engineering in Radar and Communications," (1969), Richards, C. J. (Editor), Van Nostrand Reinhold Company, London, pp. 123-203.

3. Ghiocel, D. and D. Lungu, "Wind, Snow and Temperature Effects on Structures Based on Probability," (1975), Abacus Press, pp. 215-224.

4. Hoerner, S. F., "Fluid-Dynamic Drag," (1965) published by Hoerner, S. F., pp. 3.17-3.18.

5. Melling, R. J., "Loads on Open Lattice Structures in Nominally Smooth Flow," (1978), Proc. of the 3rd Colloquium on Industrial Aerodynamics, Aachen, Pt. 1, pp. 107-127.

6. Sykes, D. M., "Wind Loads on Lattice Structures in Turbulent Airflow," (1978), Proc. of the 3rd Colloquium on Industrial Aerodynamics, Aachen, Pt. 1, pp. 129-148.

7. Clow, D. G., "Loads on Open Lattice Structures - A Comparative Study," (1978), Proc. of the 3rd Colloquium on Industrial Aerodynamics, Aachen, Pt. 1, pp. 165-177.

8. Jacobs, B. E. A., "Determination of Shielding Factors for Multiple Frame Structures," (1978), Proc. of the 3rd Colloquium on Industrial Aerodynamics, Aachen, Pt. 1, pp. 149-164.

9. Whitbread, R. E., "The Influence of Shielding on the Wind Forces Experienced by Arrays of Lattice Frames," (1979), Proc. of the 5th Int. Conf. on Wind Engineering, Fort Collins, Colorado, USA, pp. 405-420.

10. Kamei, I., E. Kimura and I. Matsushita, "Experimental Study of Wind Force Coefficient of SHF Antennas for Telecommunication Tower Design," (1971), Proc. of the 3rd Int. Conf. on Wind Effects on Buildings and Structures, Tokyo, Japan, pp. 357-364.

11. Mackey, S., P. K. L. Ko and L. C. H. Lam, "Response of a 180-ft Latticed Tower to High Winds," (1974), Proc. of the 2nd U.S.A.-Japan Research Seminar on Wind Effects on Structures, Kyoto, Japan, pp. 199-207.

12. Cermak, J. E., "Laboratory Simulation of the Atmospheric Boundary Layer," (1971), AIAA Journal, Vol. 9, No. 9, pp. 1749-1954.

13. Cermak, J. E., "Aerodynamics of Buildings," (1976), Annual Review of Fluid Mechanincs, Vol. 8, pp. 75-106.

14. Poreh, M. and J. E. Cermak, "Wind Forces and Moments on Microwave Antennas," (1976), Colorado State University, Report CER76-77MP-JEC12, Fort Collins, Colorado.

15. American National Standards Institute, "Minimum Design Loads for Buildings and Other Structures," (1982), ANSI Standard A58.1 - 1982.

FIGURES

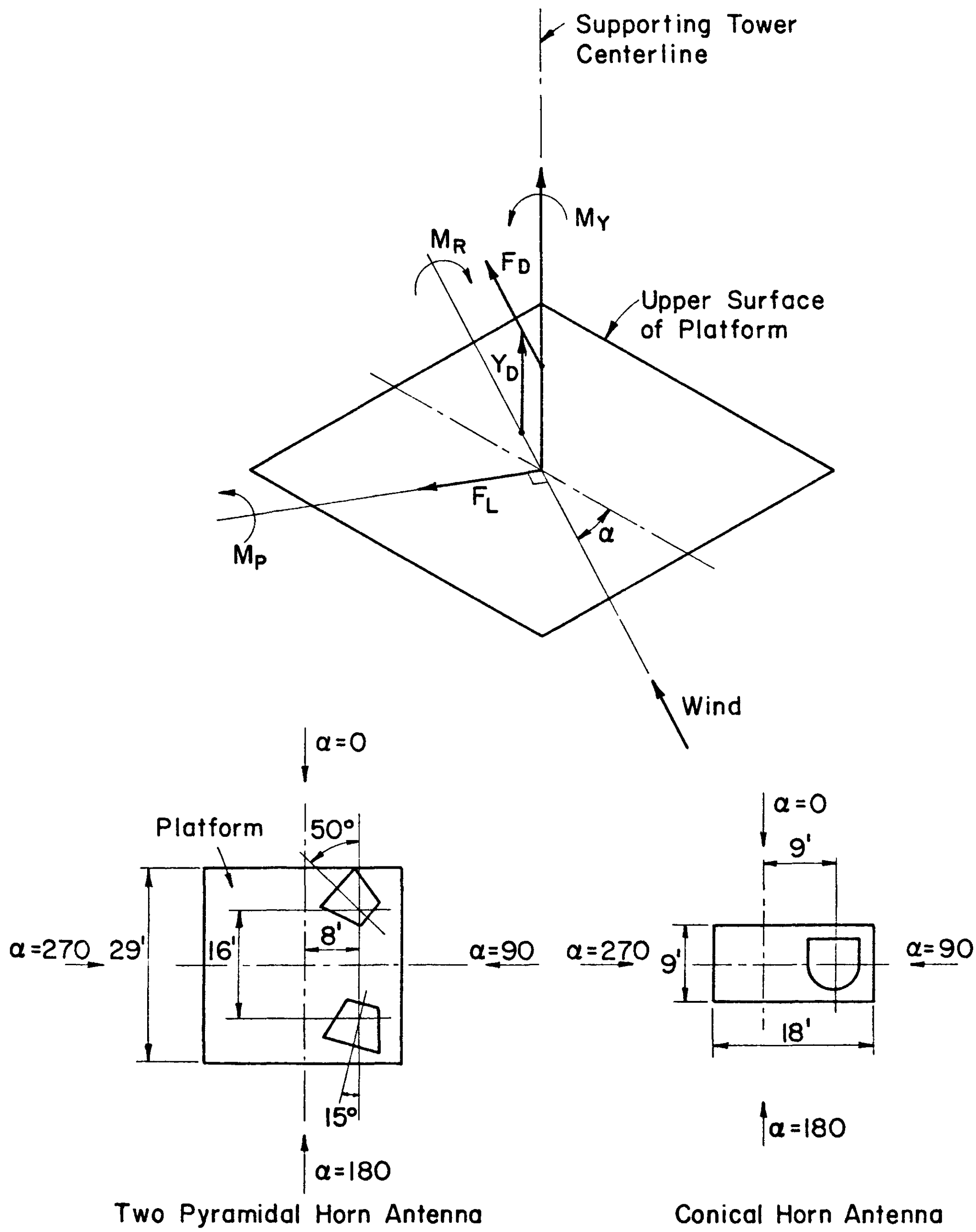

Figure 1. Definitions of Forces and Moments on Horn Antennas

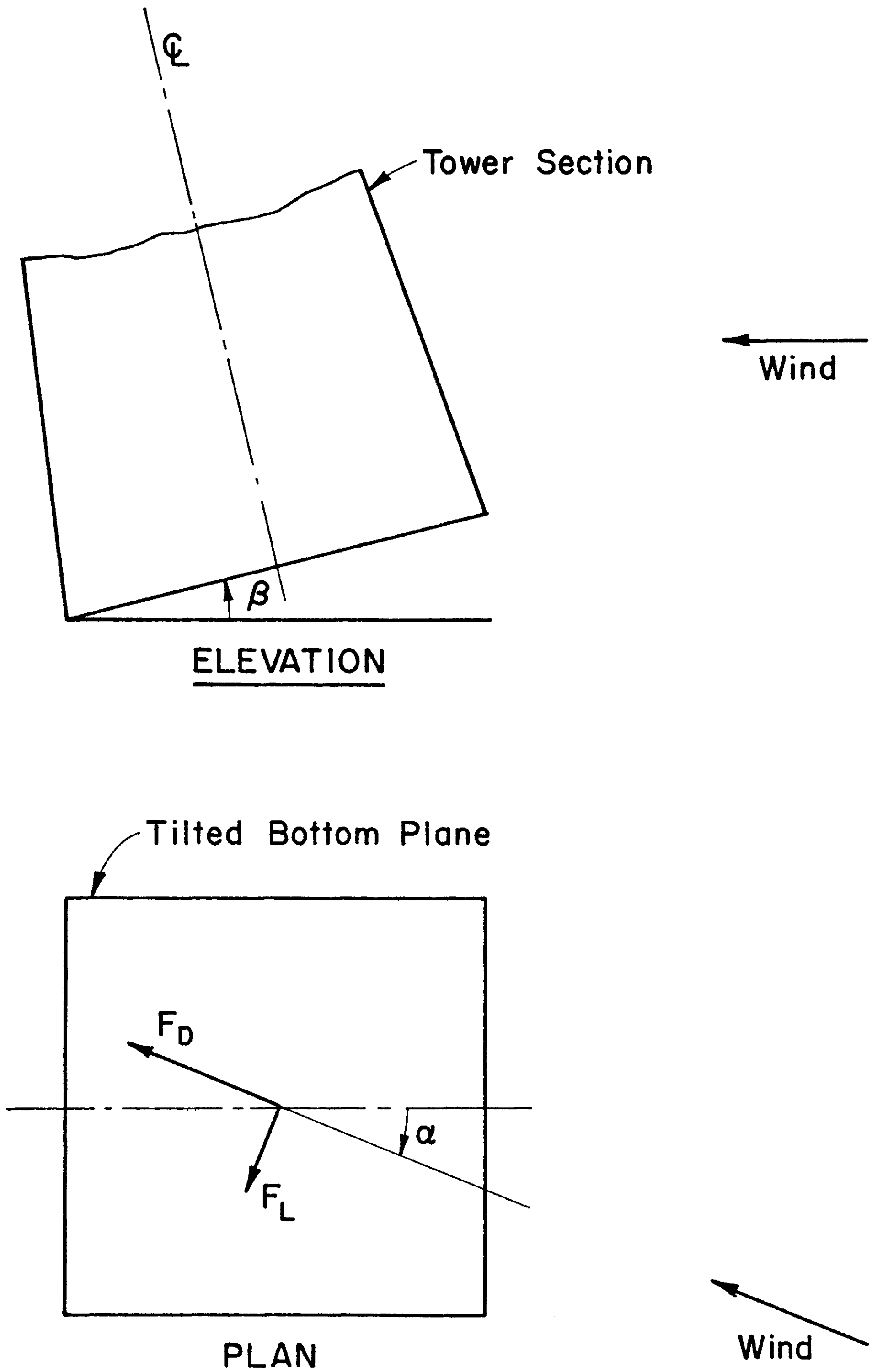

Figure 2. Definition of Forces on Tower Section

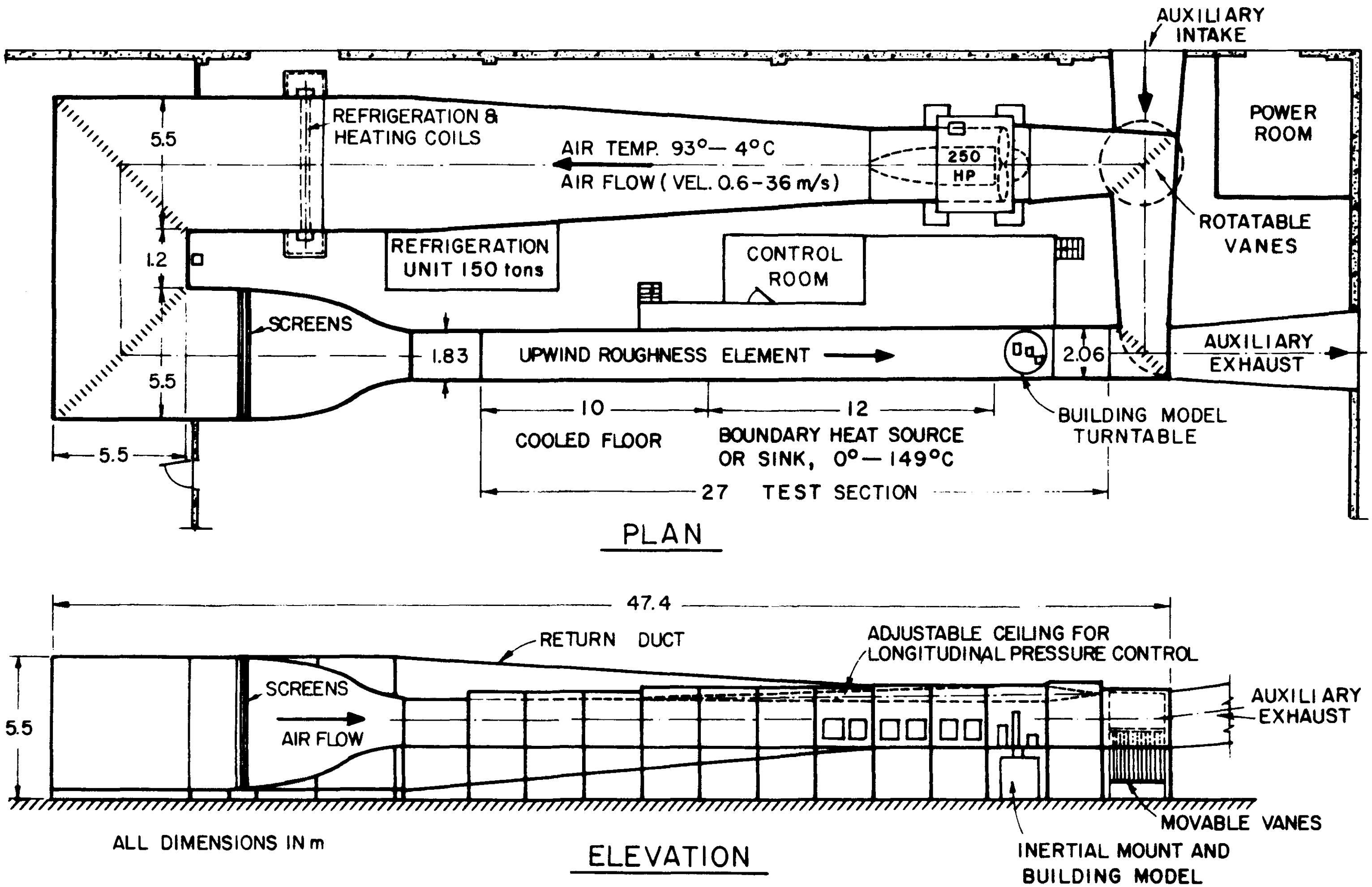

Figure 3. Meteorological Wind Tunnel

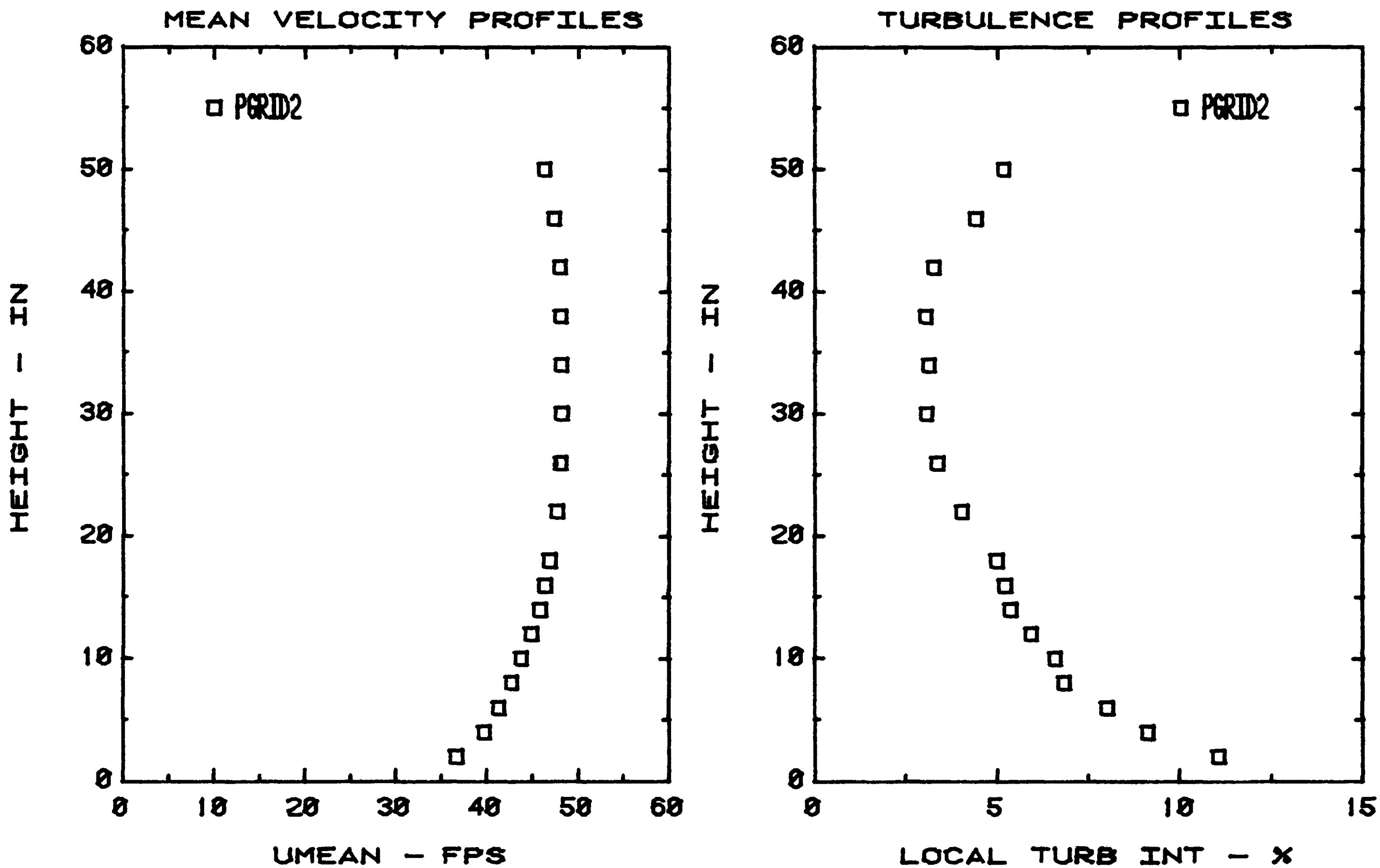

Figure 4. Wind Profile - Horn Antenna Tests

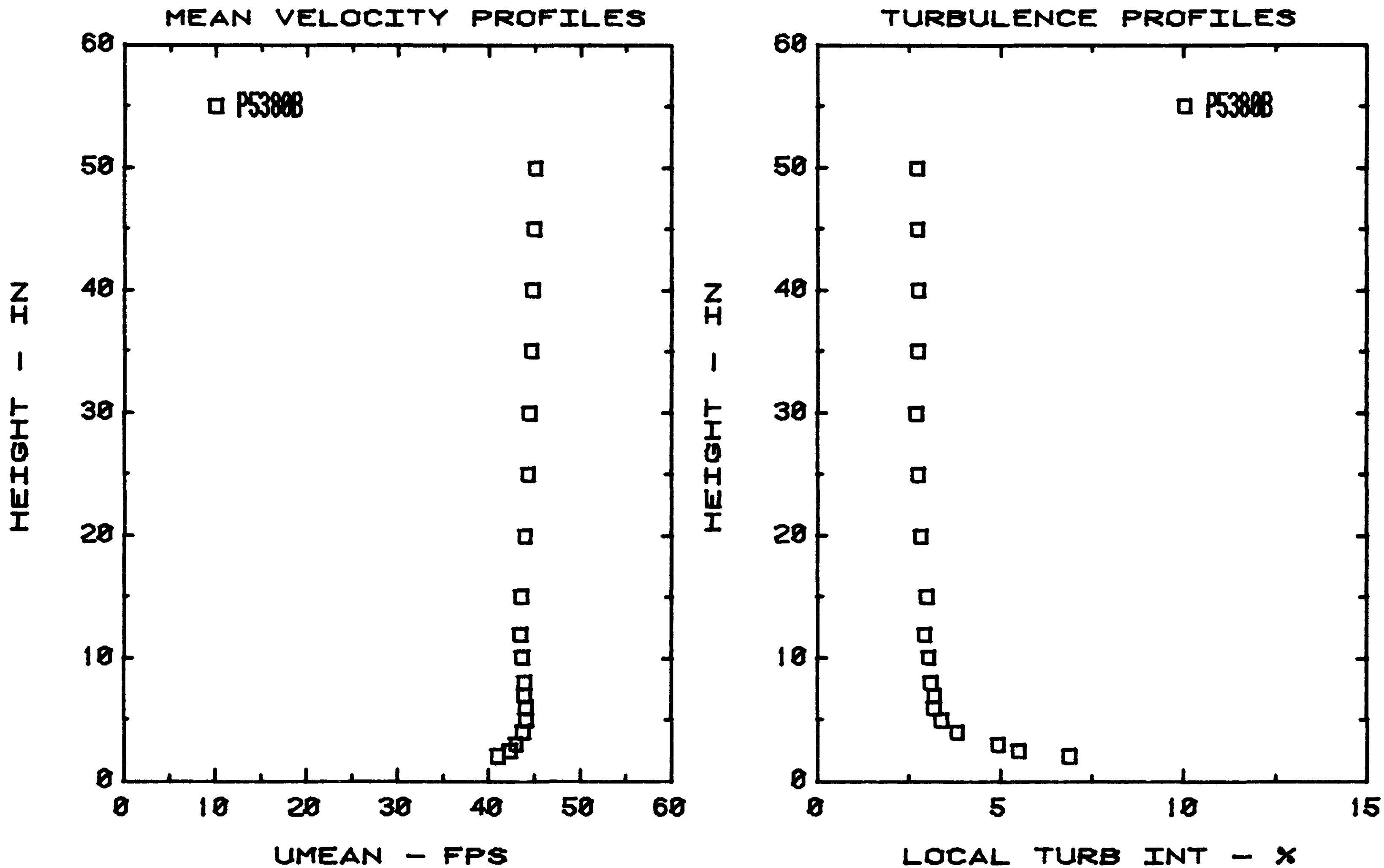

Figure 5. Wind Profile - Tower Section Tests

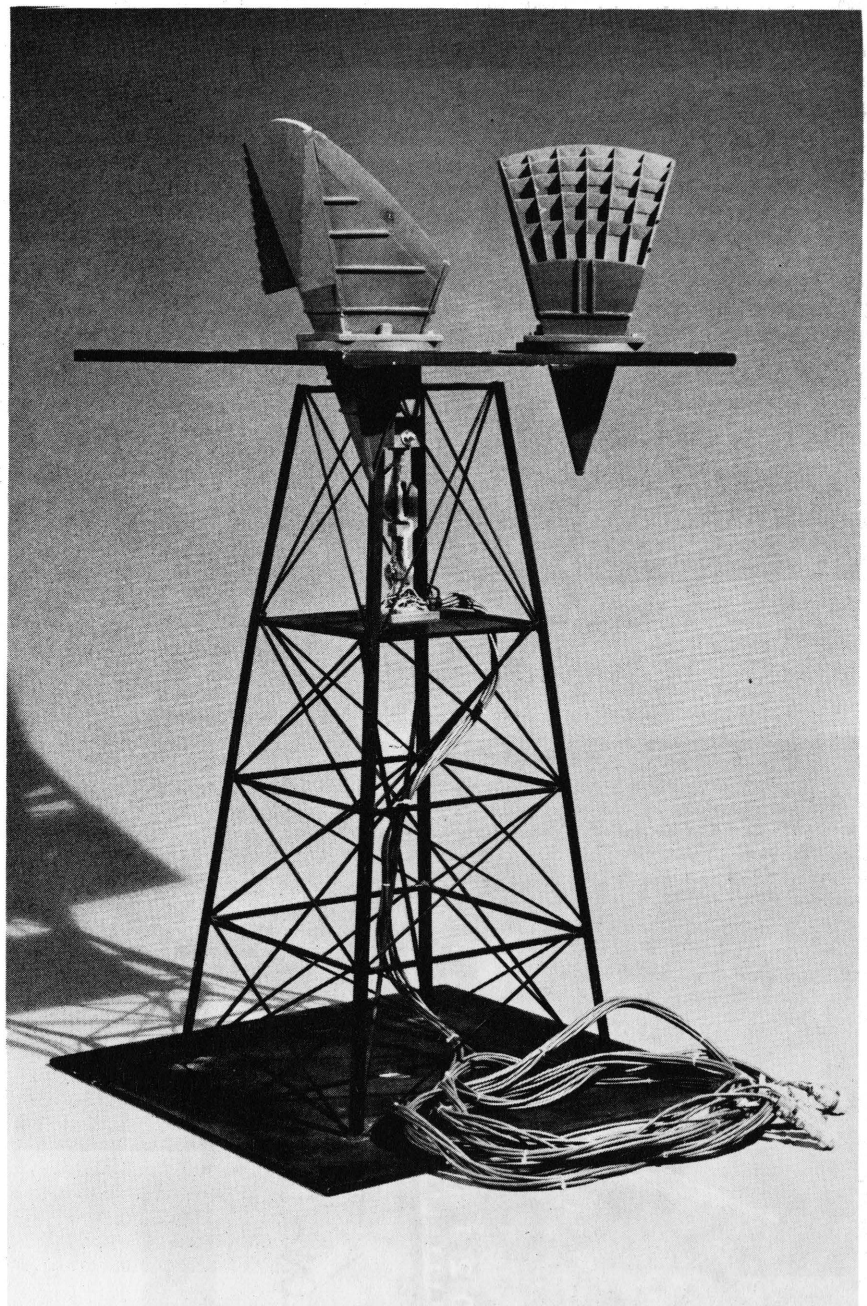

Figure 6. Two Pyramidal Horn Antenna Cluster

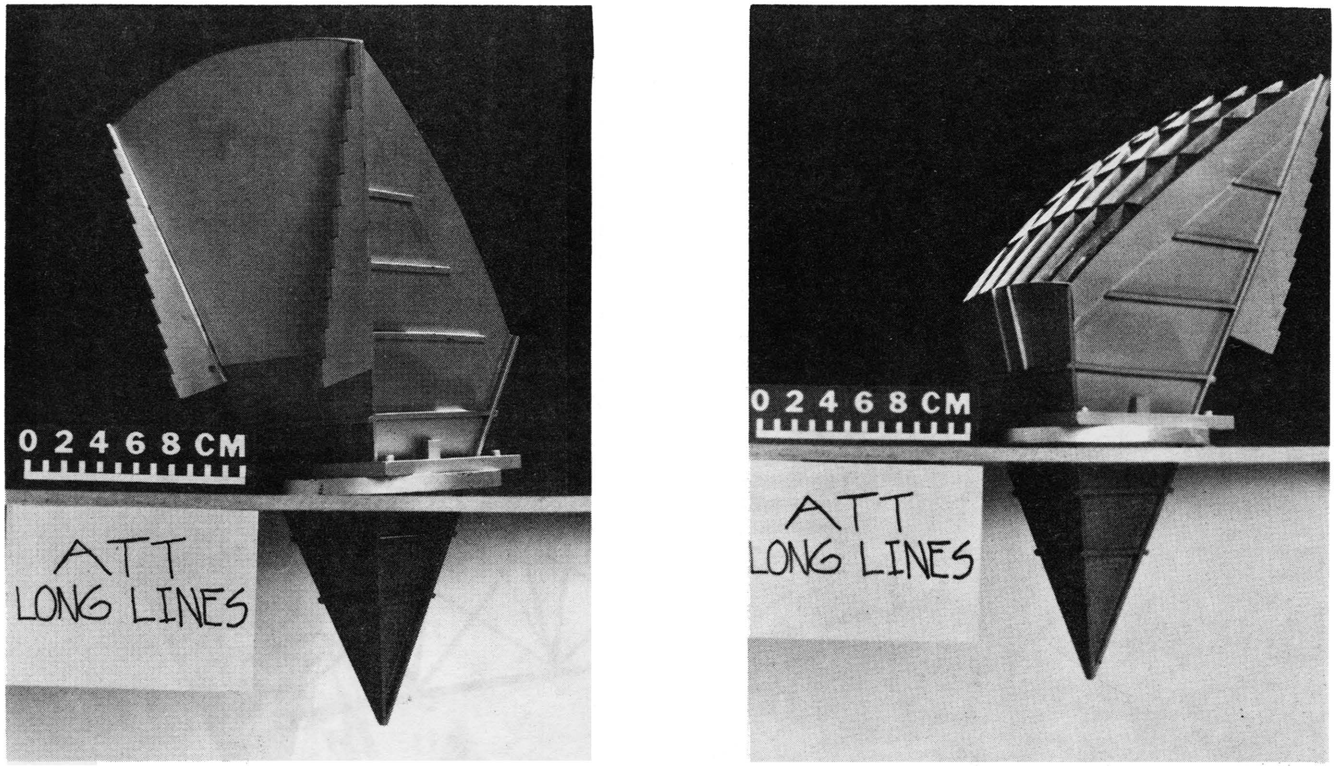

Figure 7. Pyramidal Horn Antenna

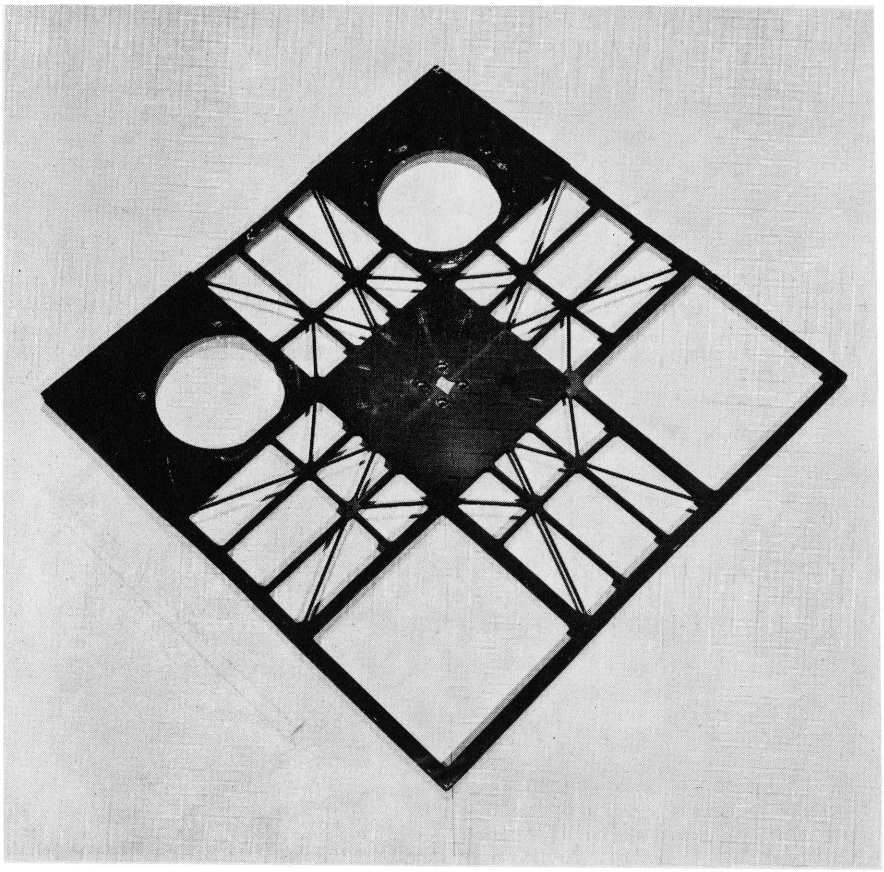

Figure 8. Pyramidal Horn Antenna Platform

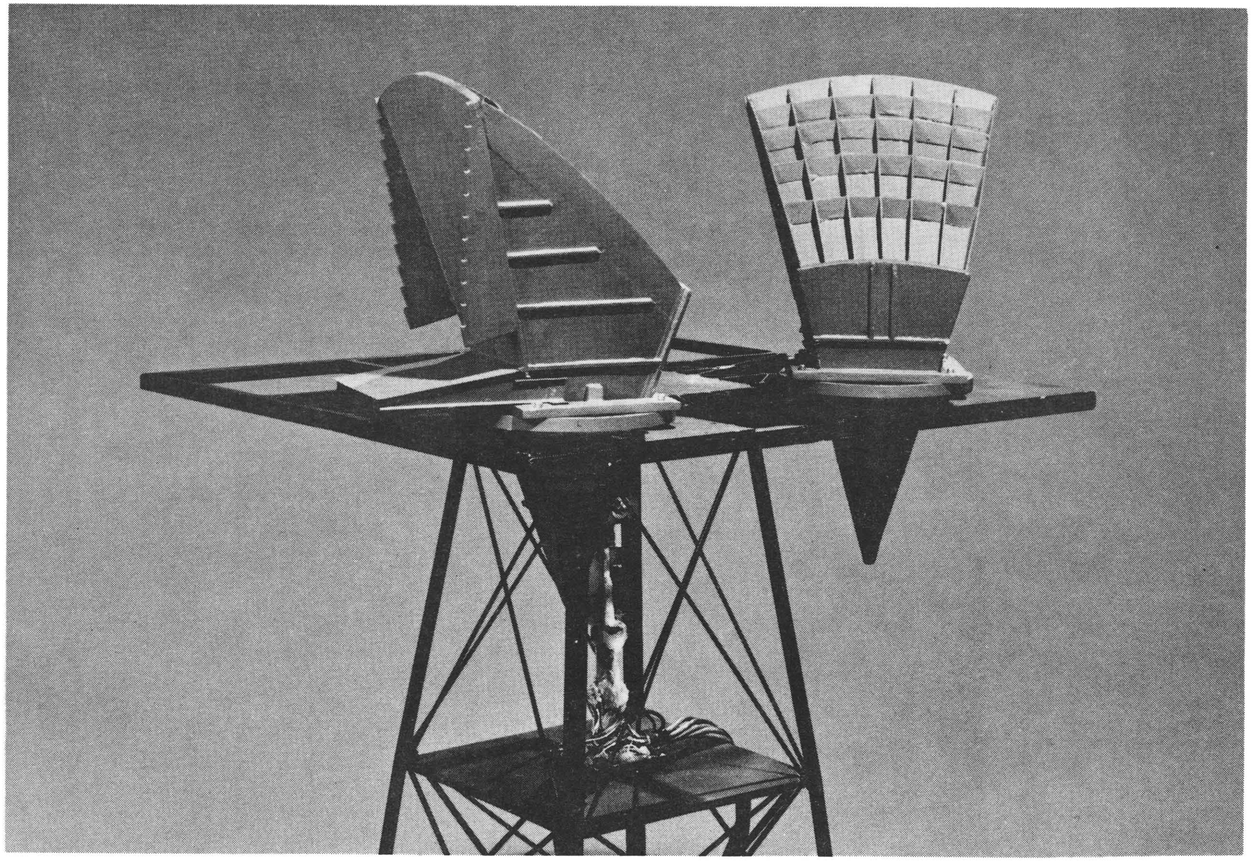

Figure 9. Bottom Edge Blinder

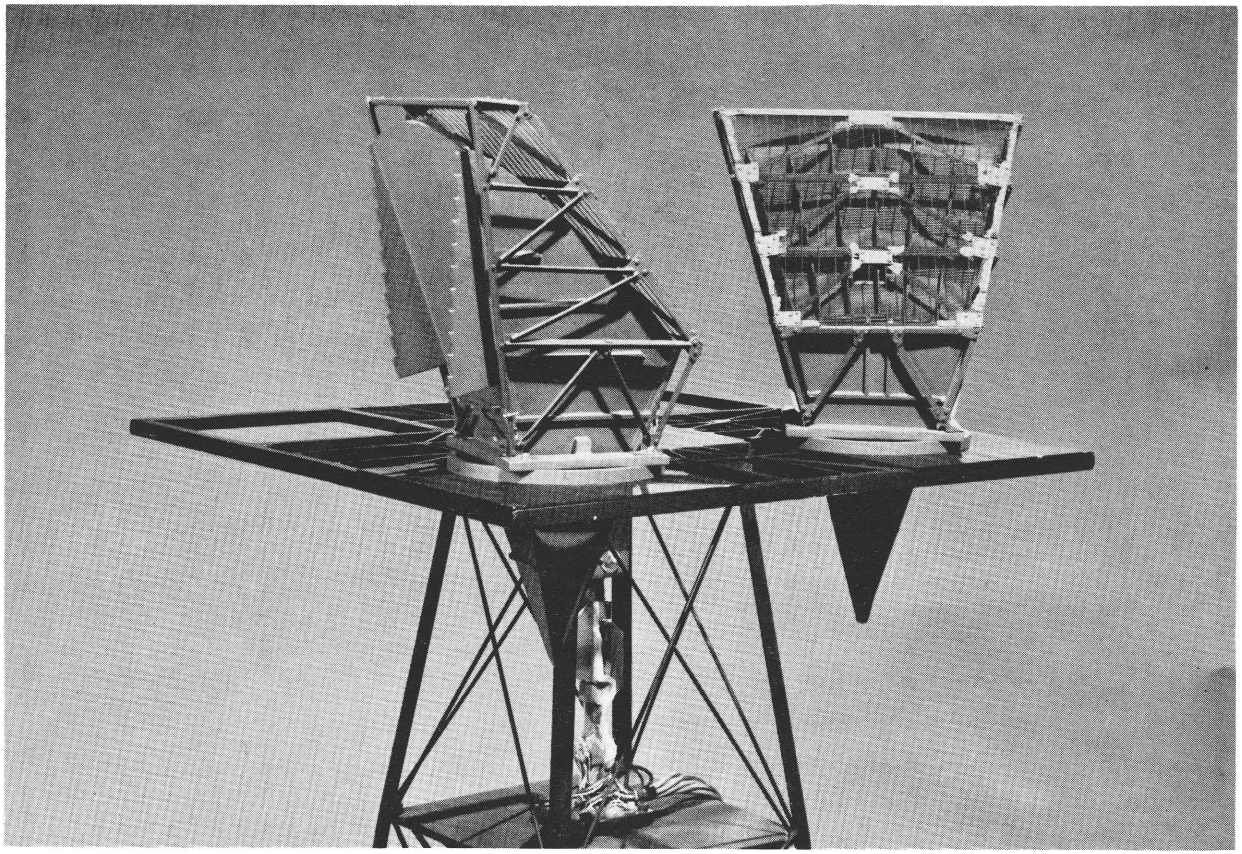

Figure 10. Ice Protection Canopy

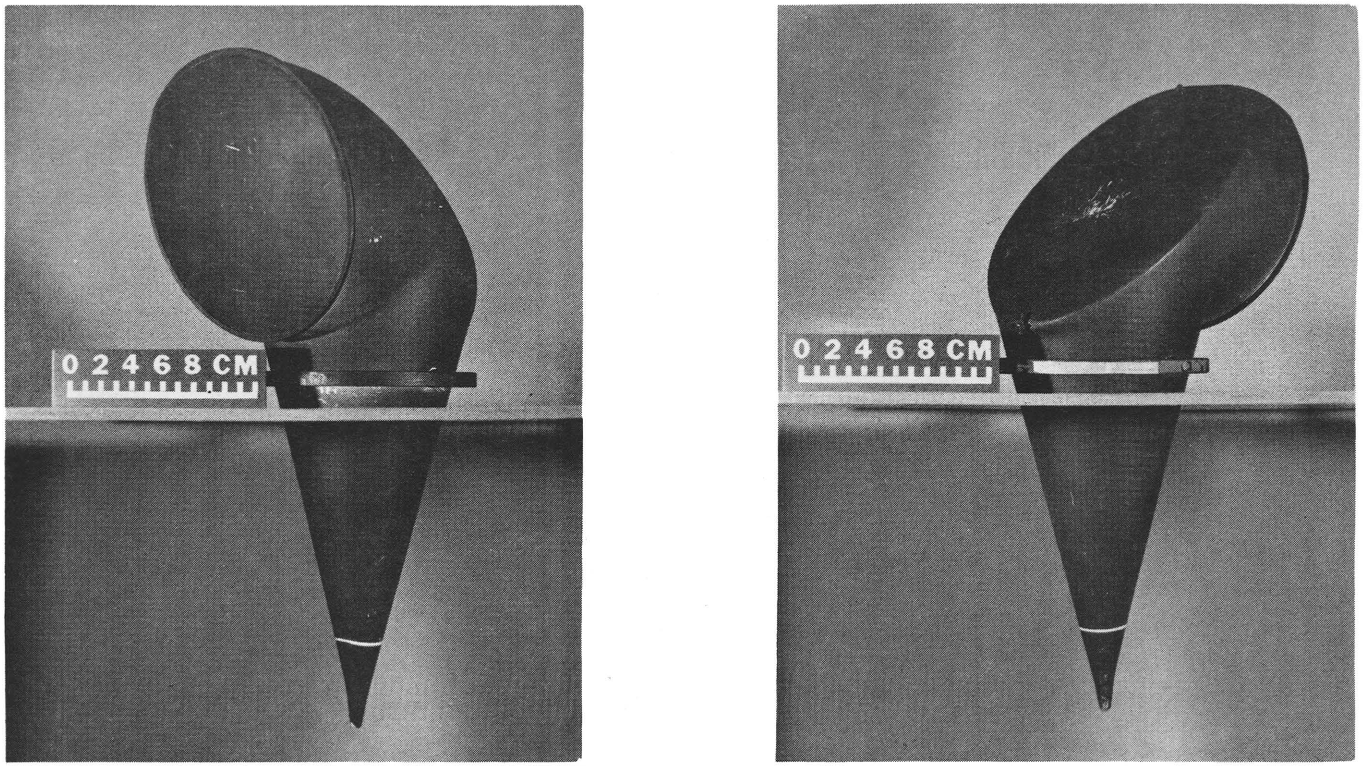

Figure 11. Conical Horn Antenna - AFC CH10

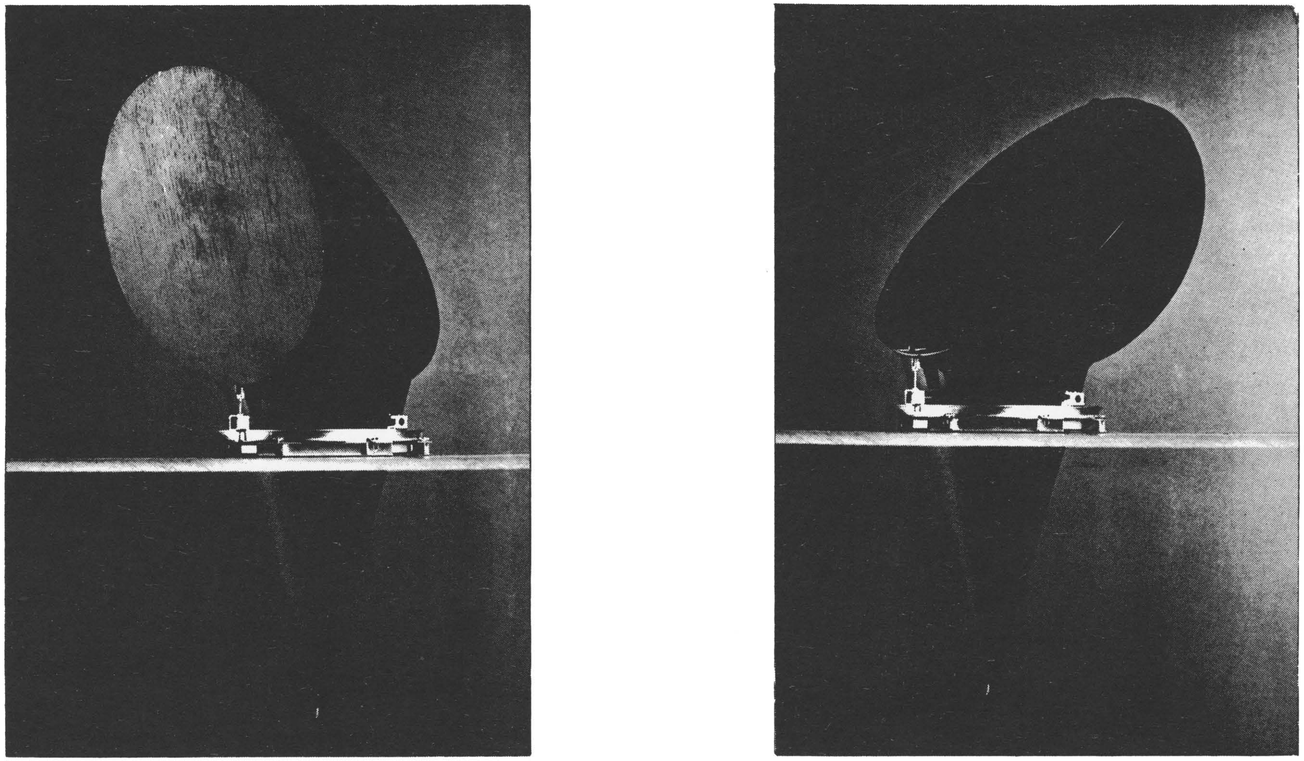

Figure 12. Conical Horn Antenna - ANDREW SHX10

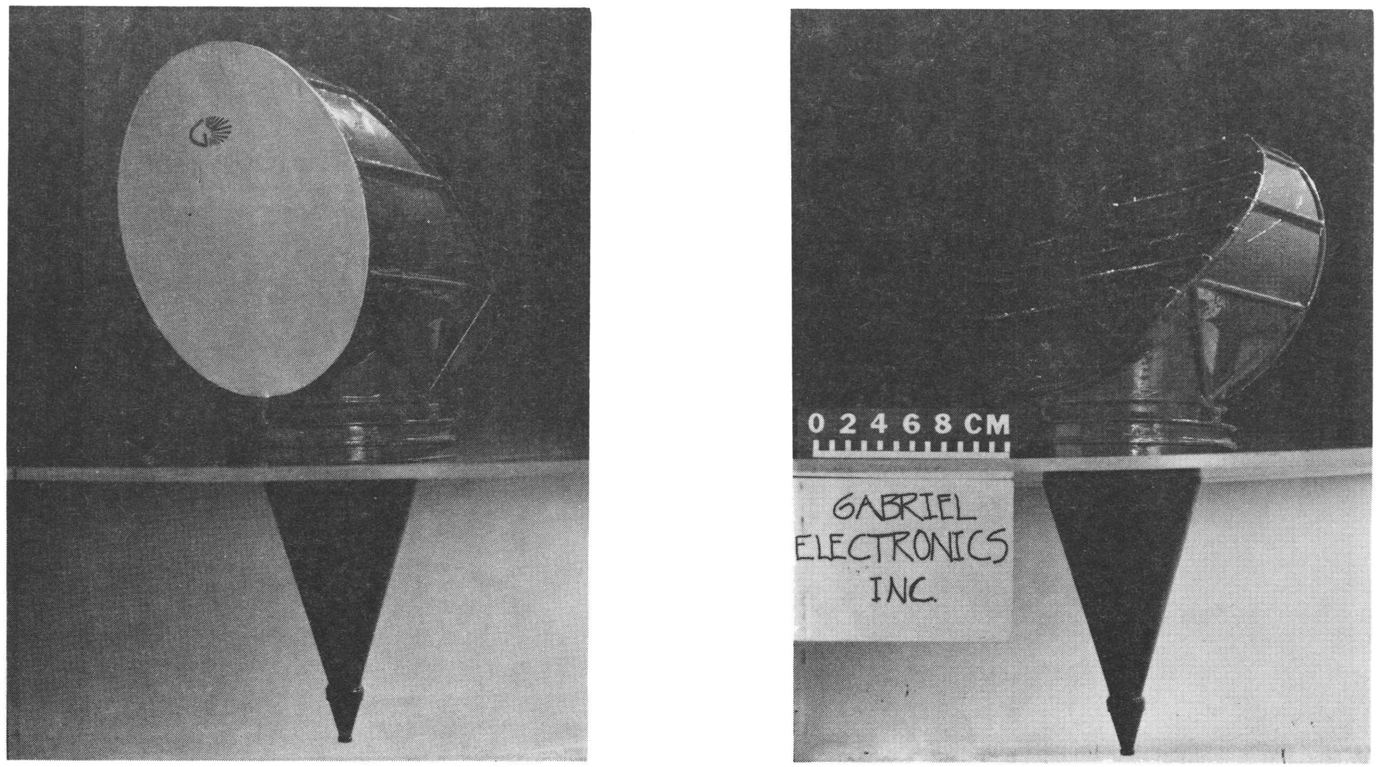

Figure 13. Conical Horn Antenna - GABRIEL UHR10 D

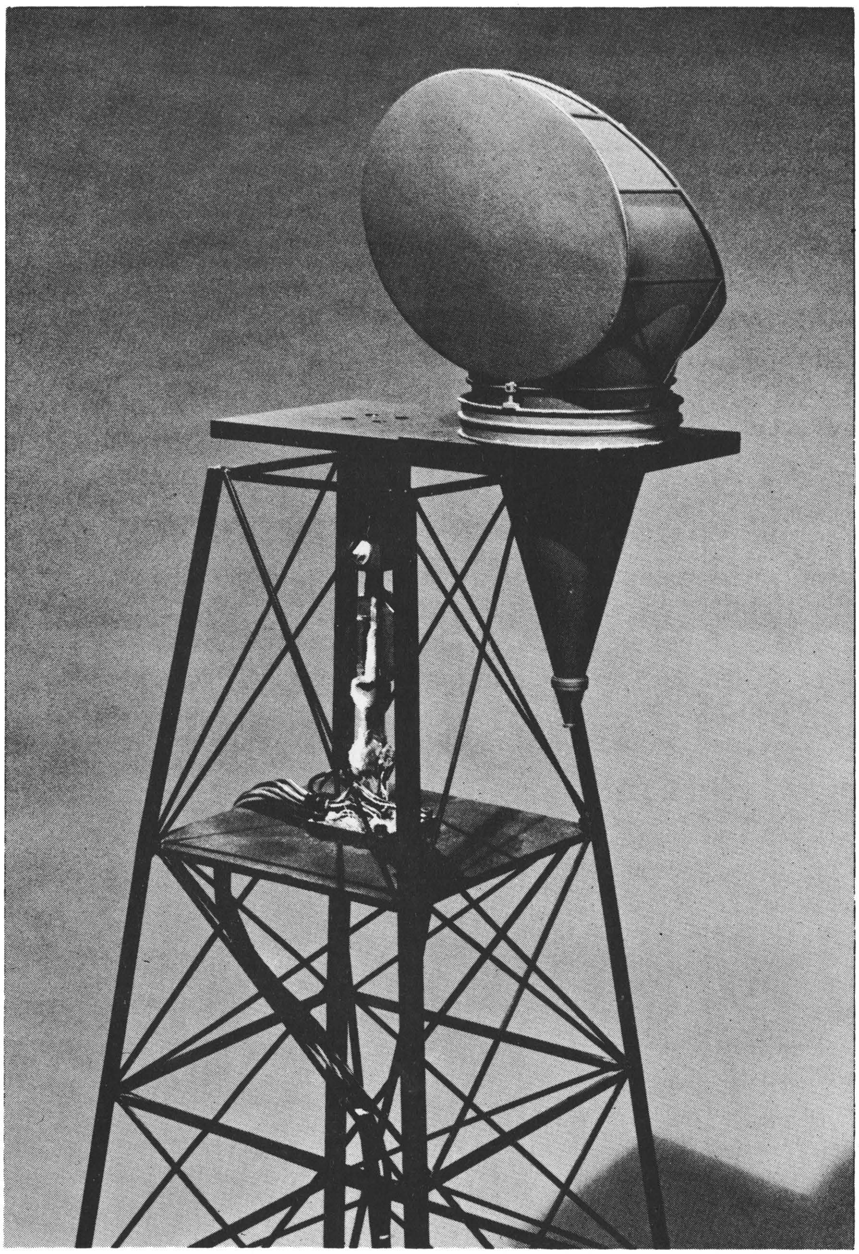

Figure 14. Conical Horn Antenna Cluster

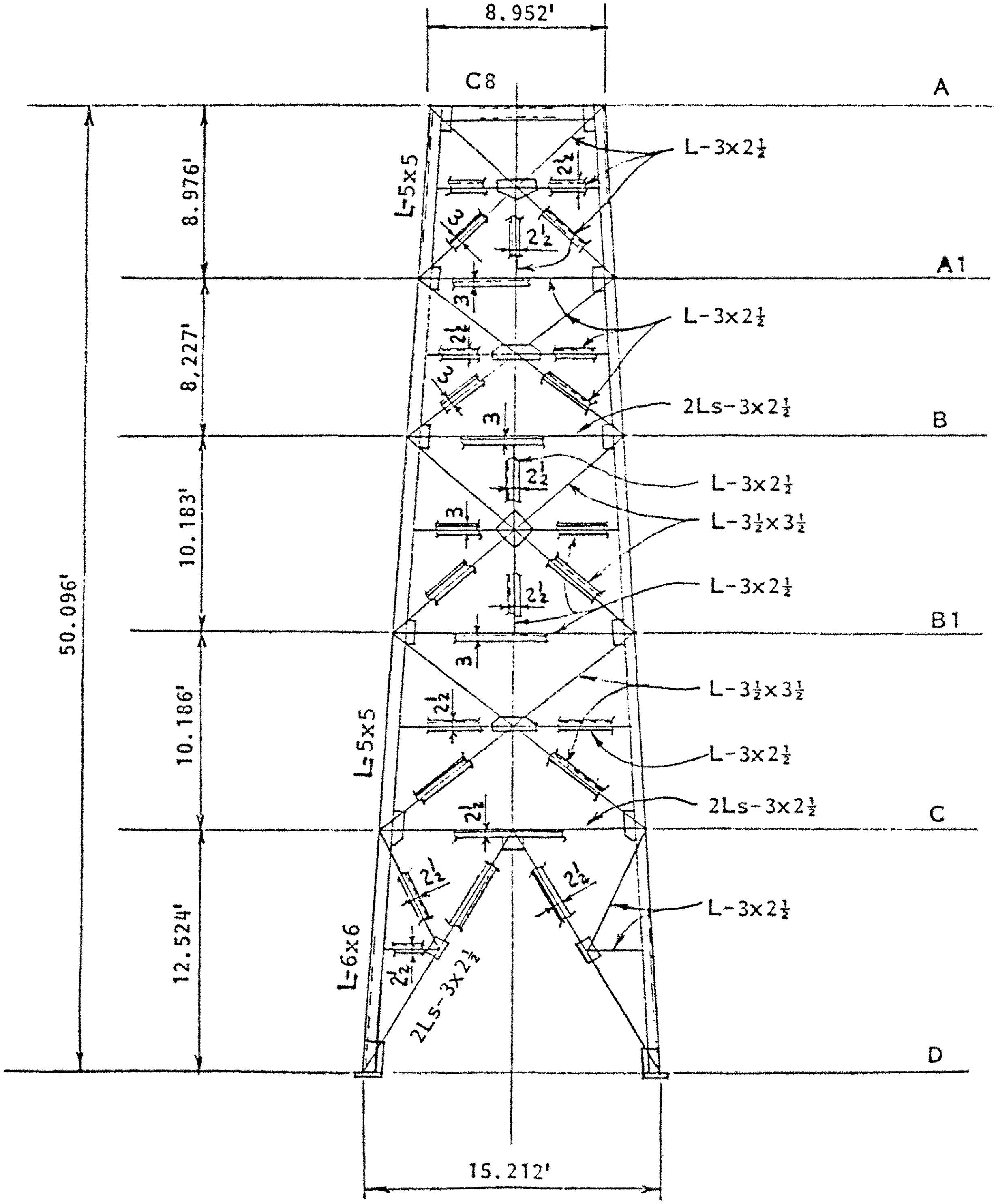

Figure 15a. Conceptional Sketch of Antenna Tower

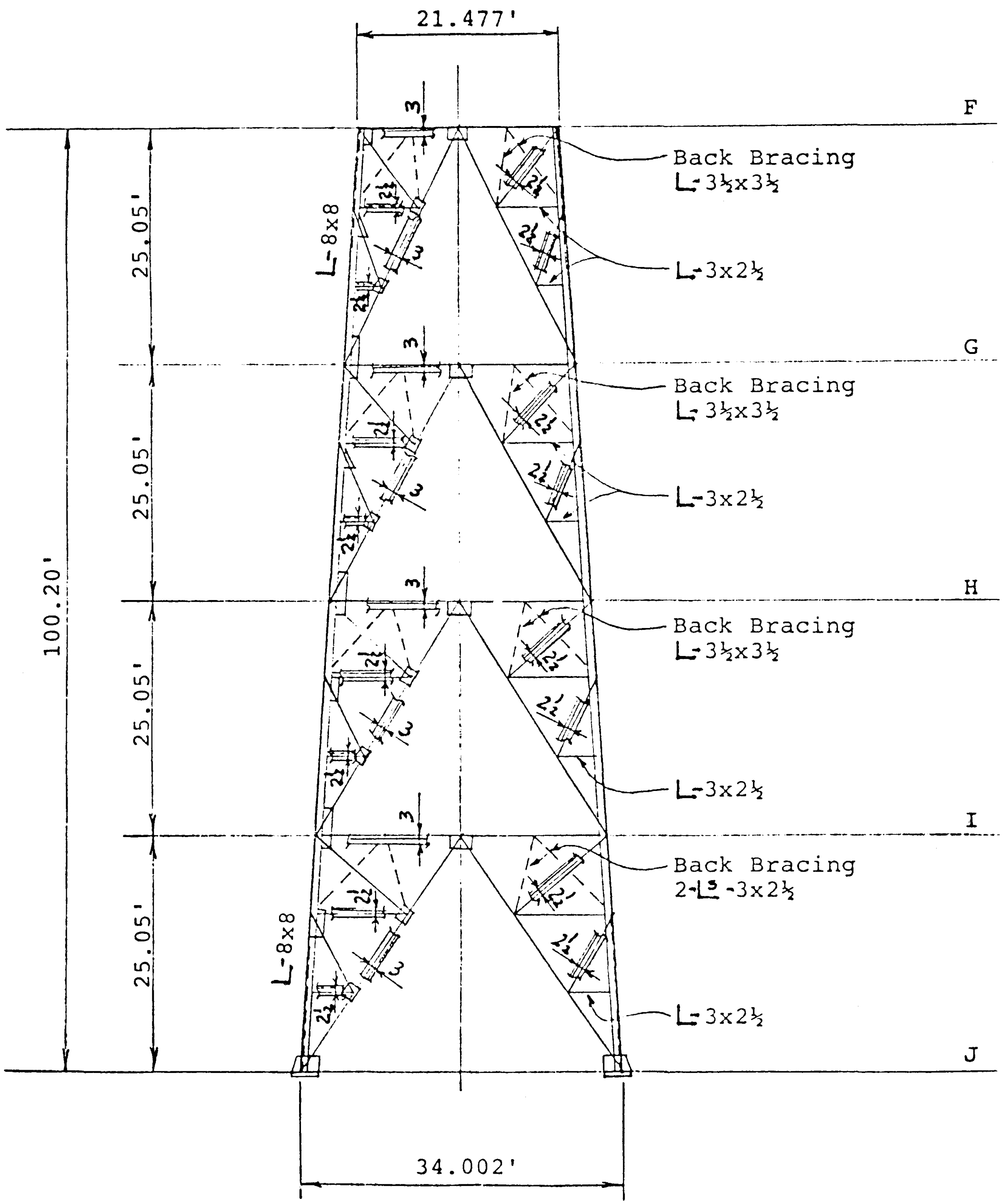

Figure 15b. Conceptional Sketch of Antenna Tower

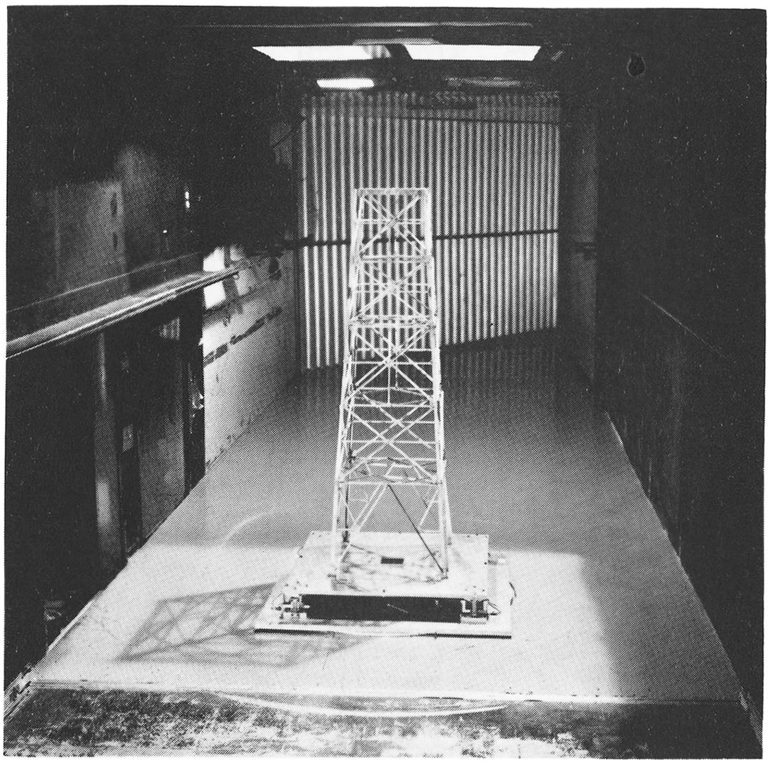

AA - DD

Figure 16a. Selected Tower Section

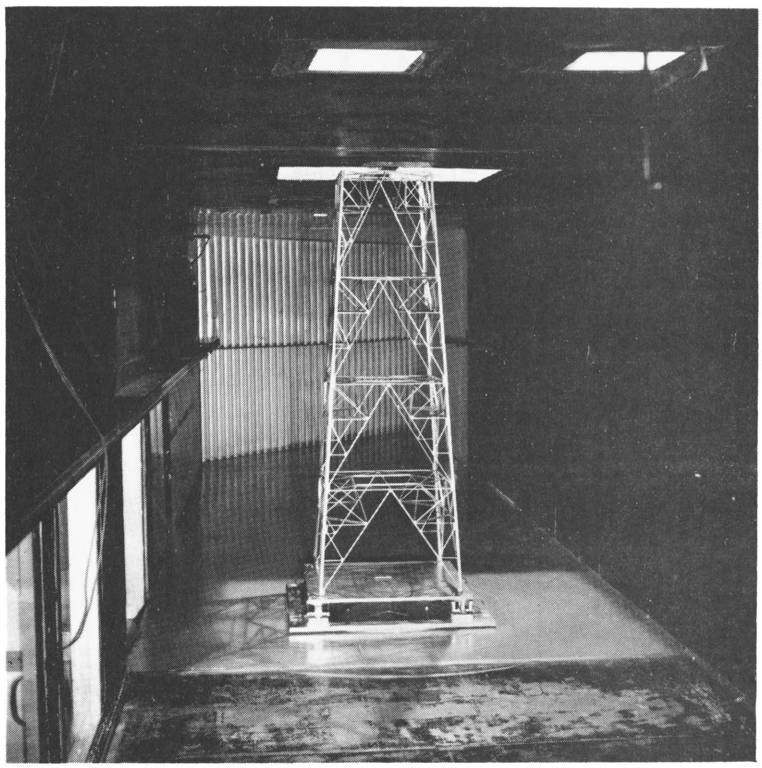

FF - JJ

Figure 16b. Selected Tower Section

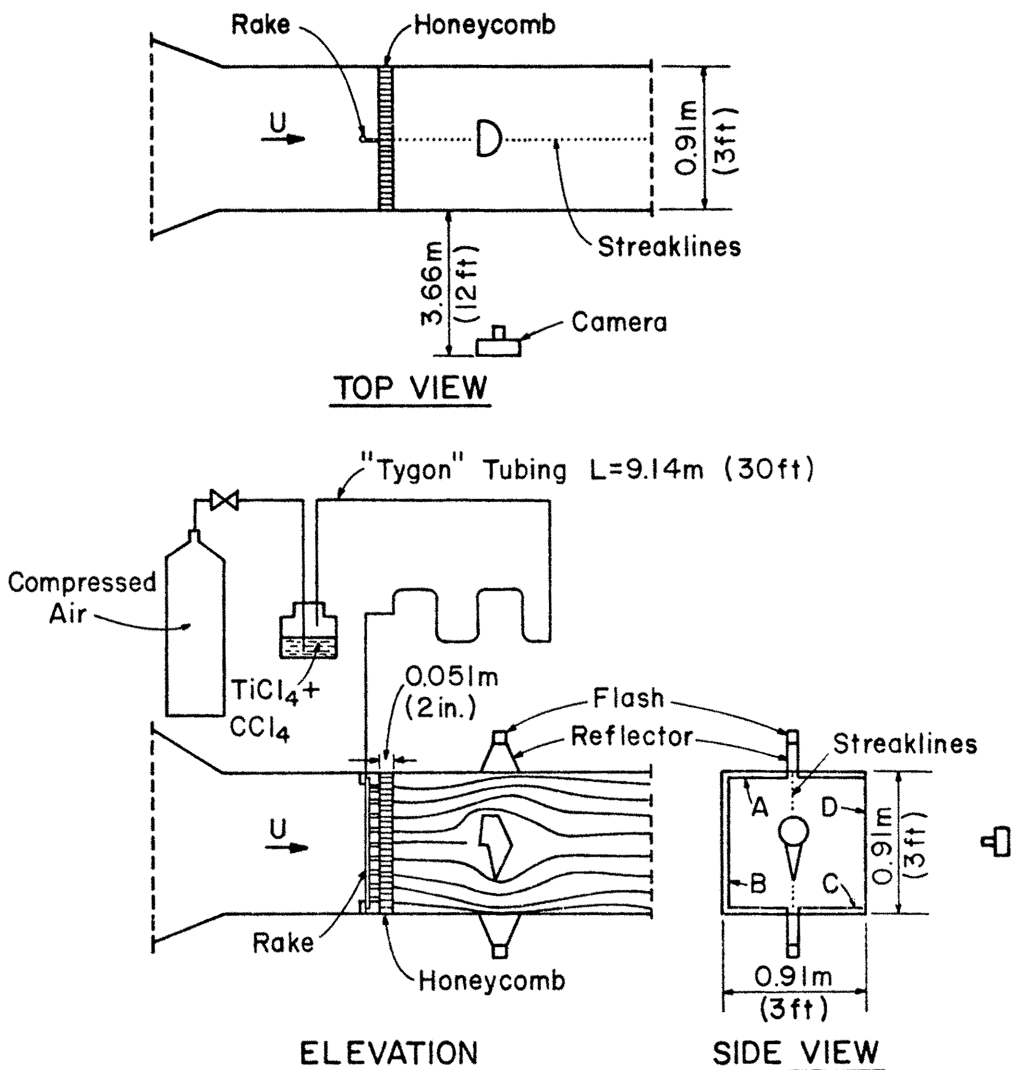

Figure 17. Flow Visualization Arrangement

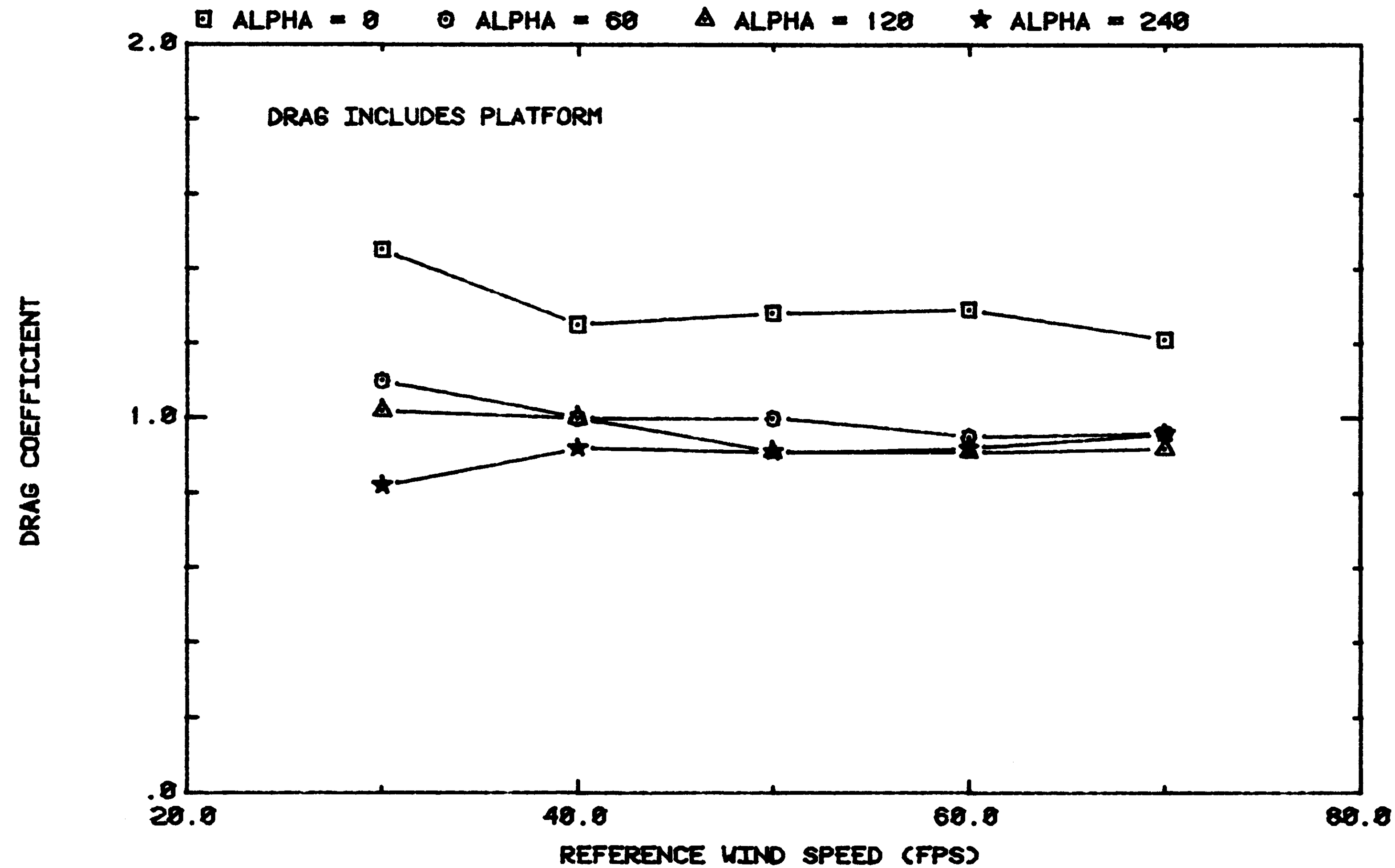

Figure 18. Effects of Wind Speed on the Drag of ANDREW SHX10

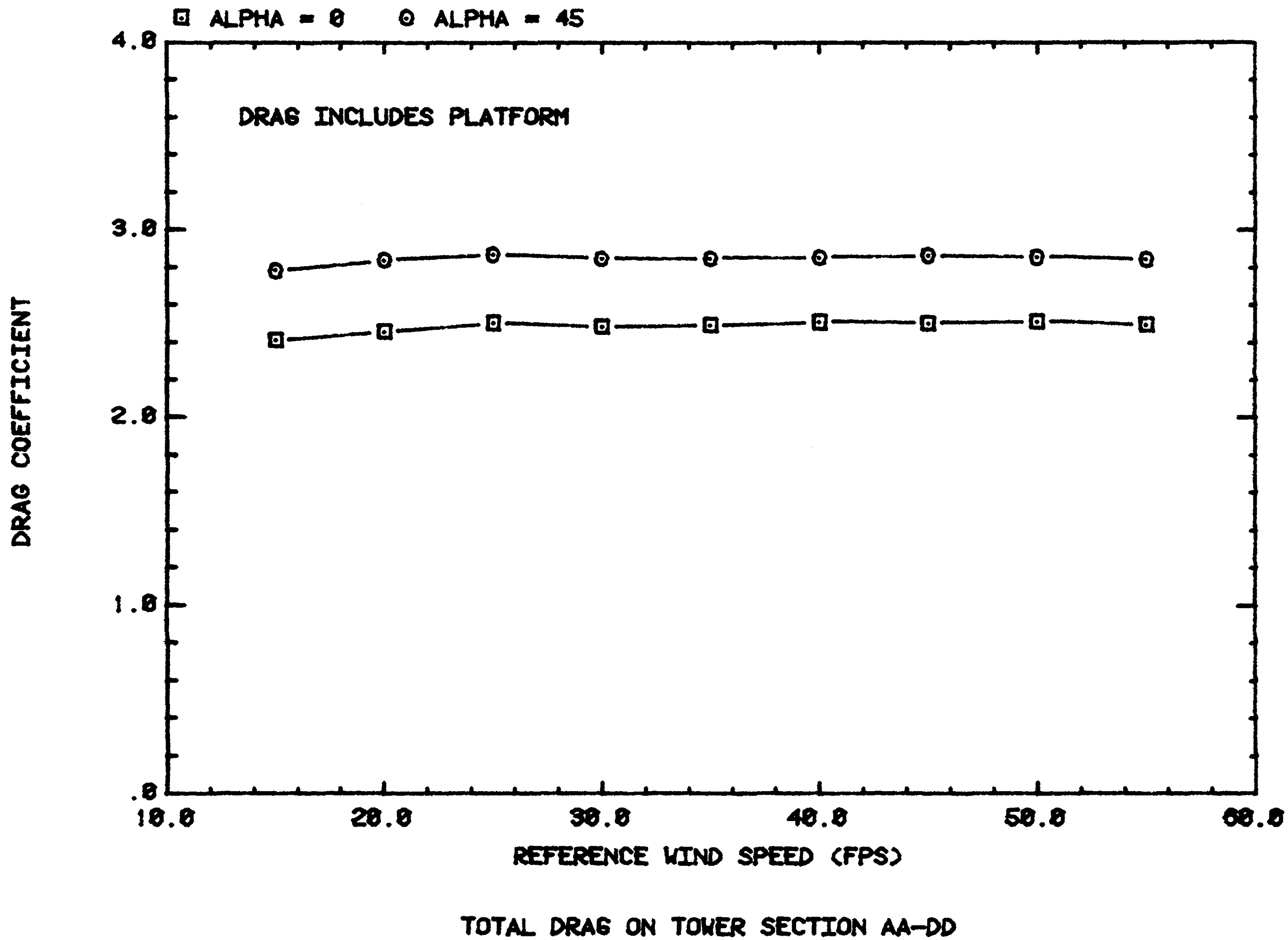

Figure 19. Effects of Wind Speed on the Drag of the Tower Section AA-DD

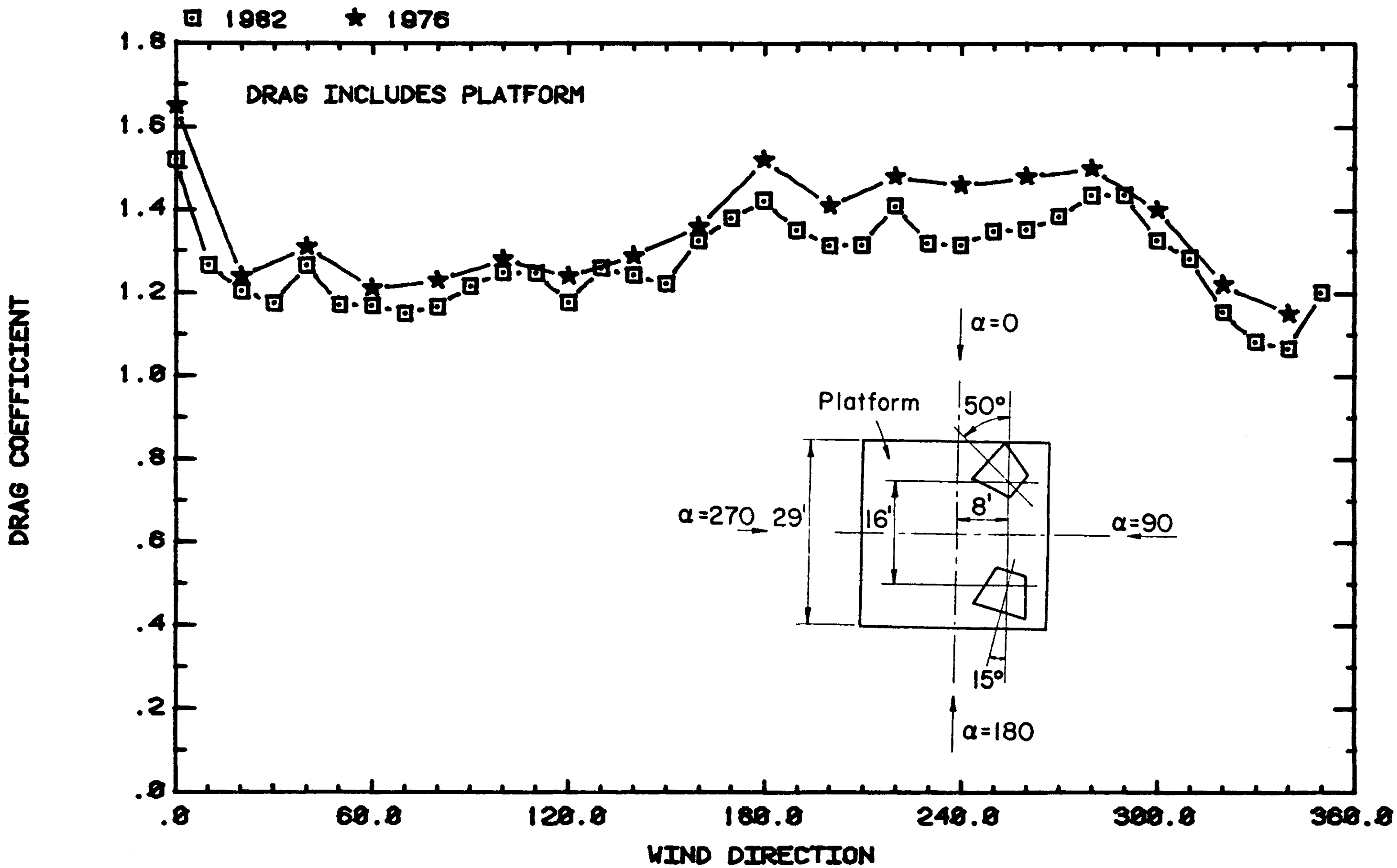

Figure 20. Comparison of the Drag on the Two Pyramidal Horn Antenna Cluster

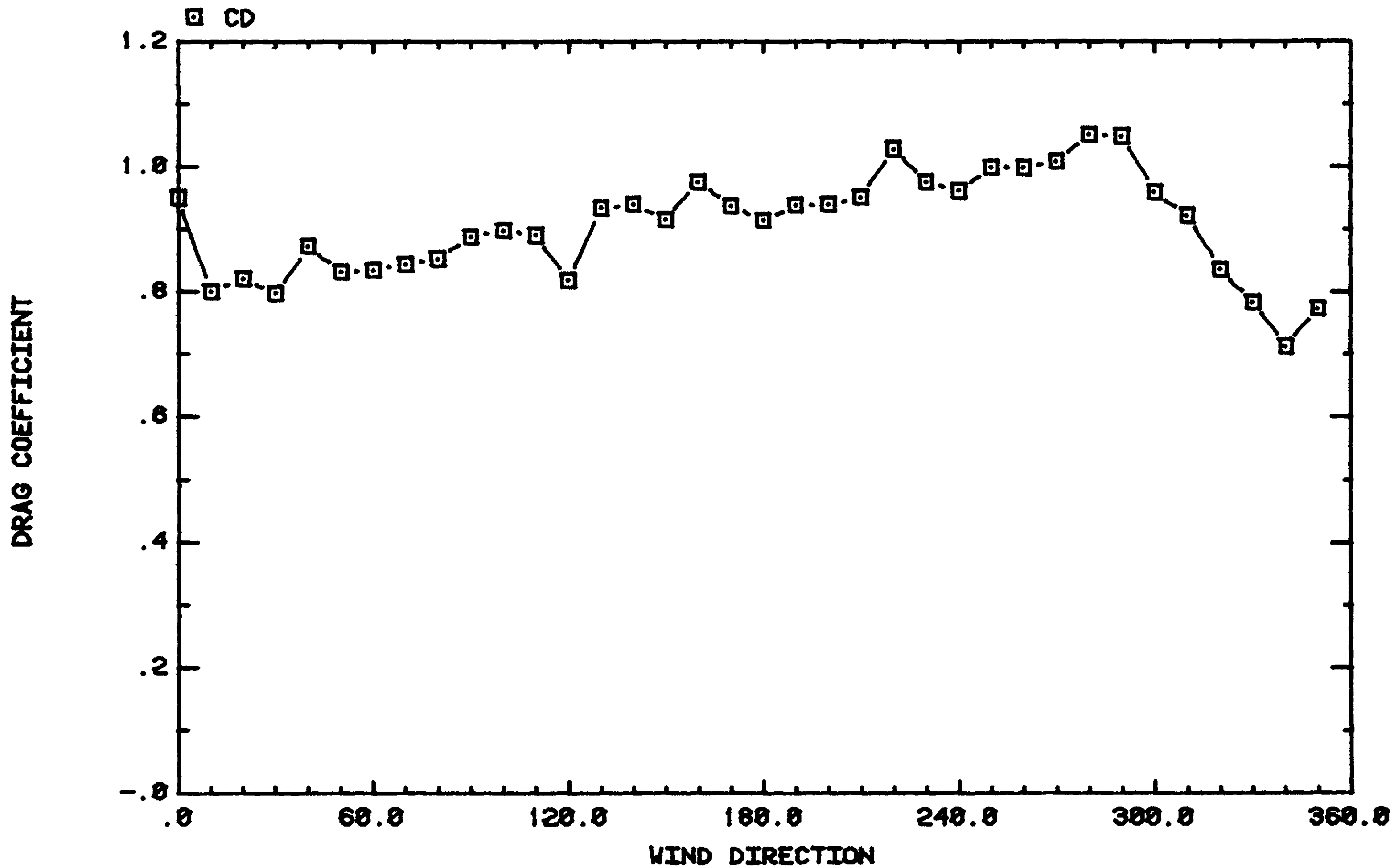

Figure 21. Drag on the Two Pyramidal Horn Antennas

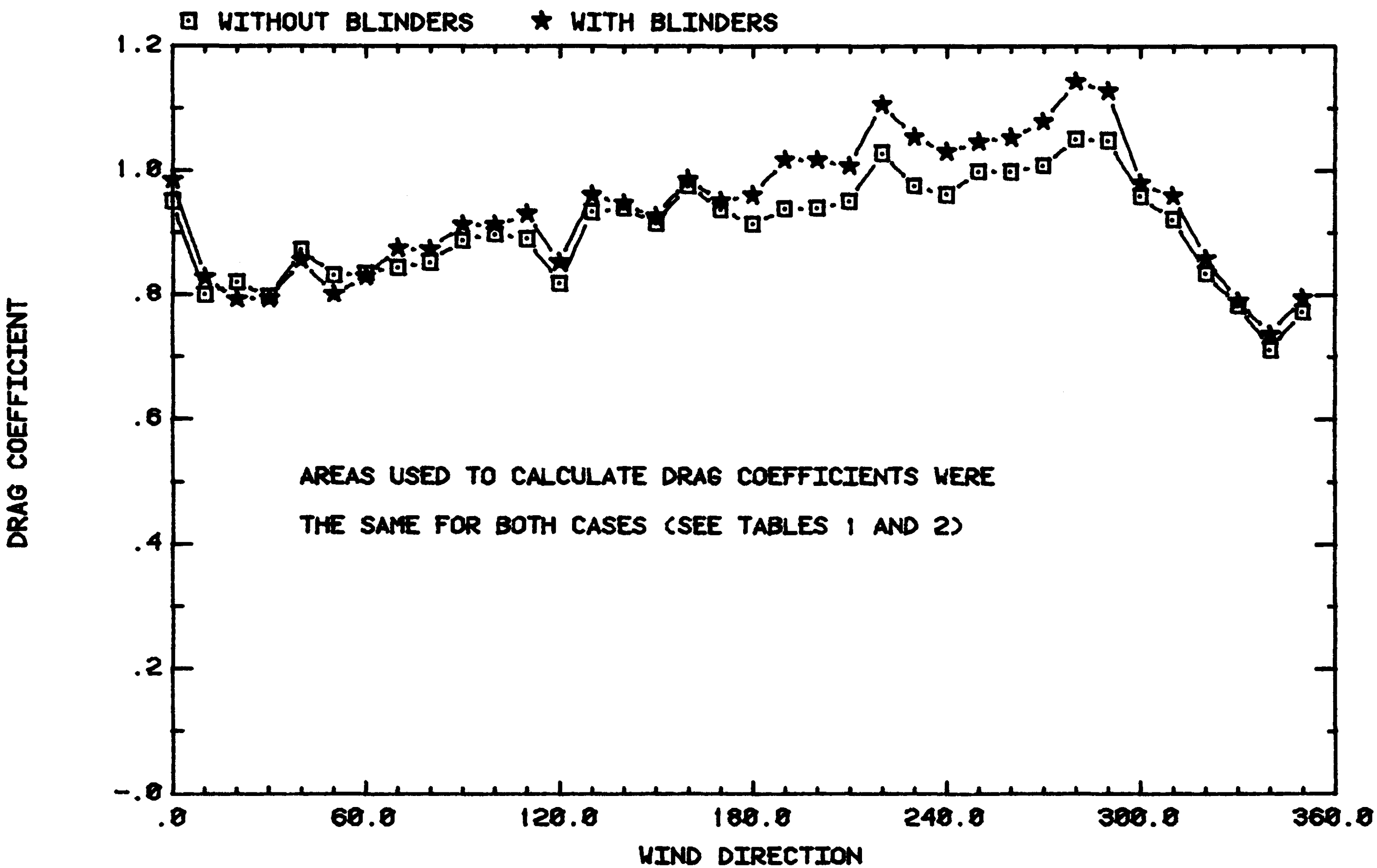

Figure 22. Effects of Bottom Edge Blinders

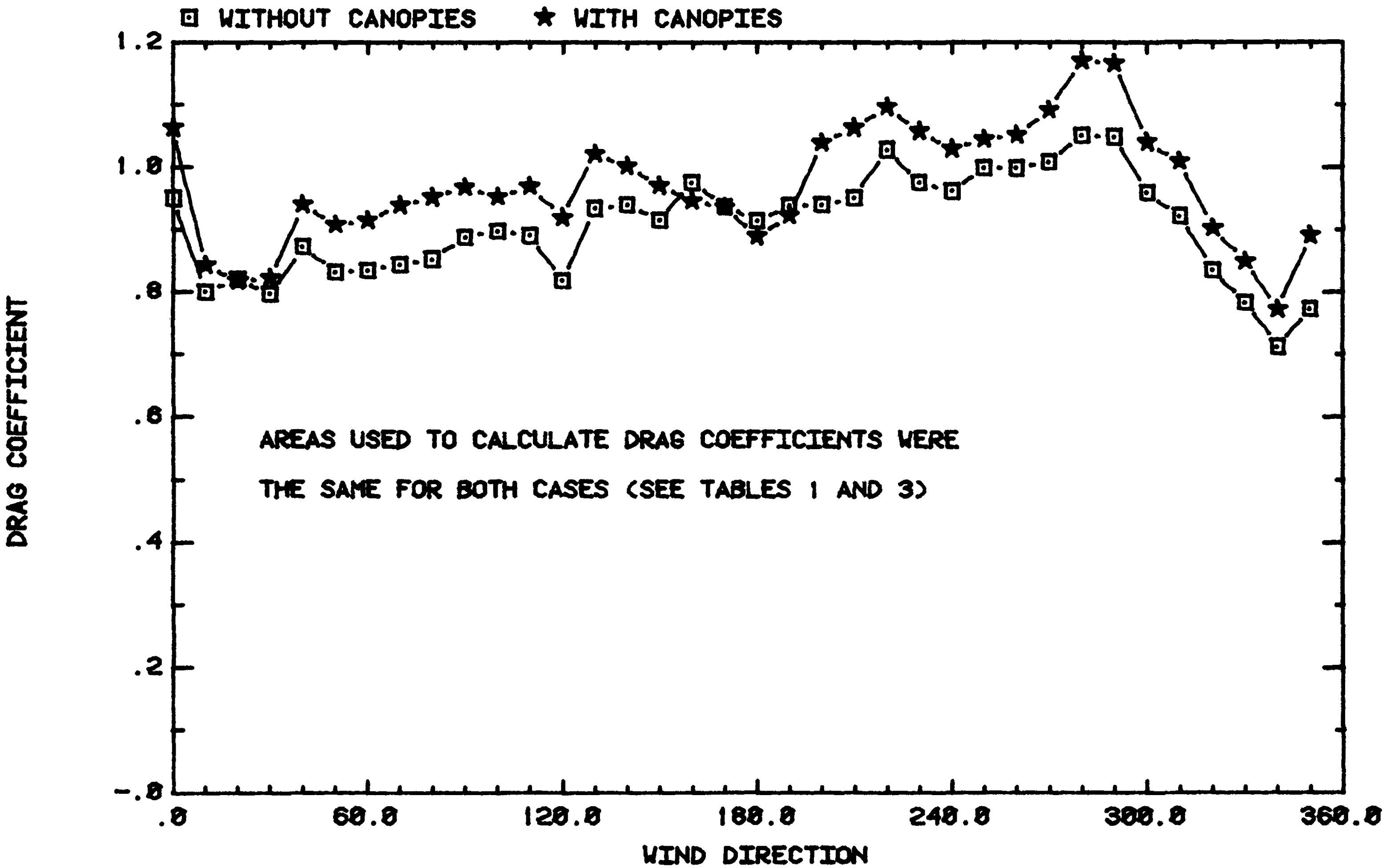

Figure 23. Effects of Ice Protection Canopies

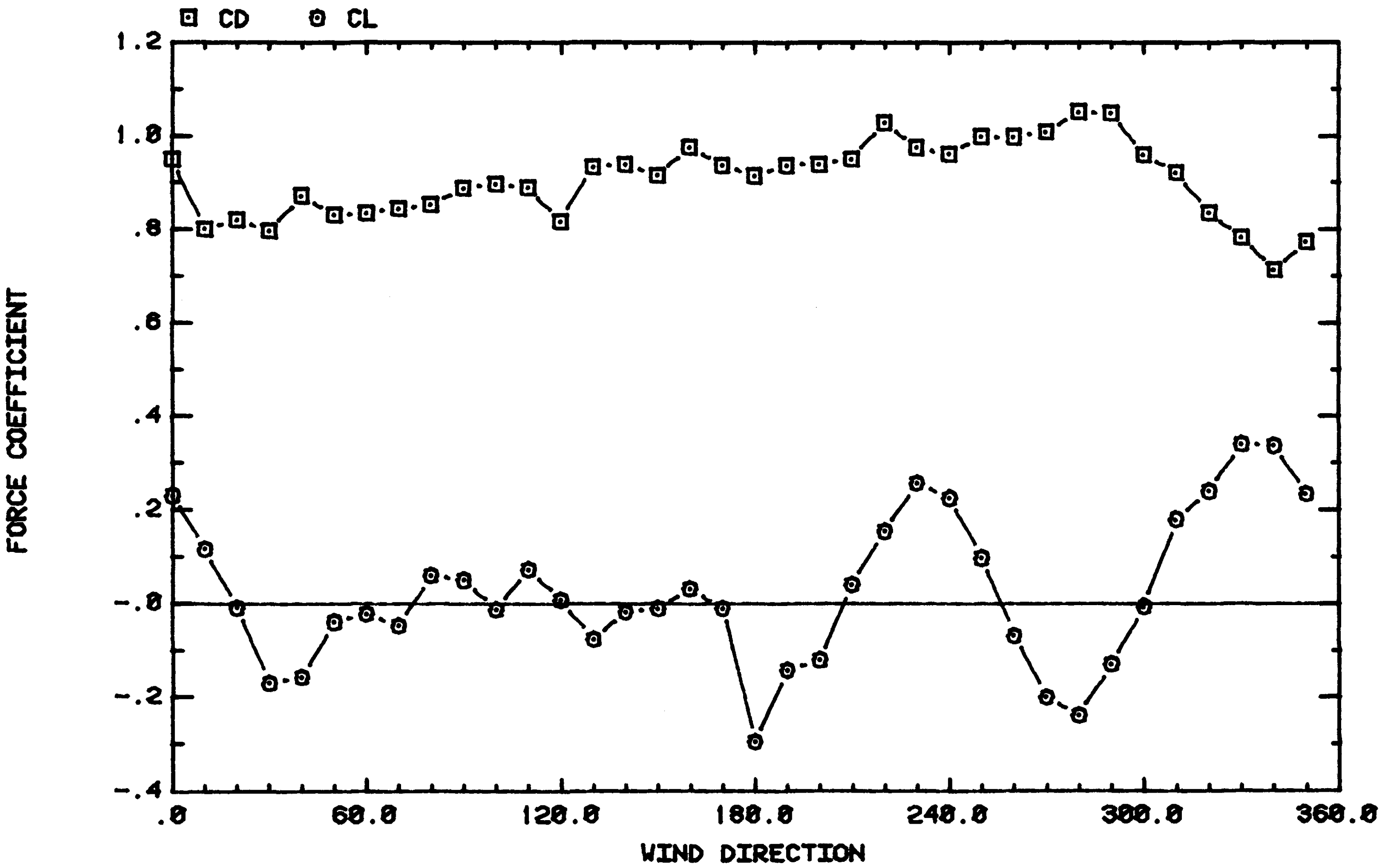

Figure 24a. Wind Loads on the Two Pyramidal Horn Antennas

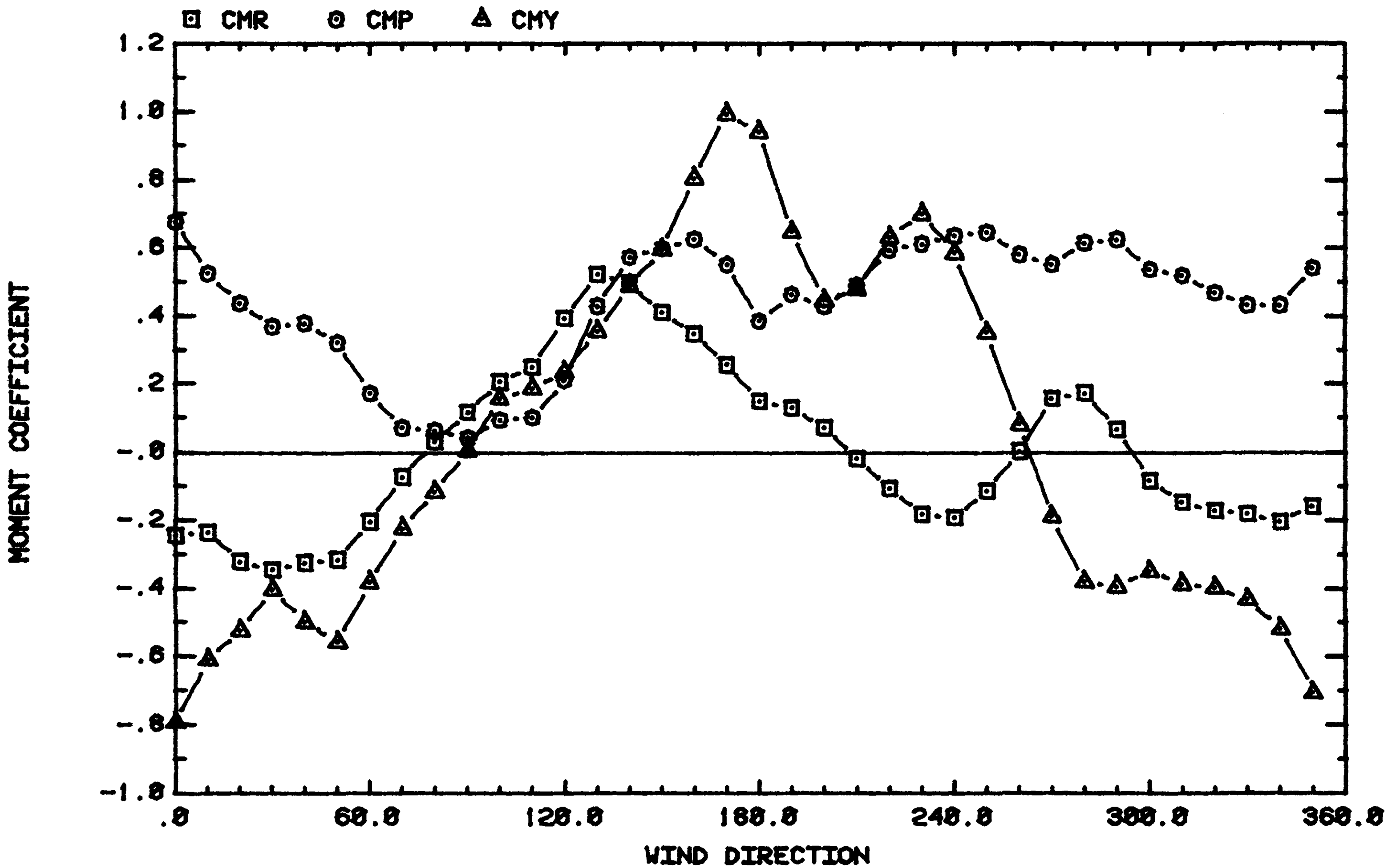

Figure 24b. Wind Loads on the Two Pyramidal Horn Antennas

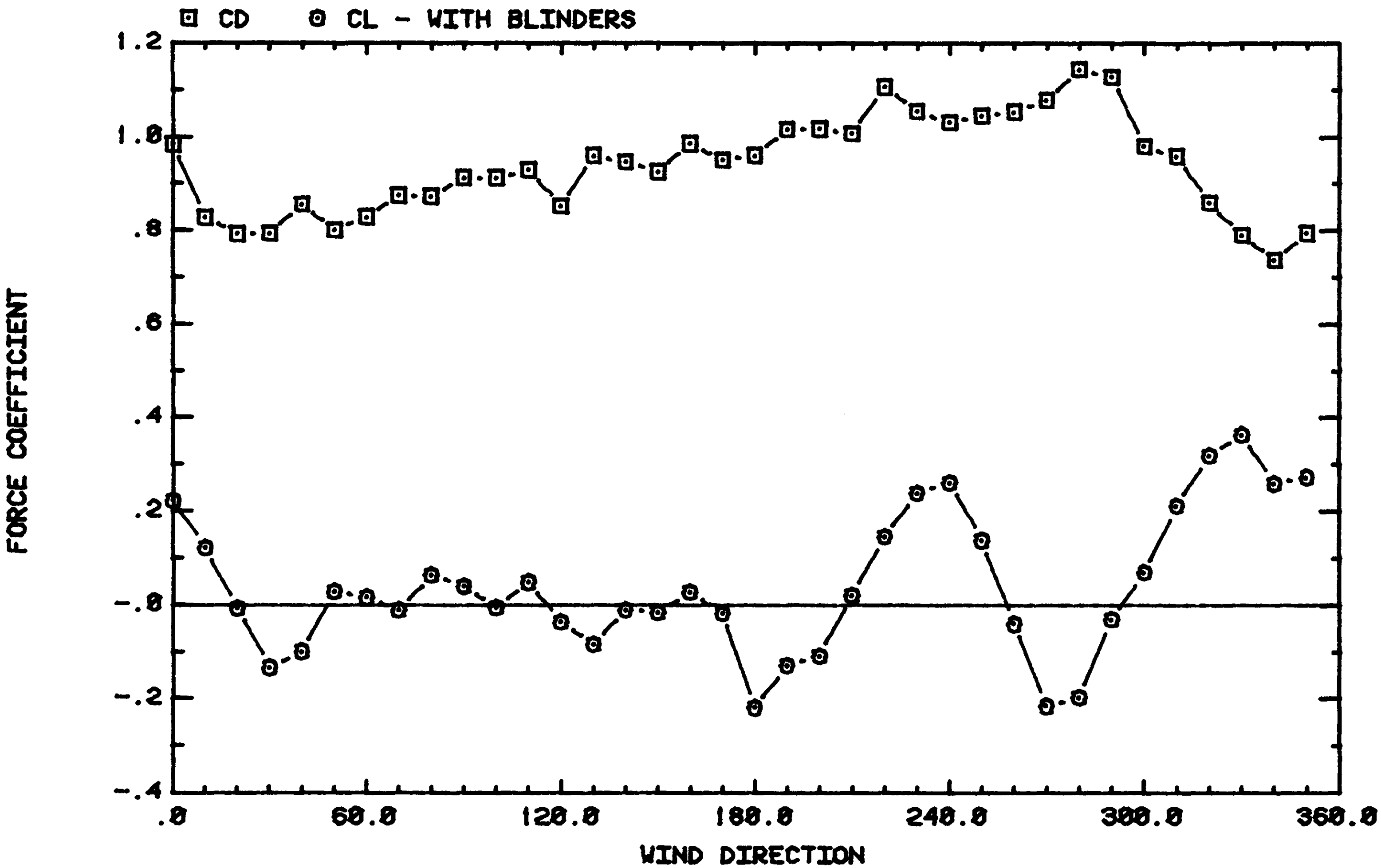

Figure 25a. Wind Loads on the Two Pyramidal Horn Antennas with Bottom Edge Blinders

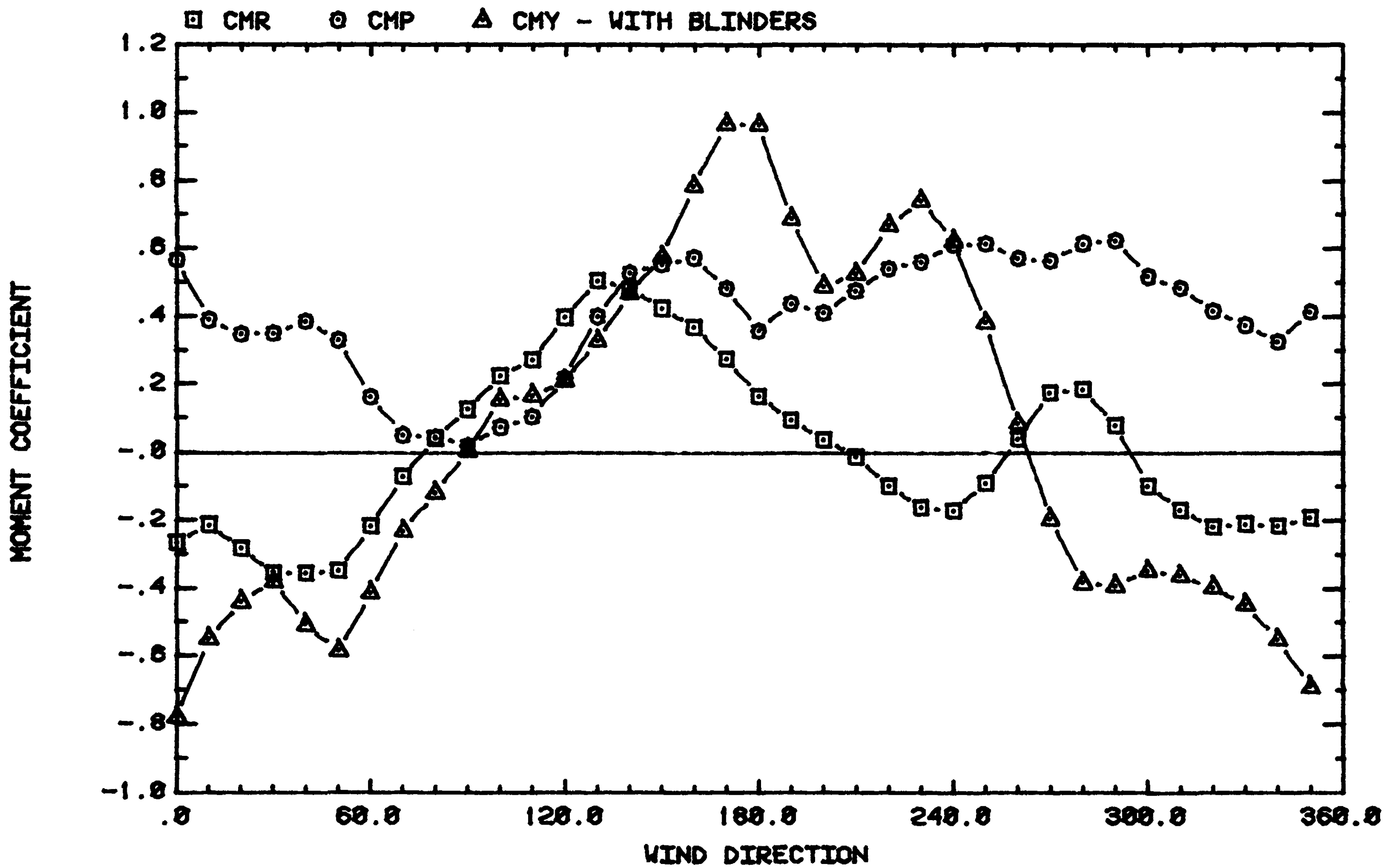

Figure 25b. Wind Loads on the Two Pyramidal Horn Antennas with Bottom Edge Blinders

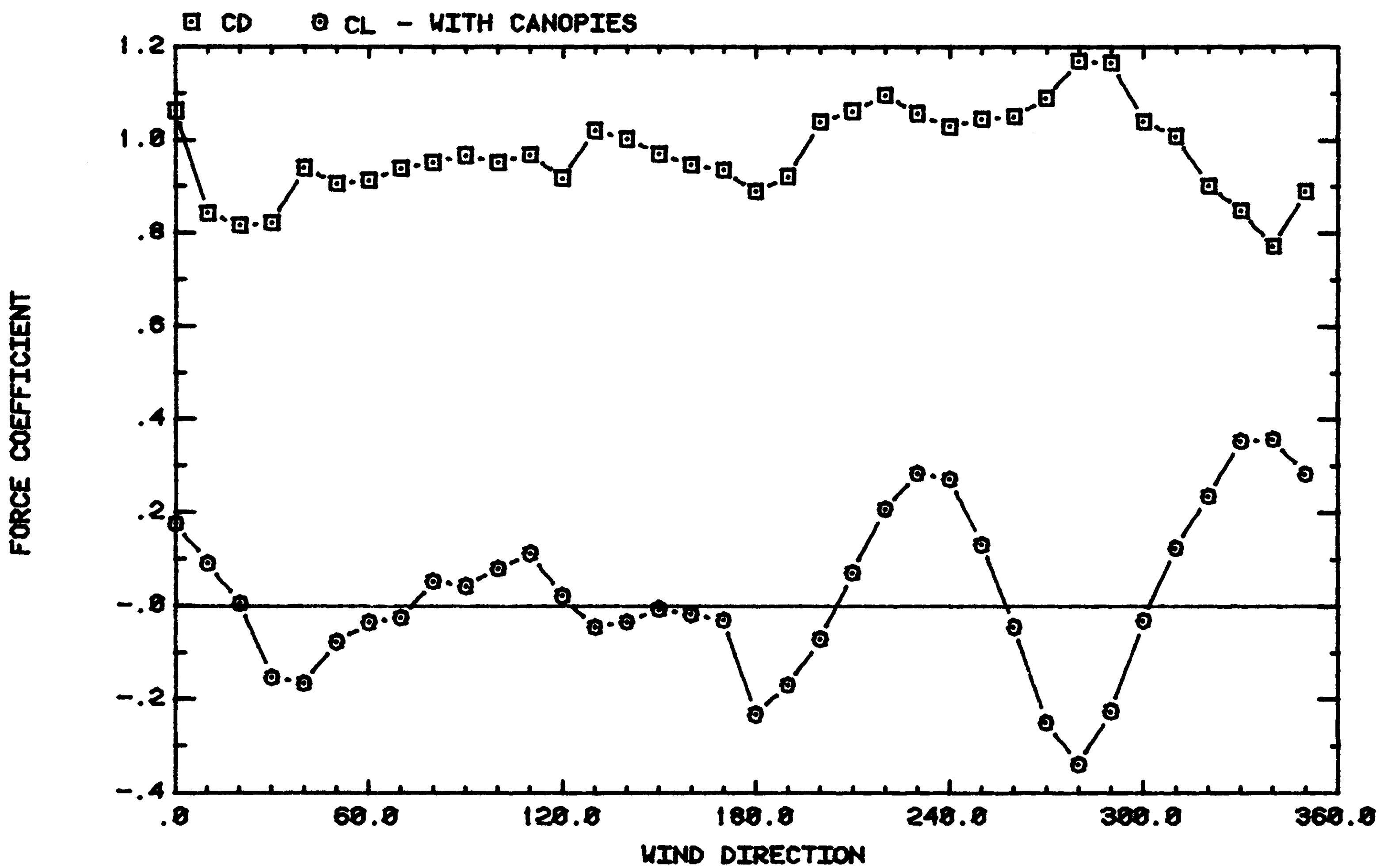

Figure 26a. Wind Loads on the Two Pyramidal Horn Antennas with Ice Protection Canopies

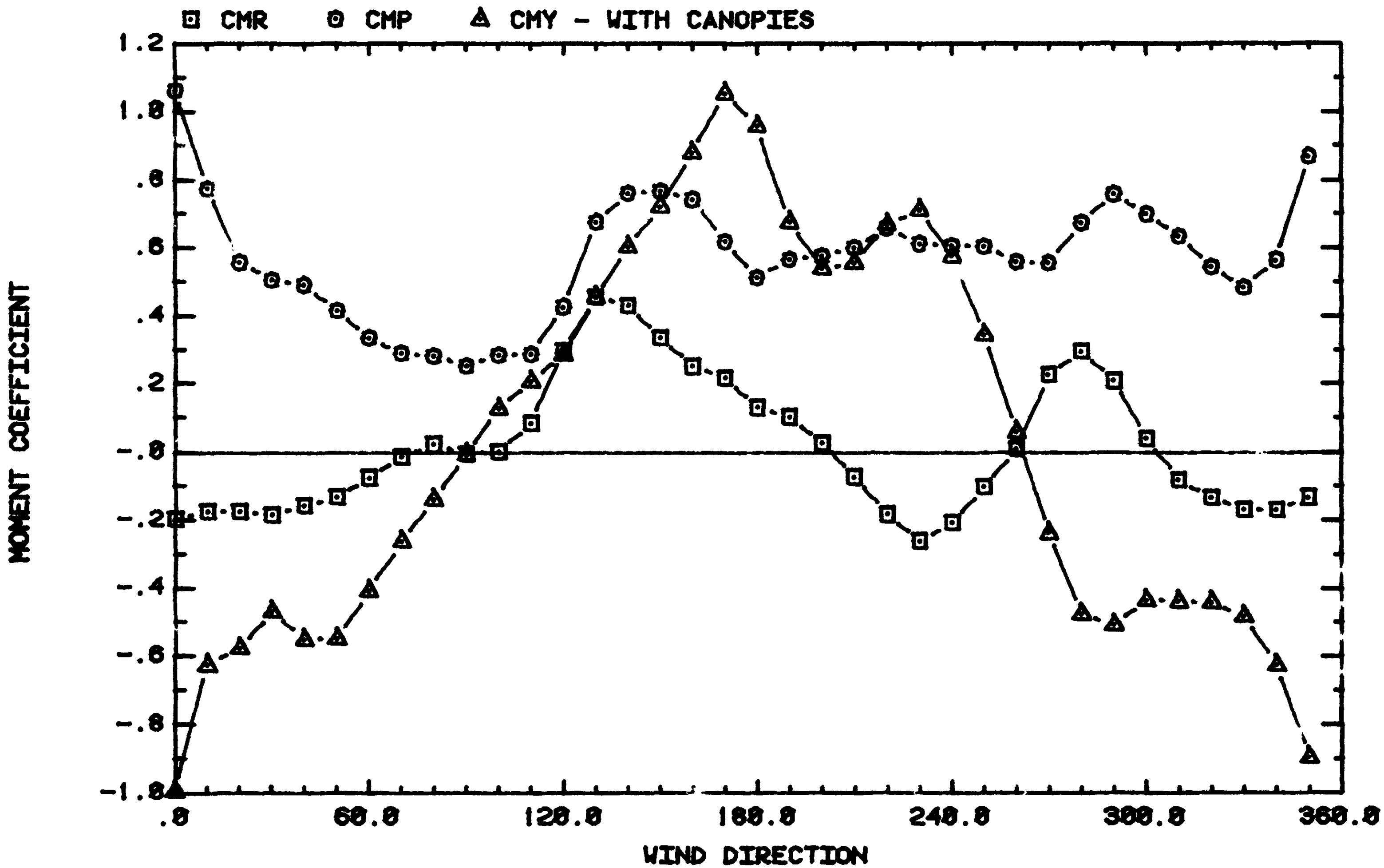

Figure 26b. Wind Loads on the Two Pyramidal Horn Antennas with Ice Protection Canopies

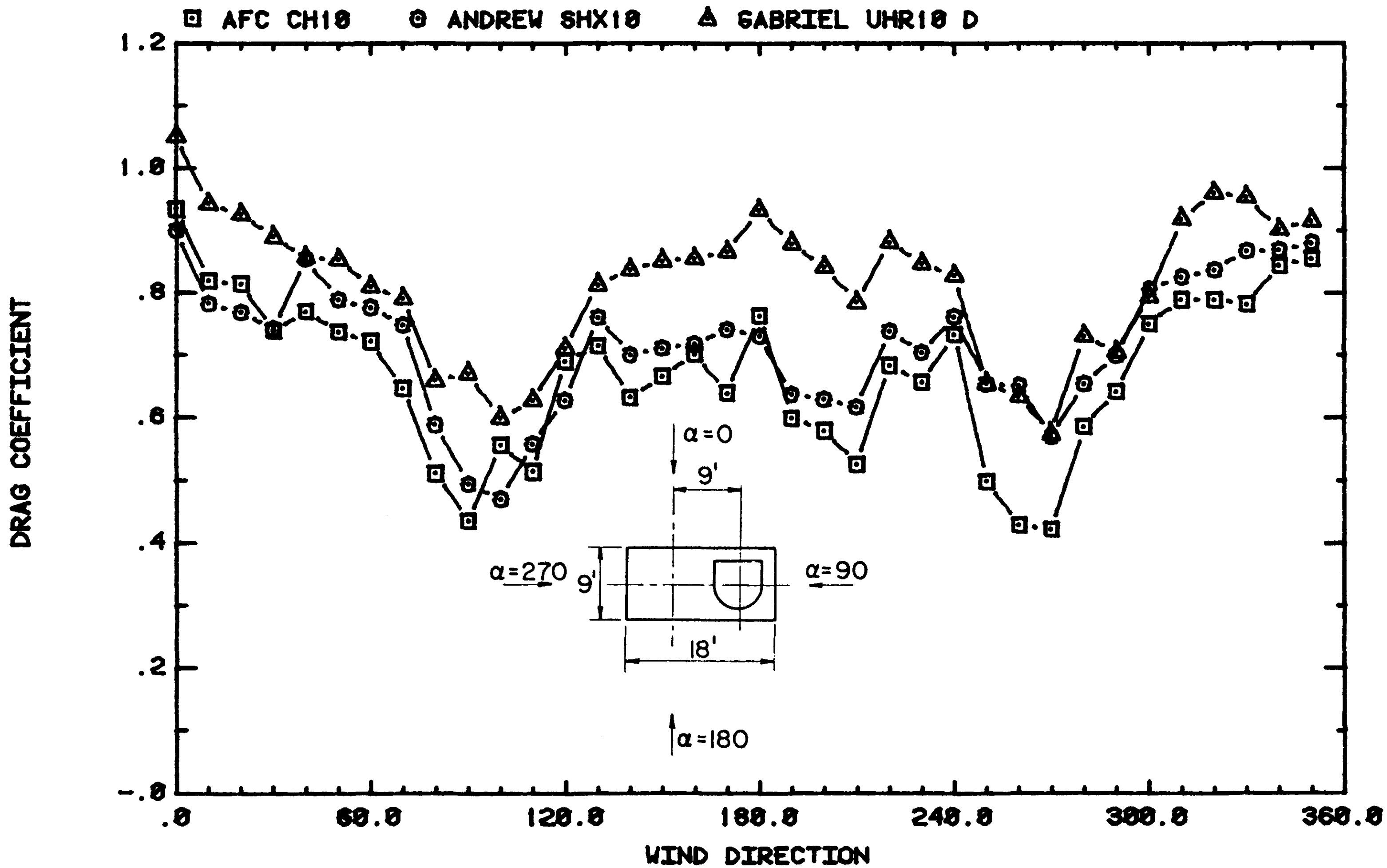

Figure 27. Drag on Various Conical Horn Antennas

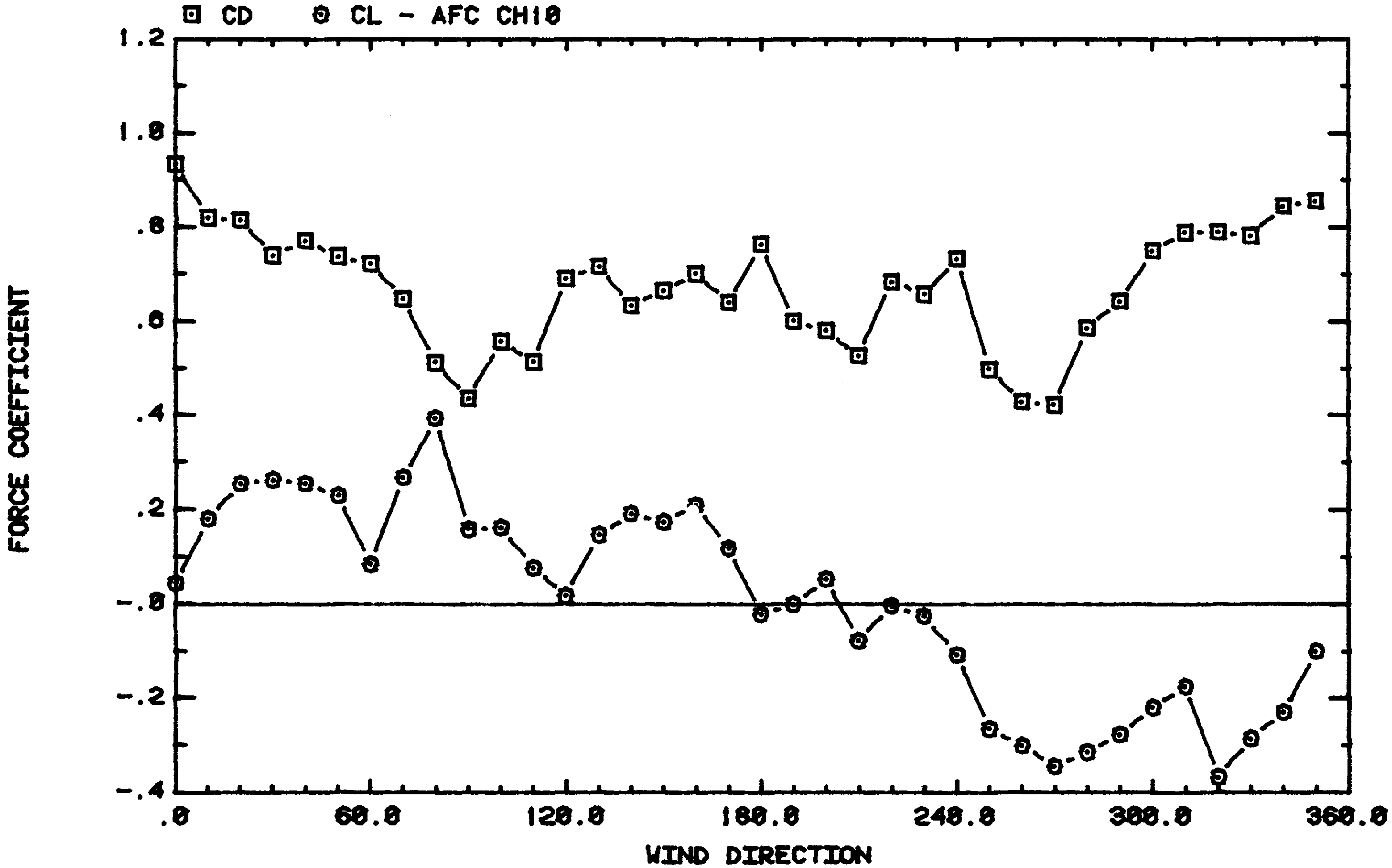

Figure 28a. Wind Loads on AFC CH10

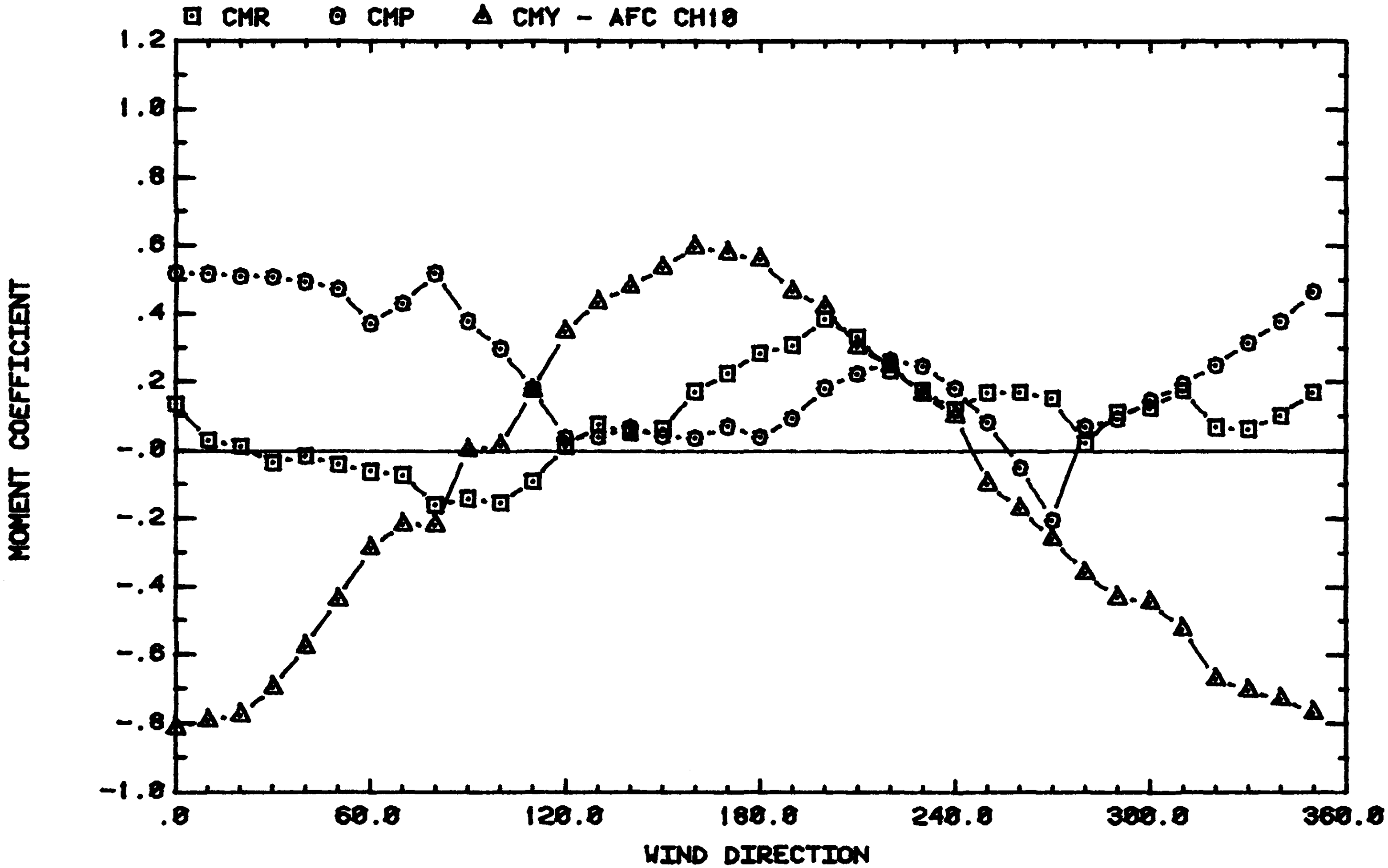

Figure 28b. Wind Loads on AFC CH10

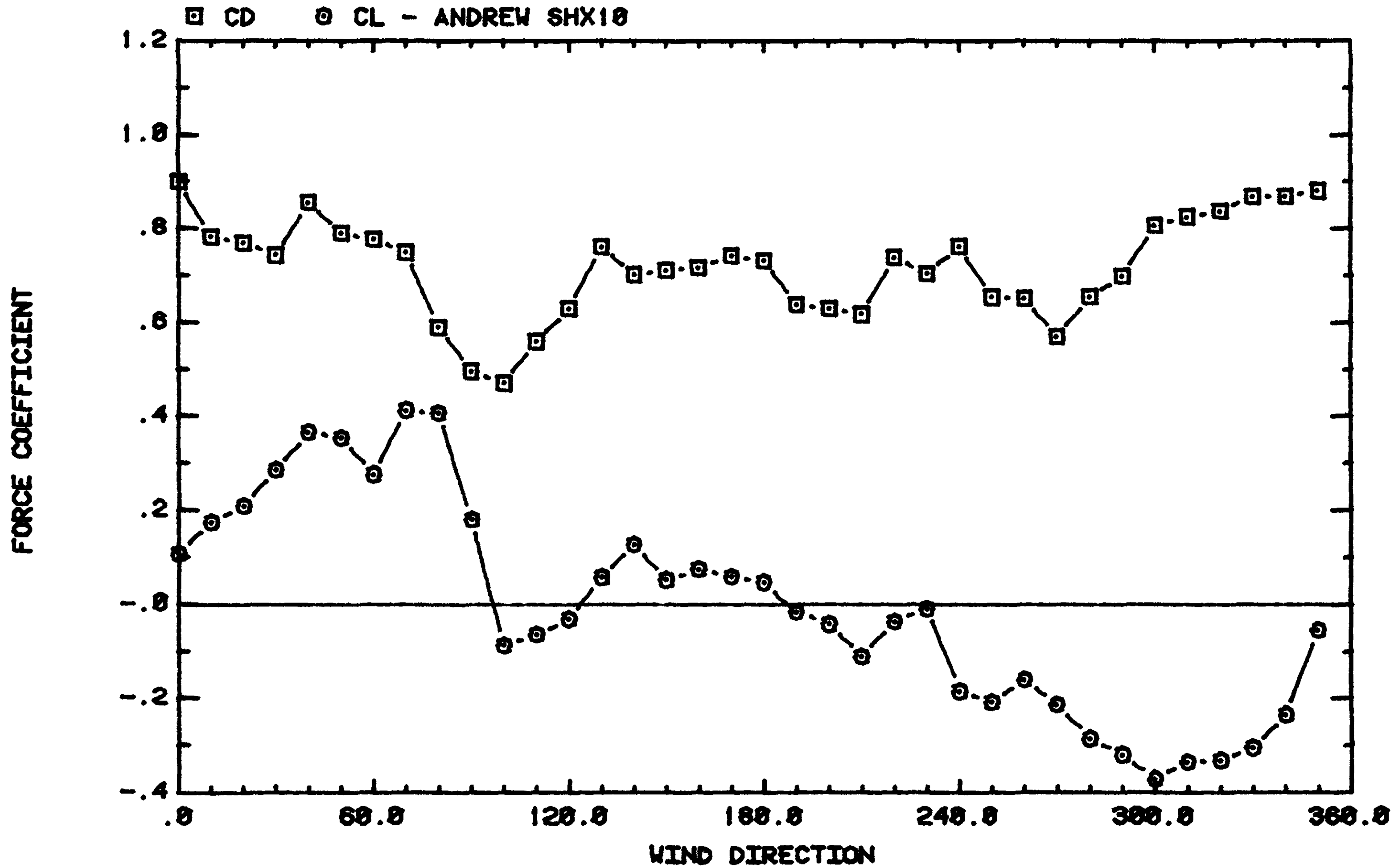

Figure 29a. Wind Loads on ANDREW SHX10

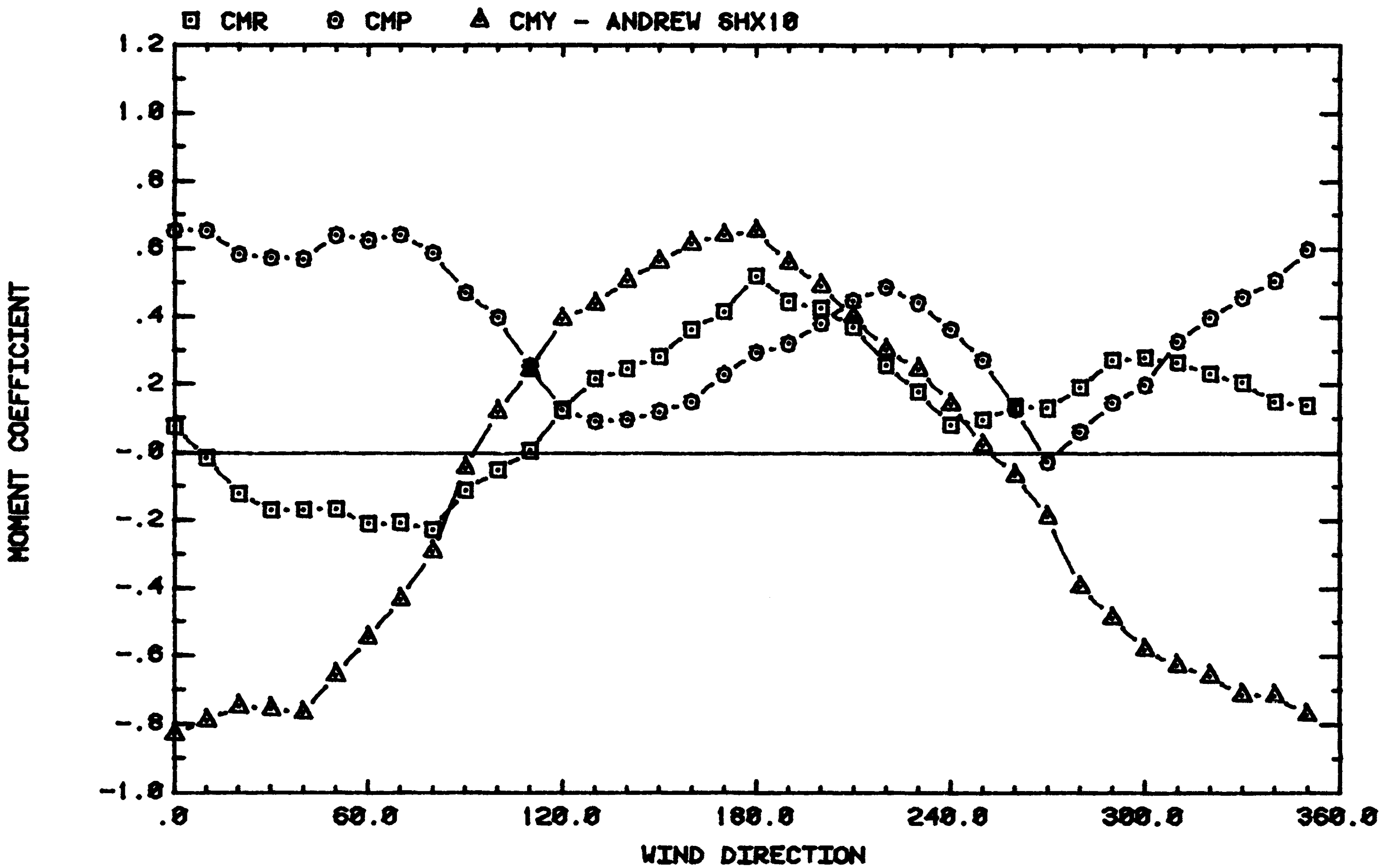

Figure 29b. Wind Loads on ANDREW SHX10

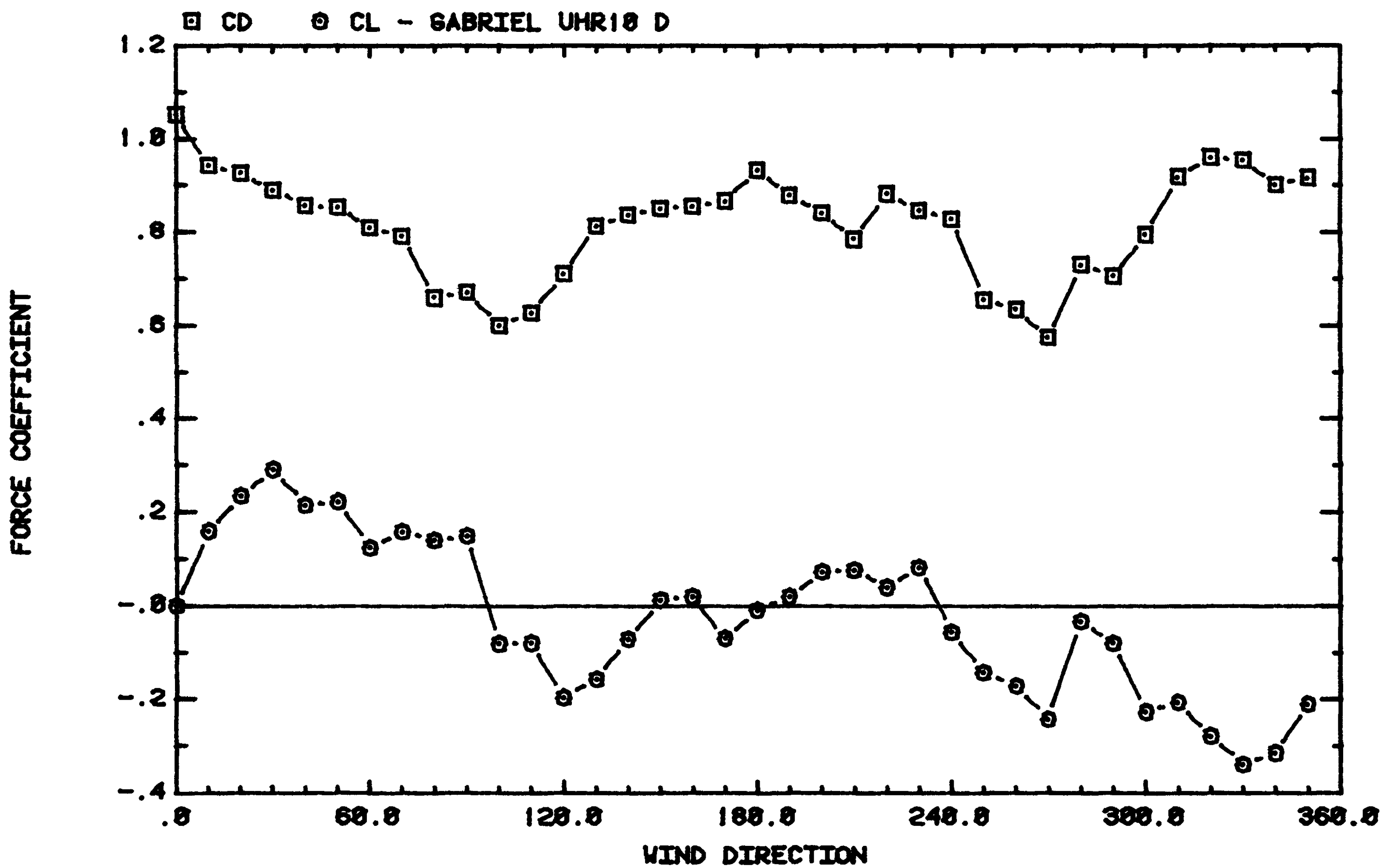

Figure 30a. Wind Loads on GABRIEL UHR10 D

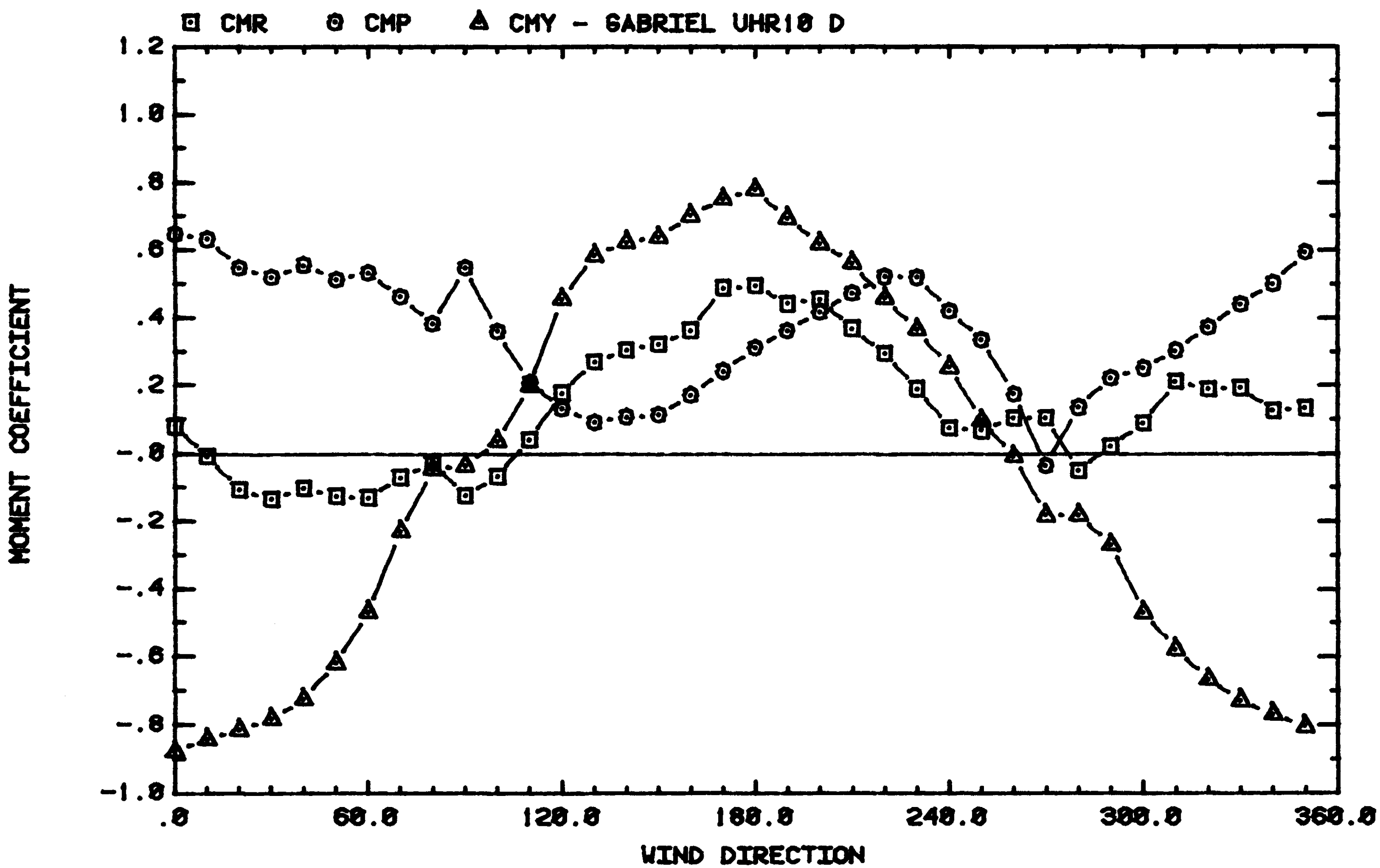

Figure 30b. Wind Loads on GABRIEL UHR10 D

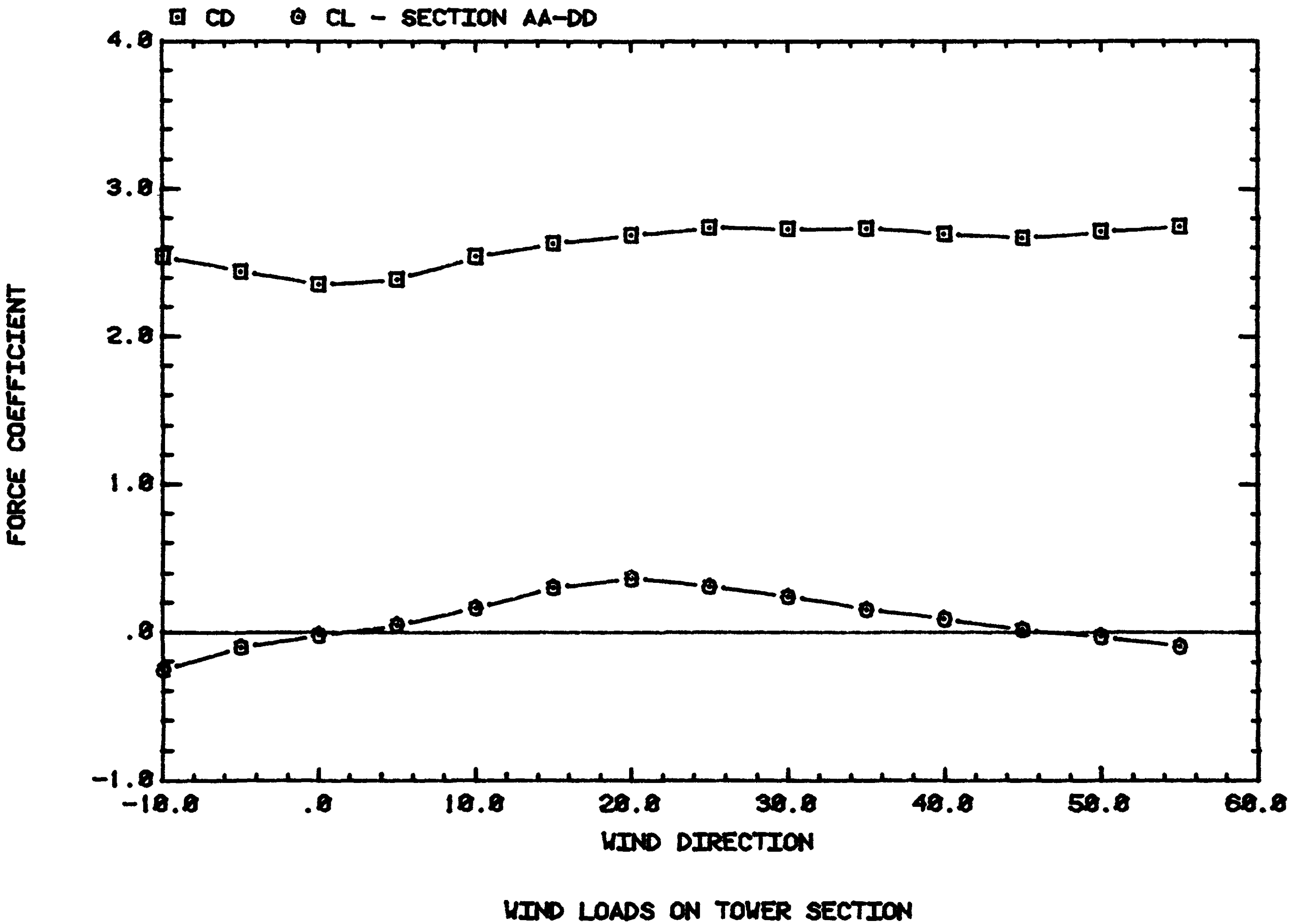

Figure 31. Wind Loads on the Tower Section AA-DD

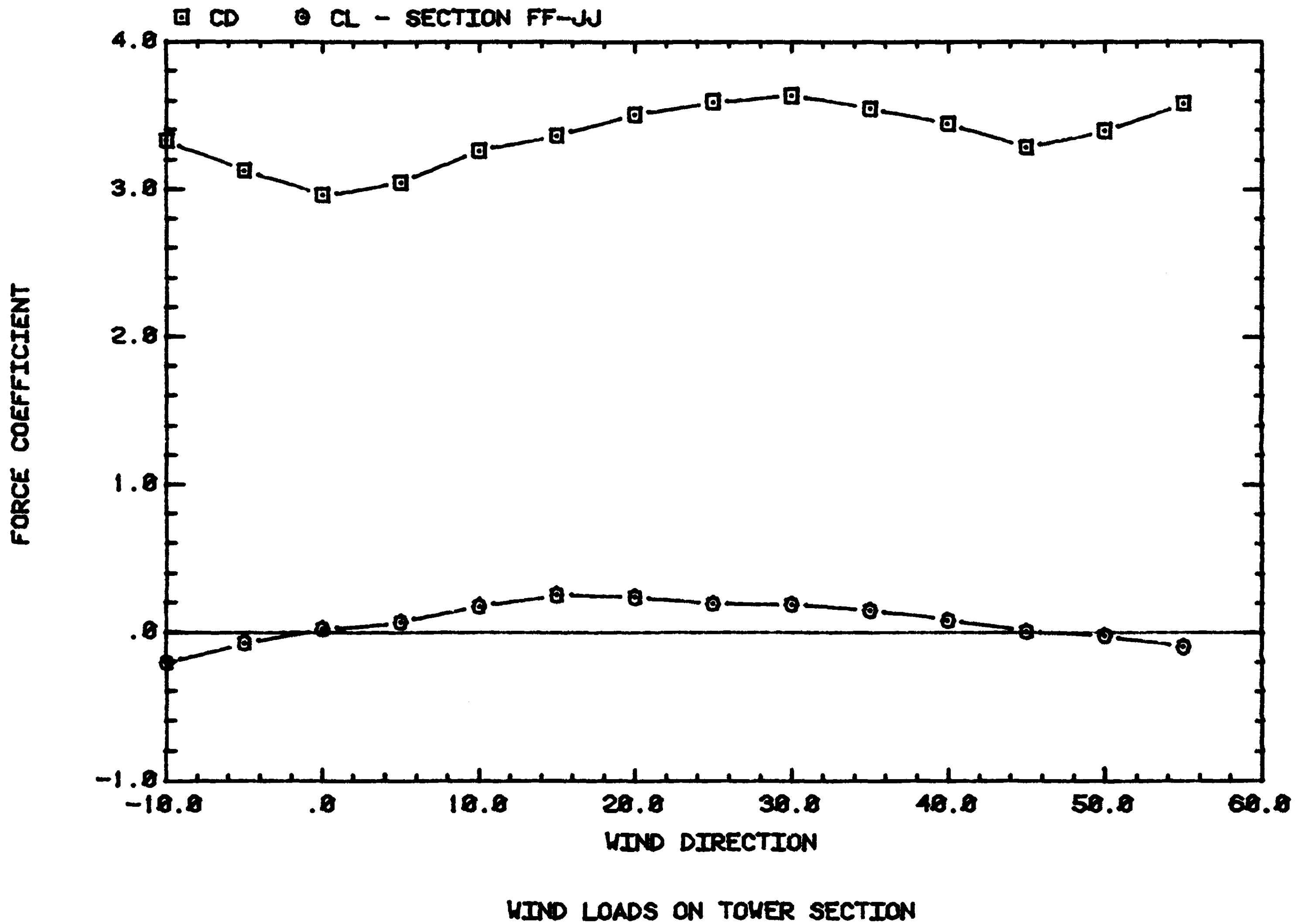

Figure 32. Wind Loads on the Tower Section FF-JJ

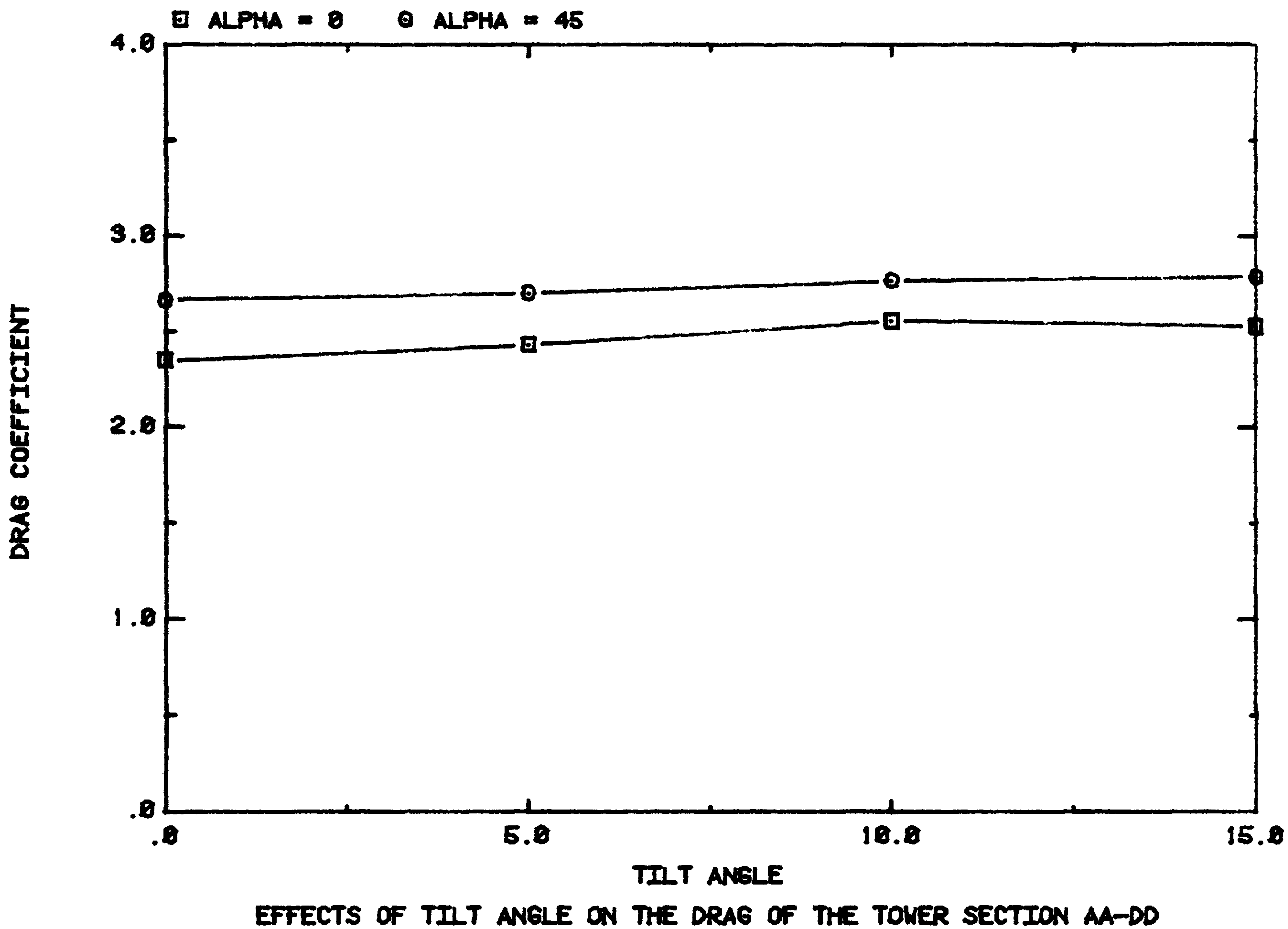

Figure 33. Effects of Tilt Angle on the Drag of the Tower Section AA-DD

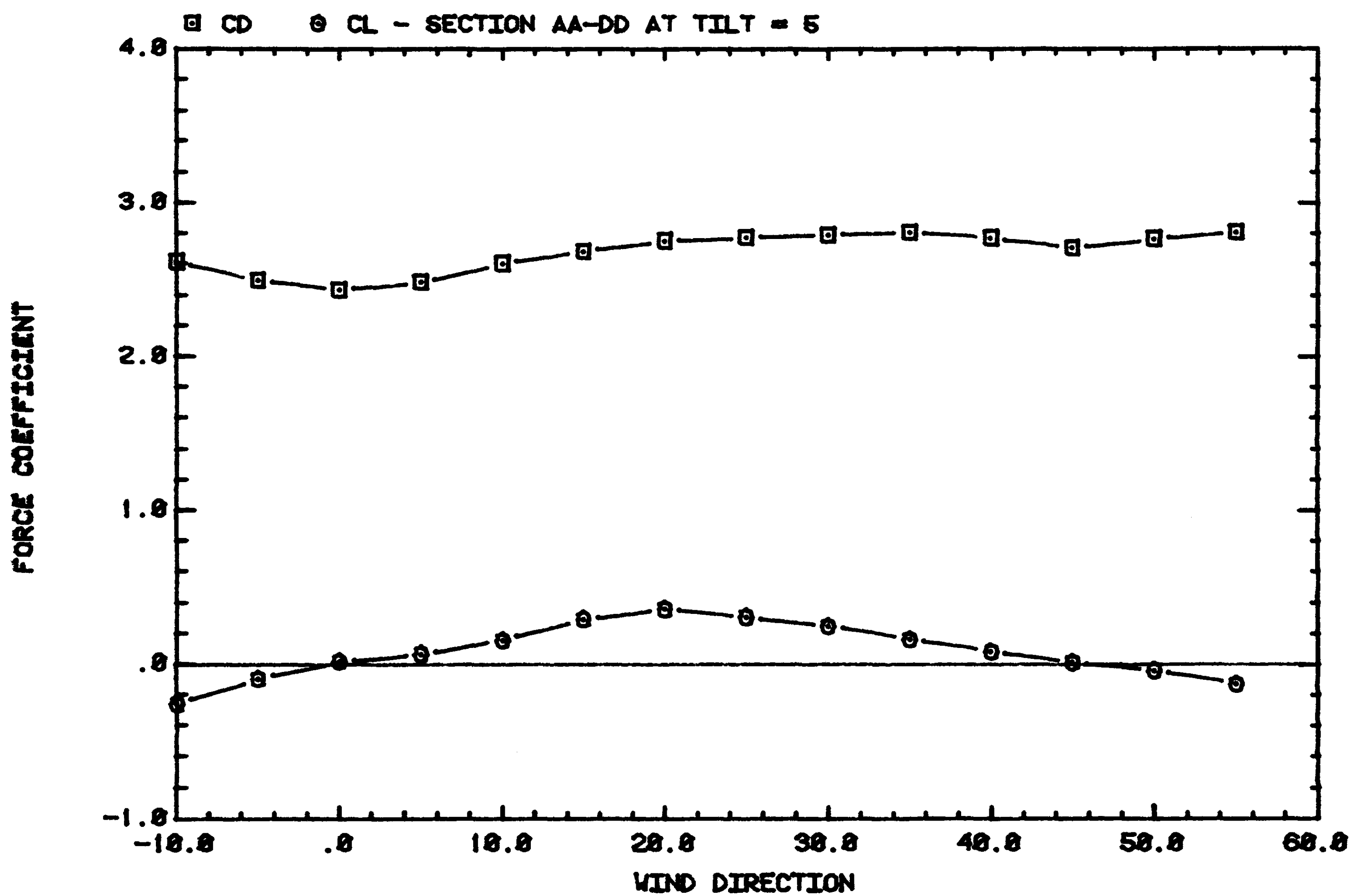

WIND LOADS ON TOWER SECTION

Figure 34. Wind Loads on the Tower Section AA-DD at Tilt Angle of 5°

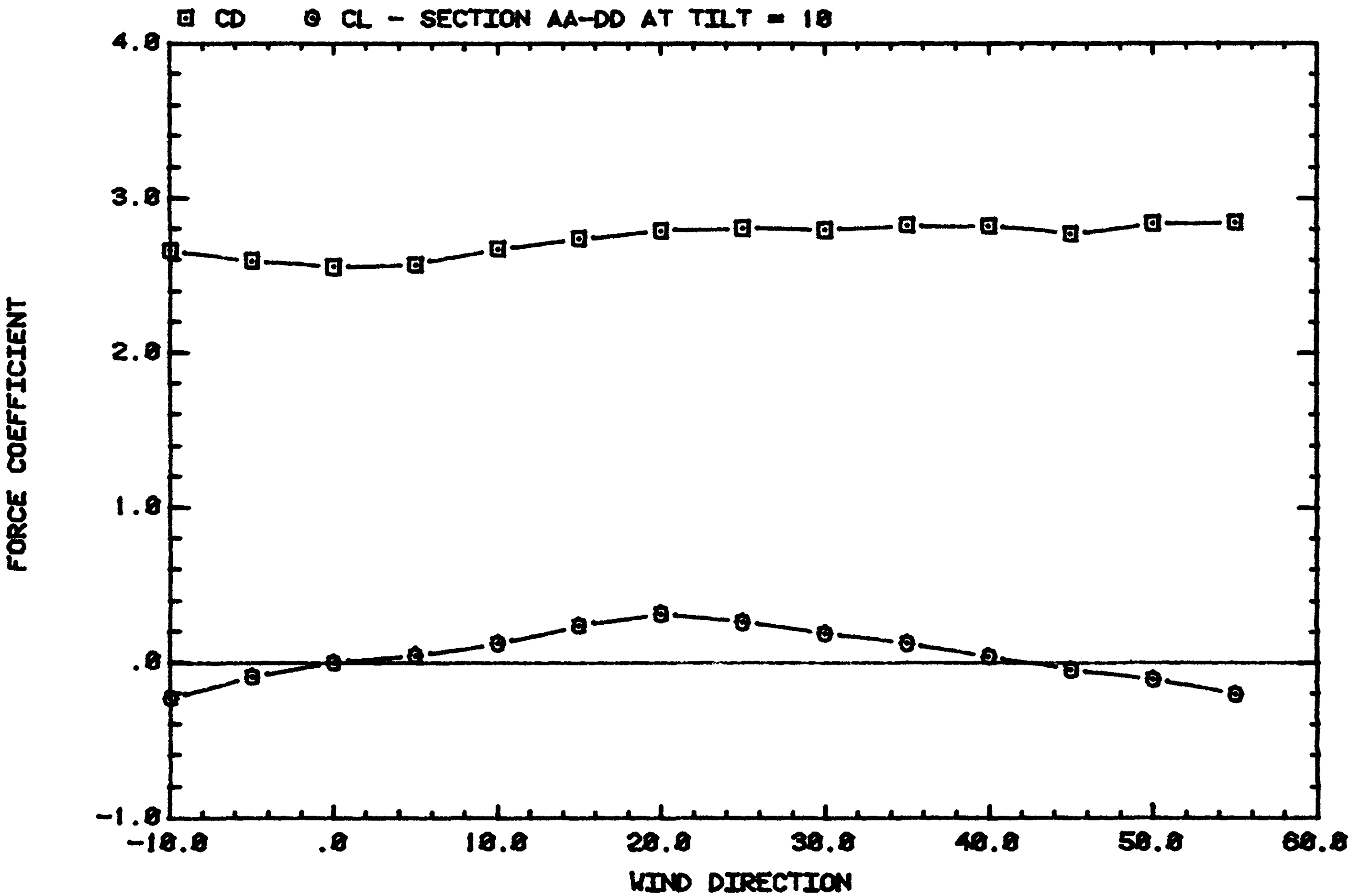

WIND LOADS ON TOWER SECTION

Figure 35. Wind Loads on the Tower Section AA-DD at Tilt Angle of 10°

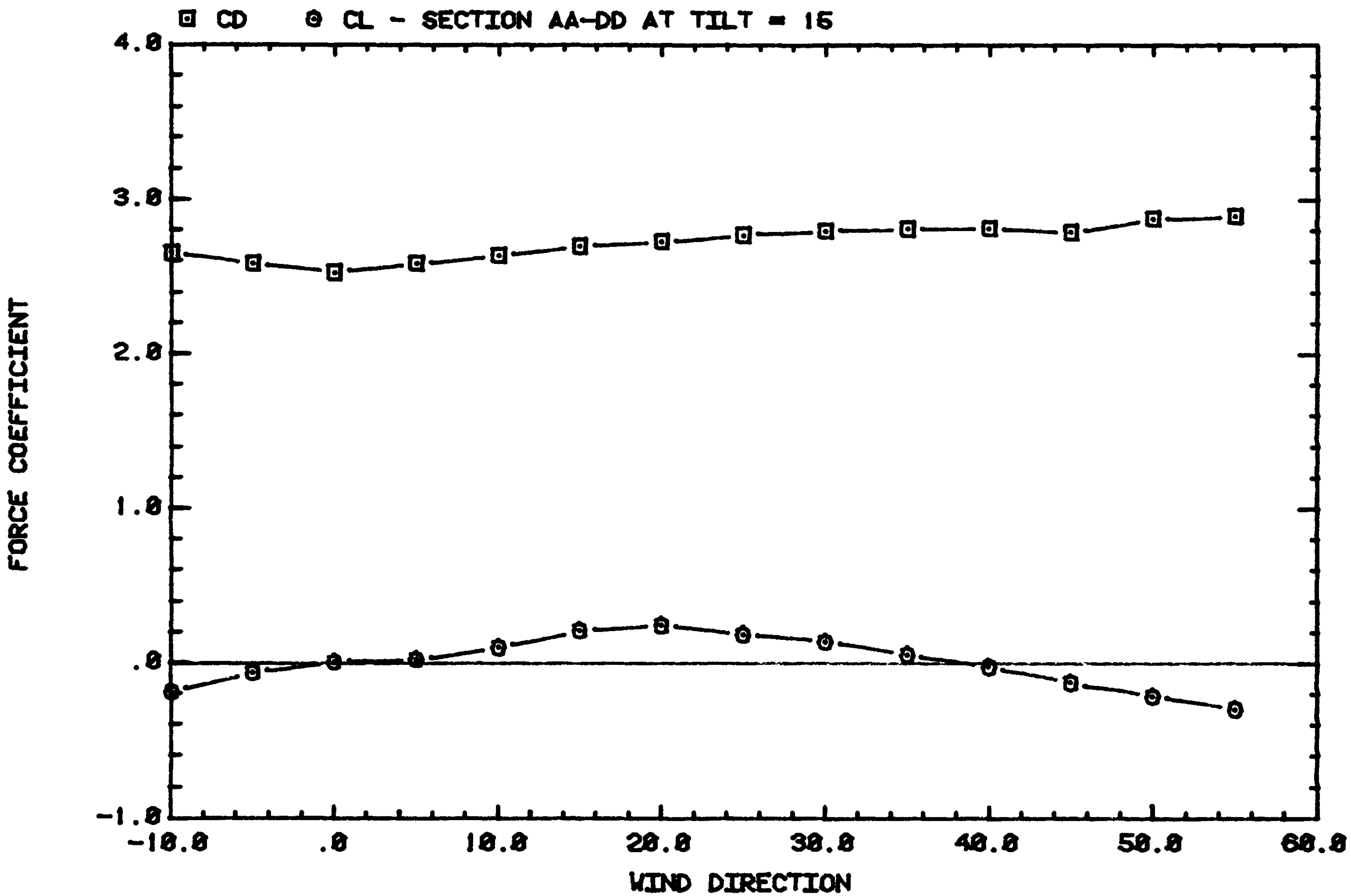

WIND LOADS ON TOWER SECTION

Figure 36. Wind Loads on the Tower Section AA-DD at Tilt Angle of 15°

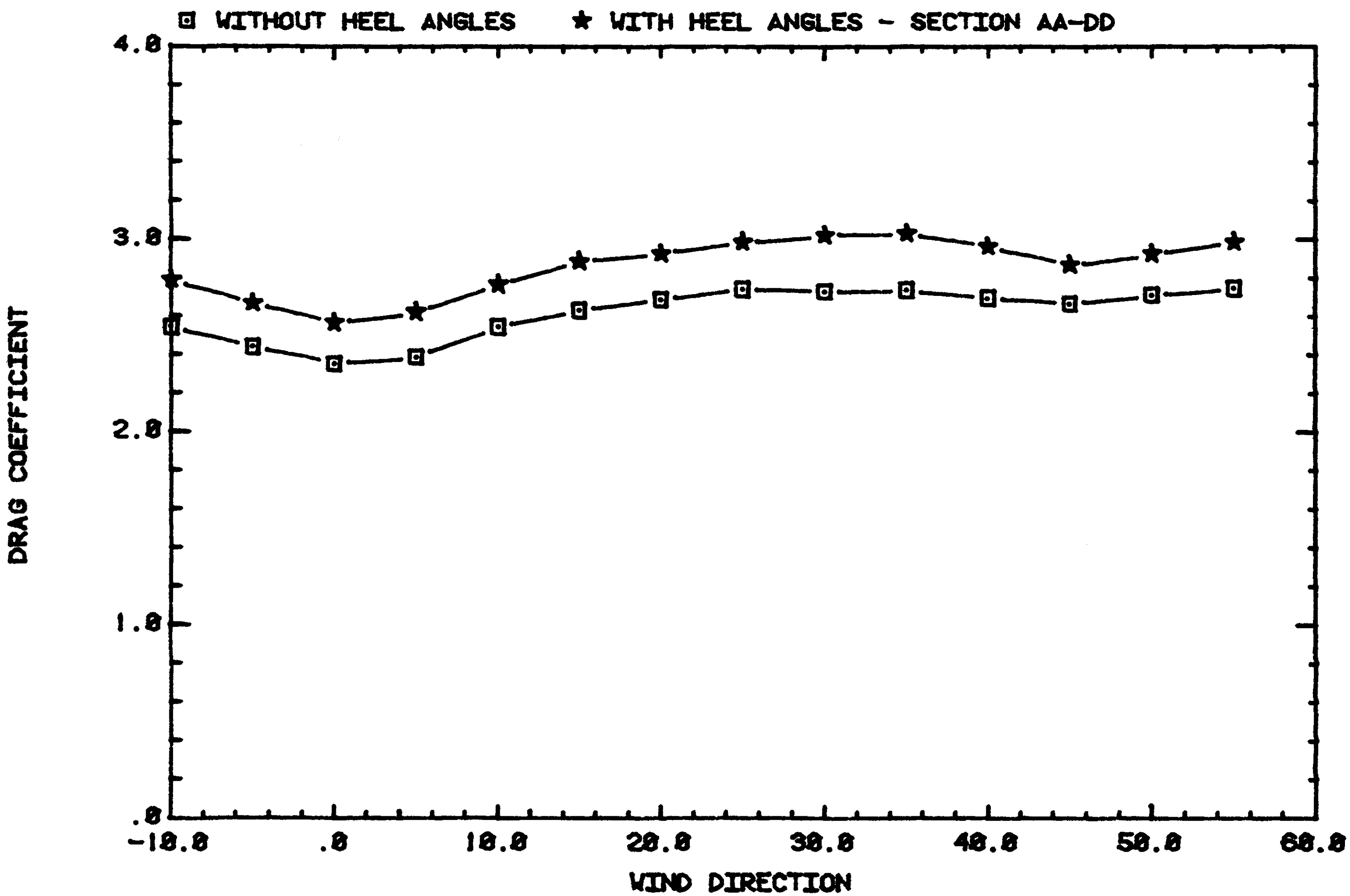

DRAG ON TOWER SECTION

Figure 37. Effects of Heel Angles on the Drag of the Tower Section AA-DD

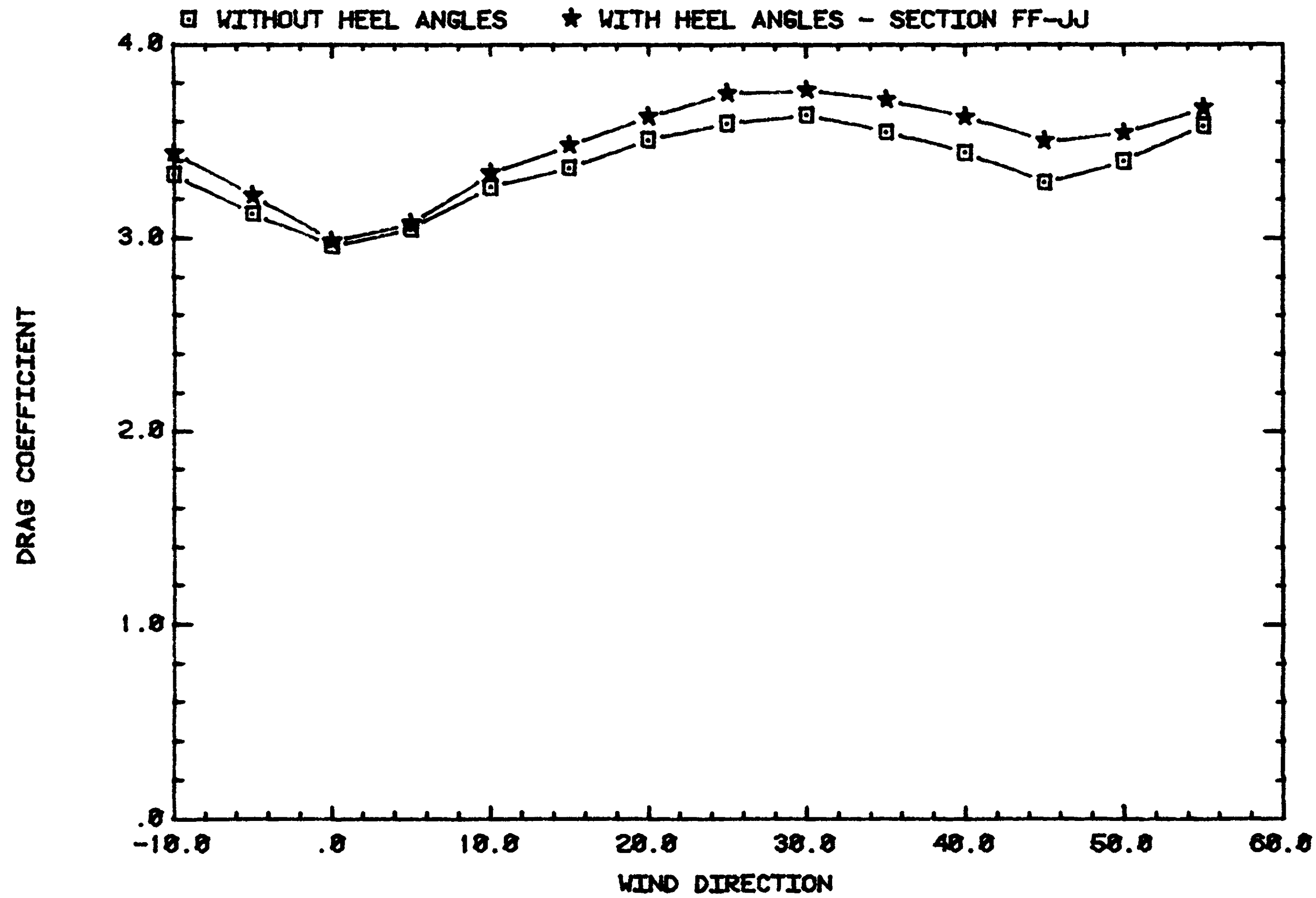

DRAG ON TOWER SECTION

Figure 38. Effects of Heel Angles on the Drag of the Tower Section FF-JJ

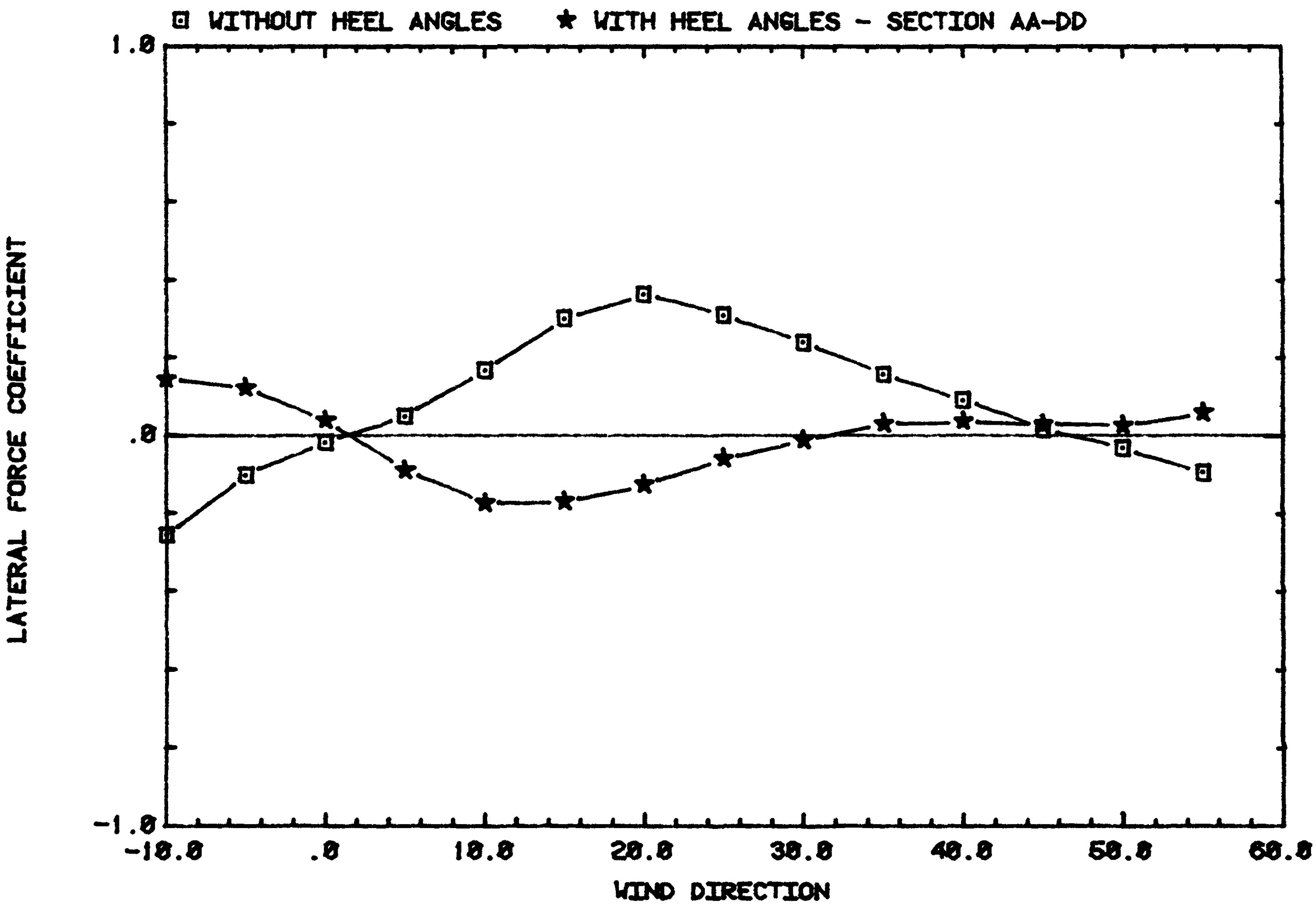

LATERAL FORCE ON TOWER SECTION

Figure 39. Effects of Heel Angles on the Lateral Force of the Tower Section AA-DD

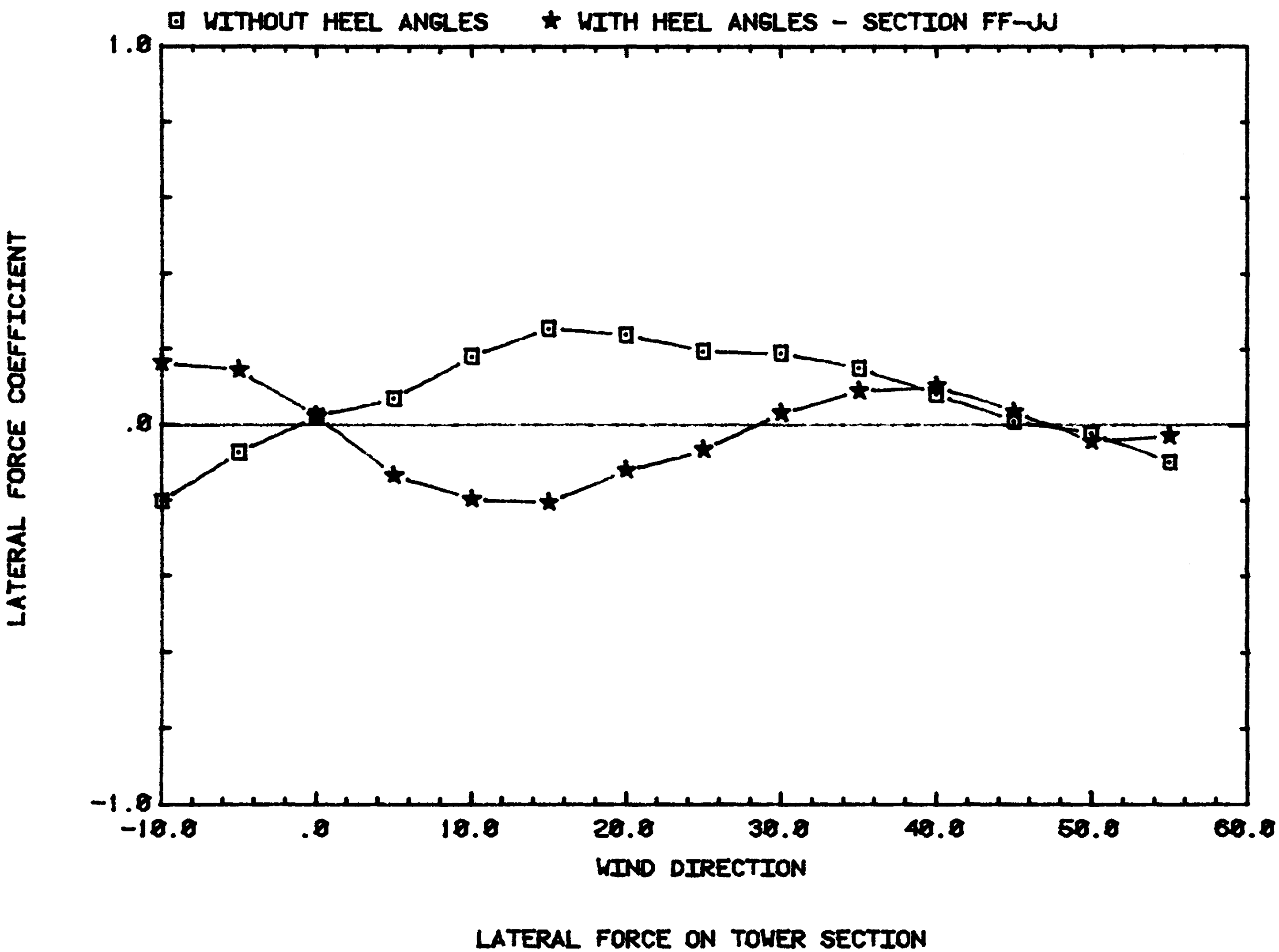

Figure 40. Effects of Heel Angles on the Lateral Force of the Tower Section FF-JJ.

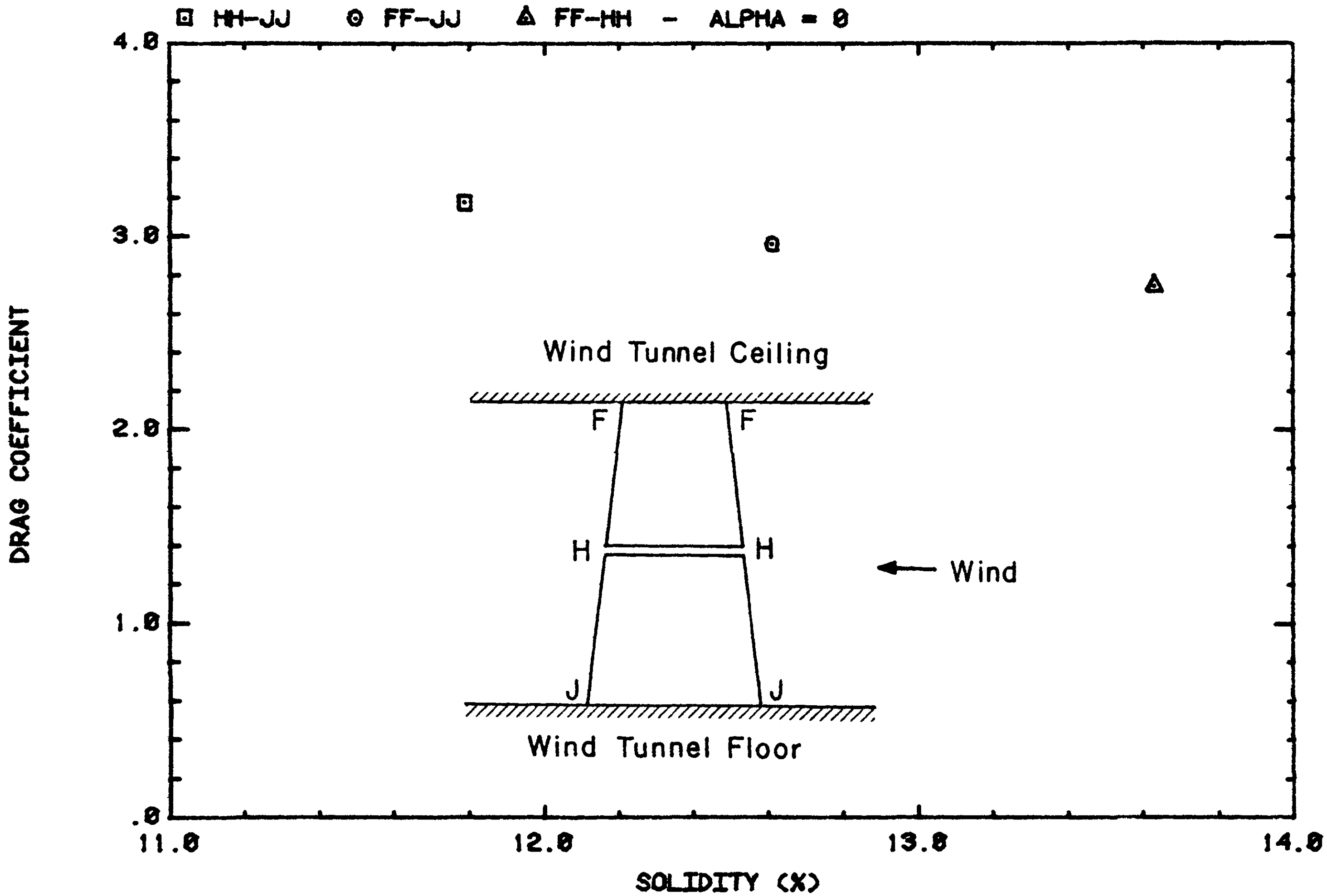

DRAG ON VARIOUS TOWER SECTIONS

Figure 41a. Effects of Solidity Ratio on the Drag of the Tower Sections

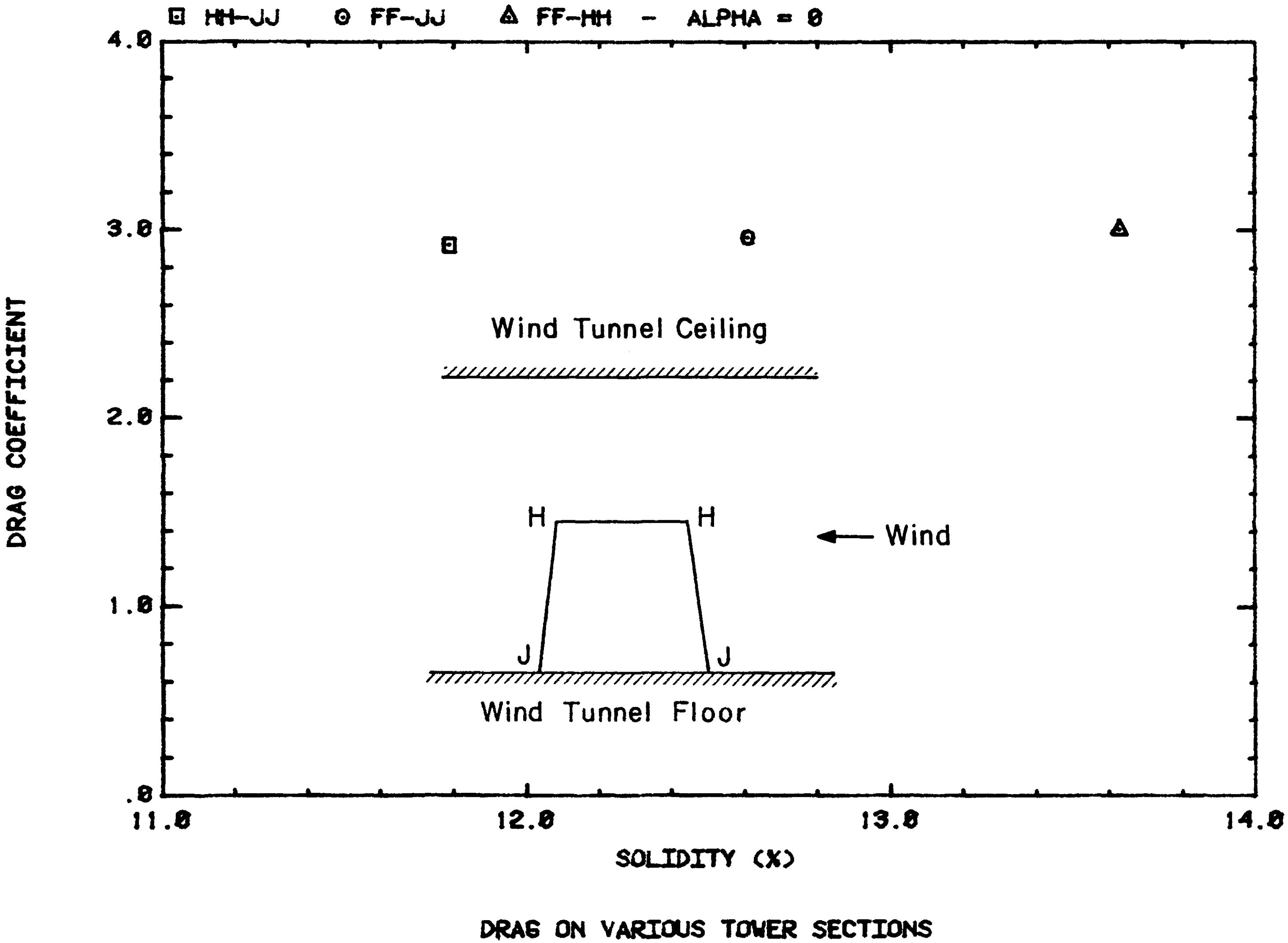

Figure 41b. Effects of Solidity Ratio on the Drag of the Tower Sections

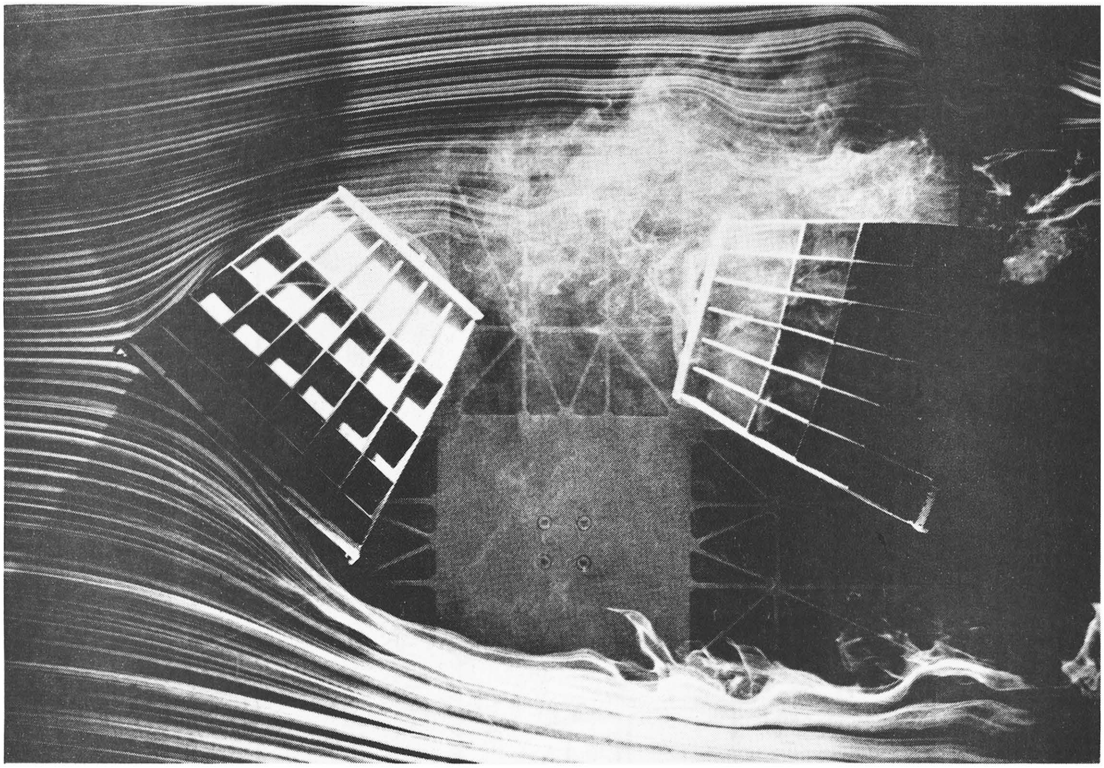

α=0°

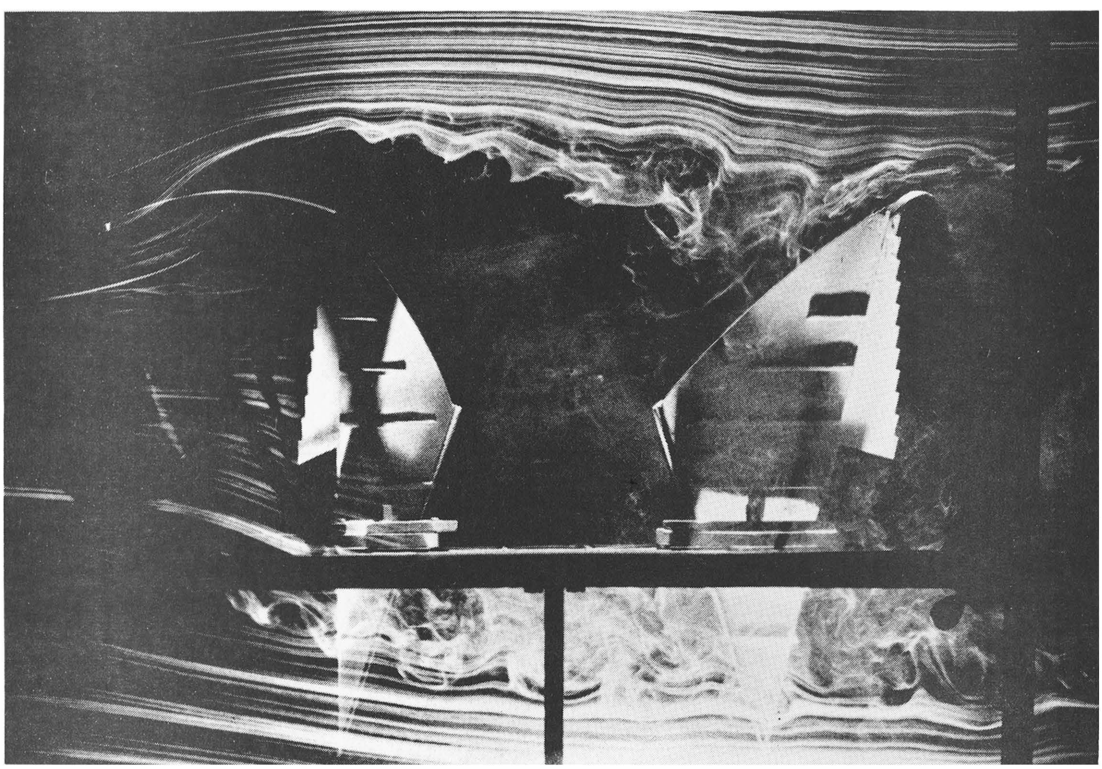

α=0°

Figure 42a. Flow Around the Two Pyramidal Horn Antennas

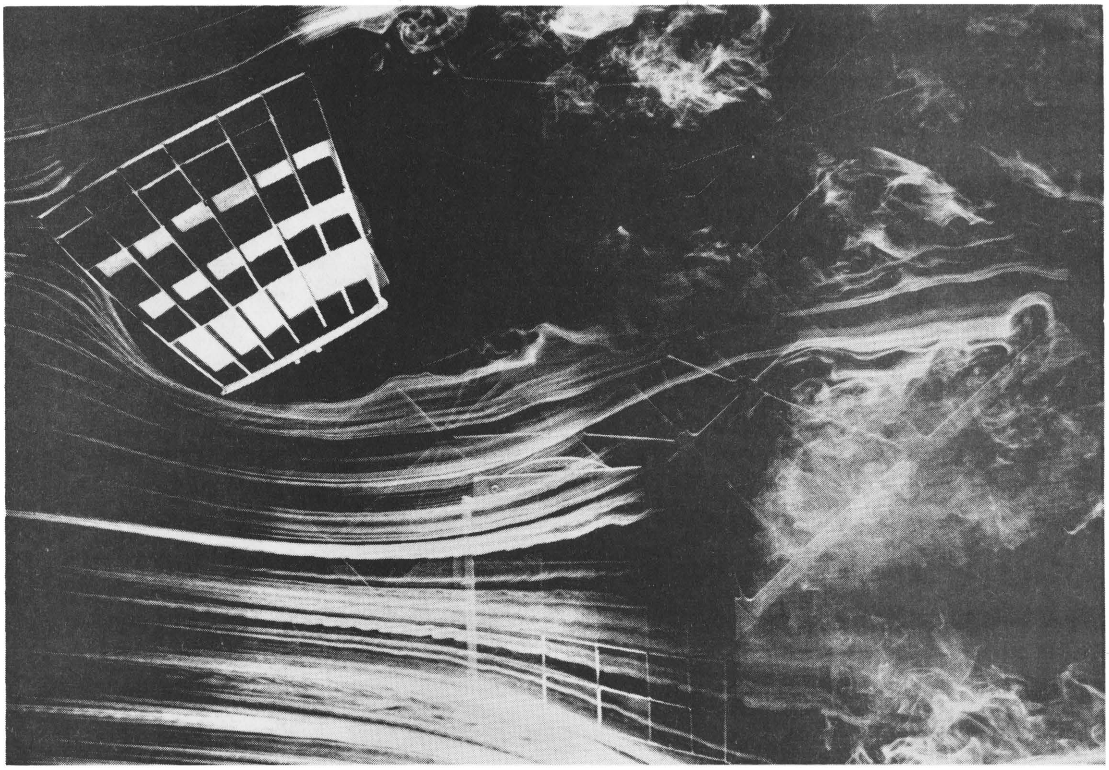

α=145°

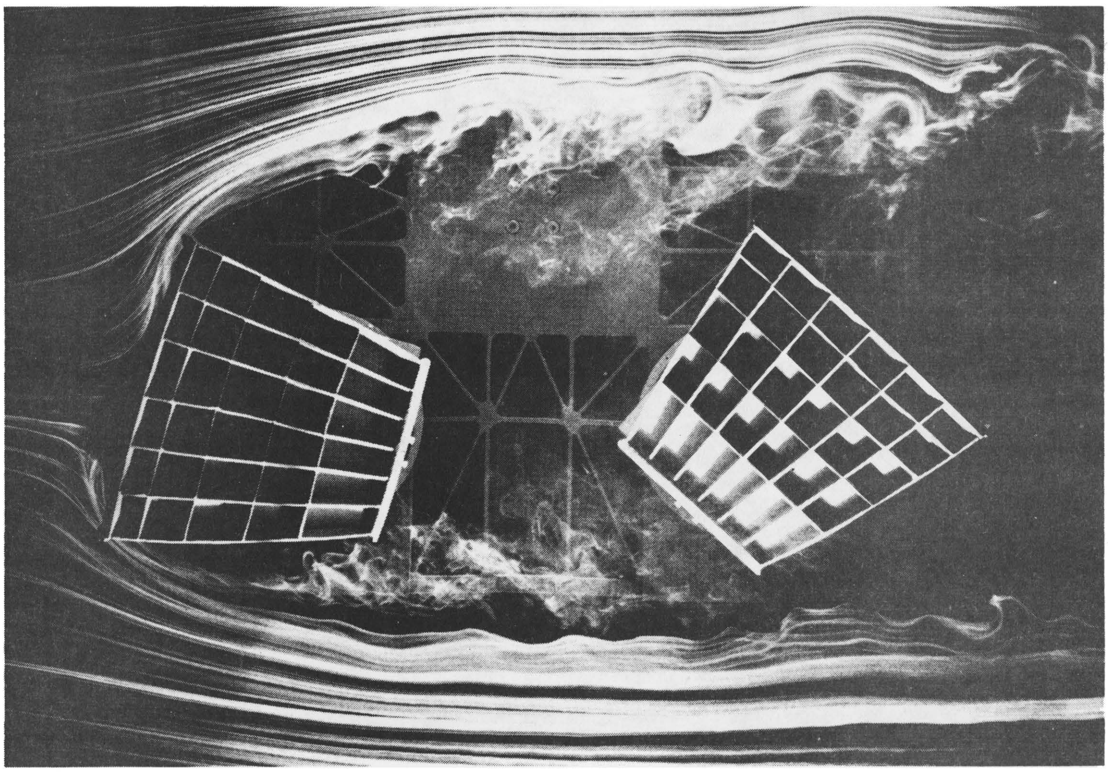

α=180°

Figure 42b. Flow Around the Two Pyramidal Horn Antennas

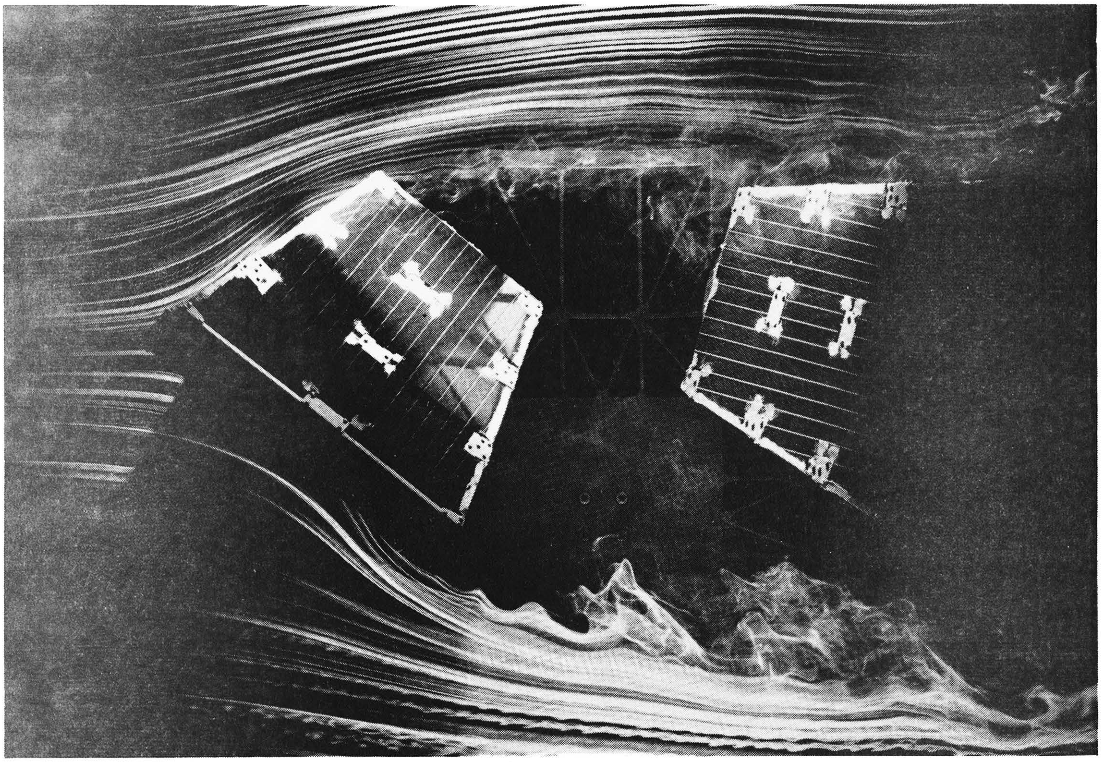

α=0°

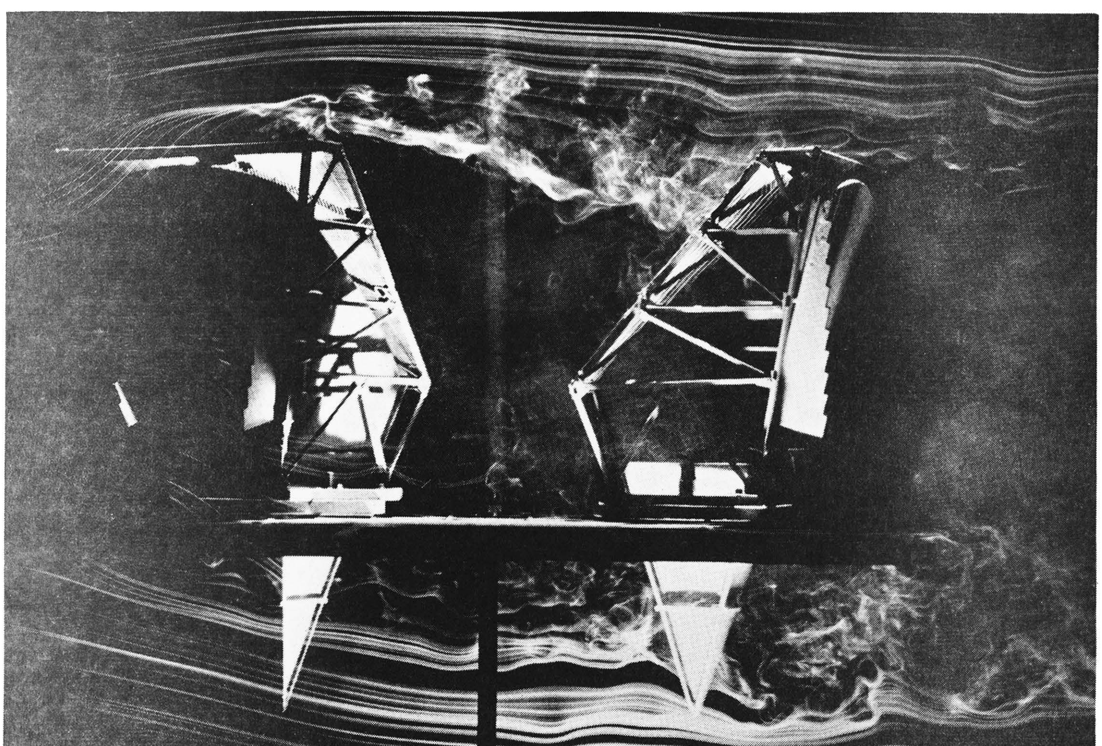

α=0°

Figure 43a. Flow Around the Two Pyramidal Horn Antennas with Ice Protection Canopies

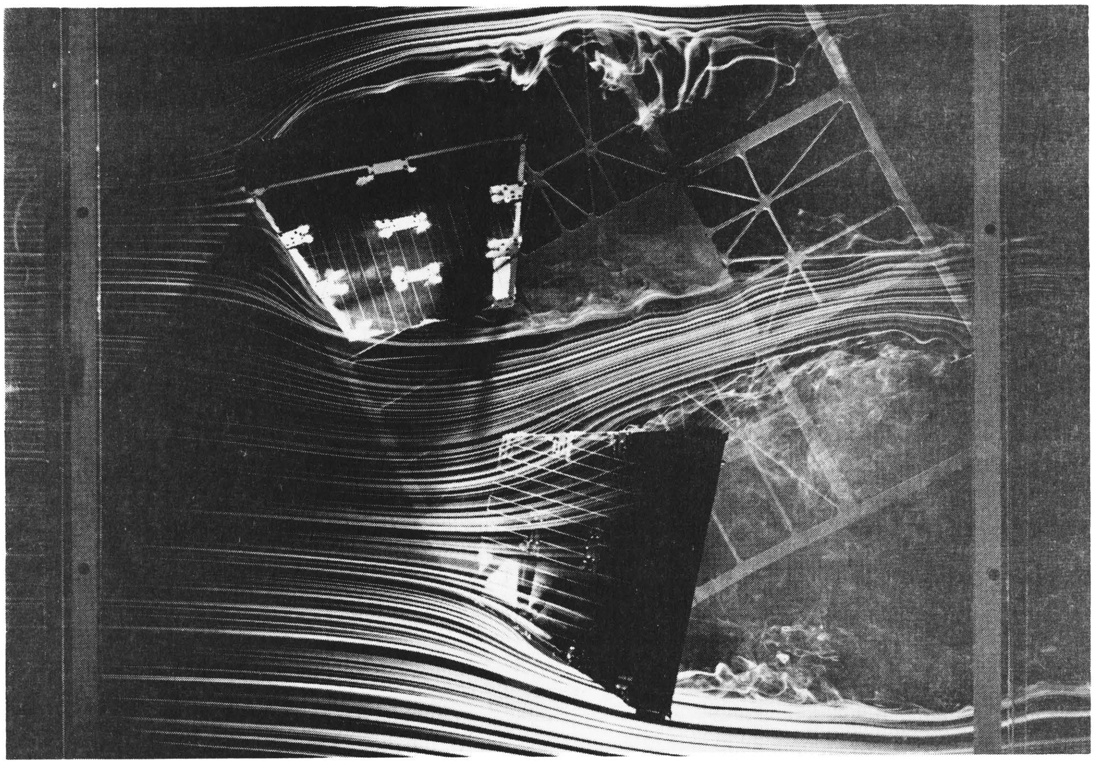

α=125°

α=180°

Figure 43b. Flow Around the Two Pyramidal Horn Antennas with Ice Protection Canopies

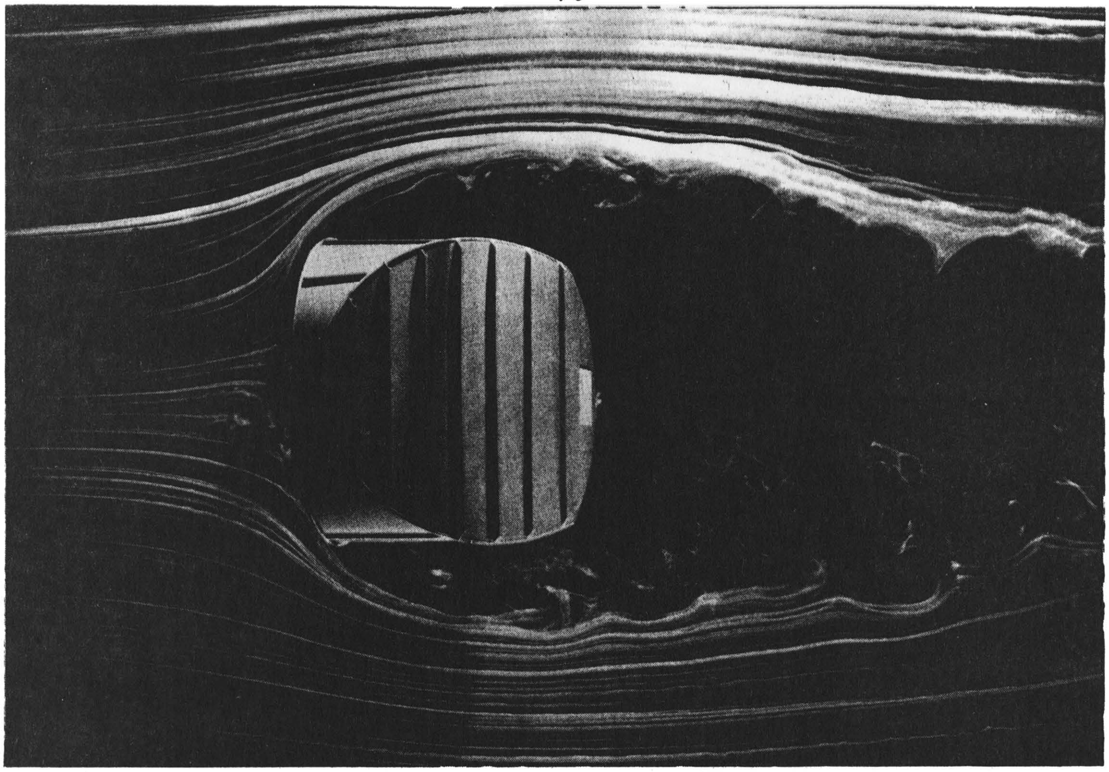

α=0°

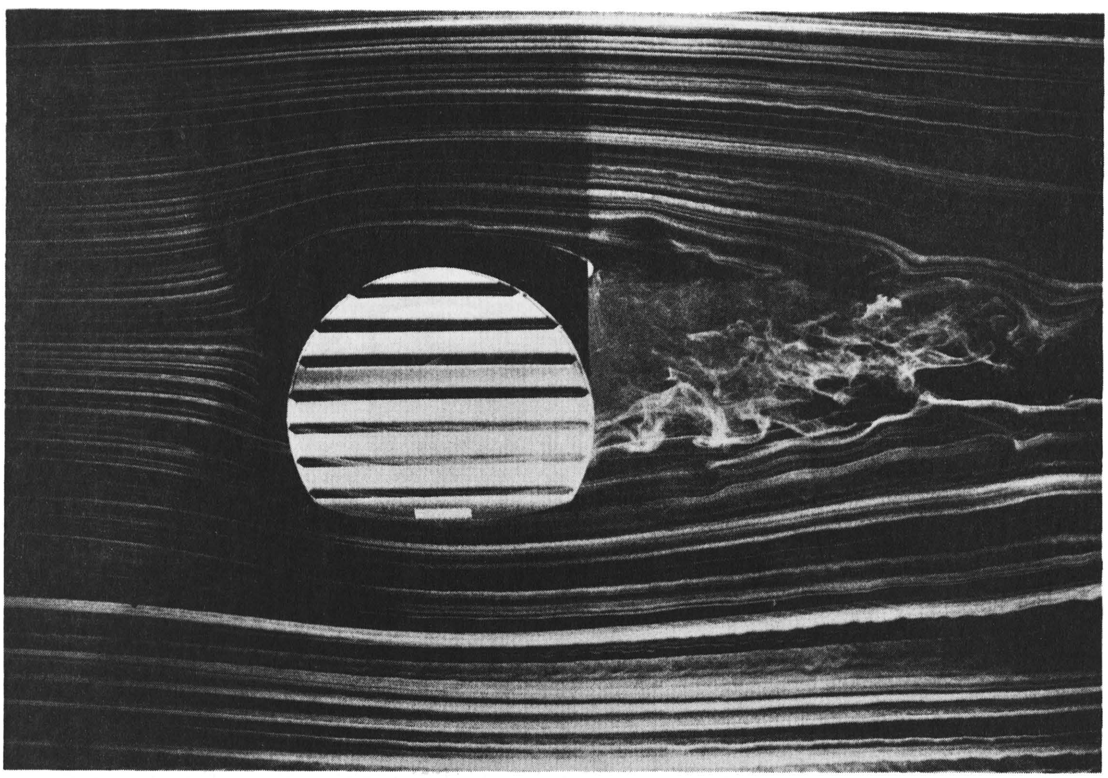

α=90°

Figure 44a. Flow Around the Conical Horn Antenna - GABRIEL UHR10 D

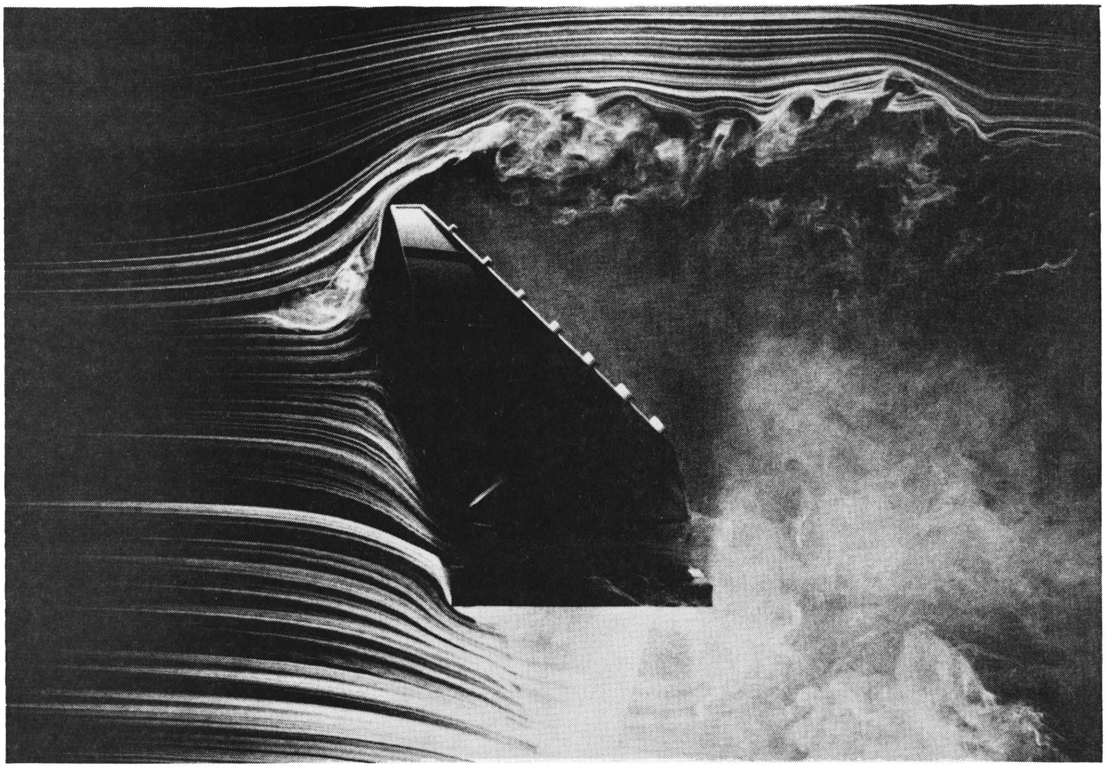

α=0°

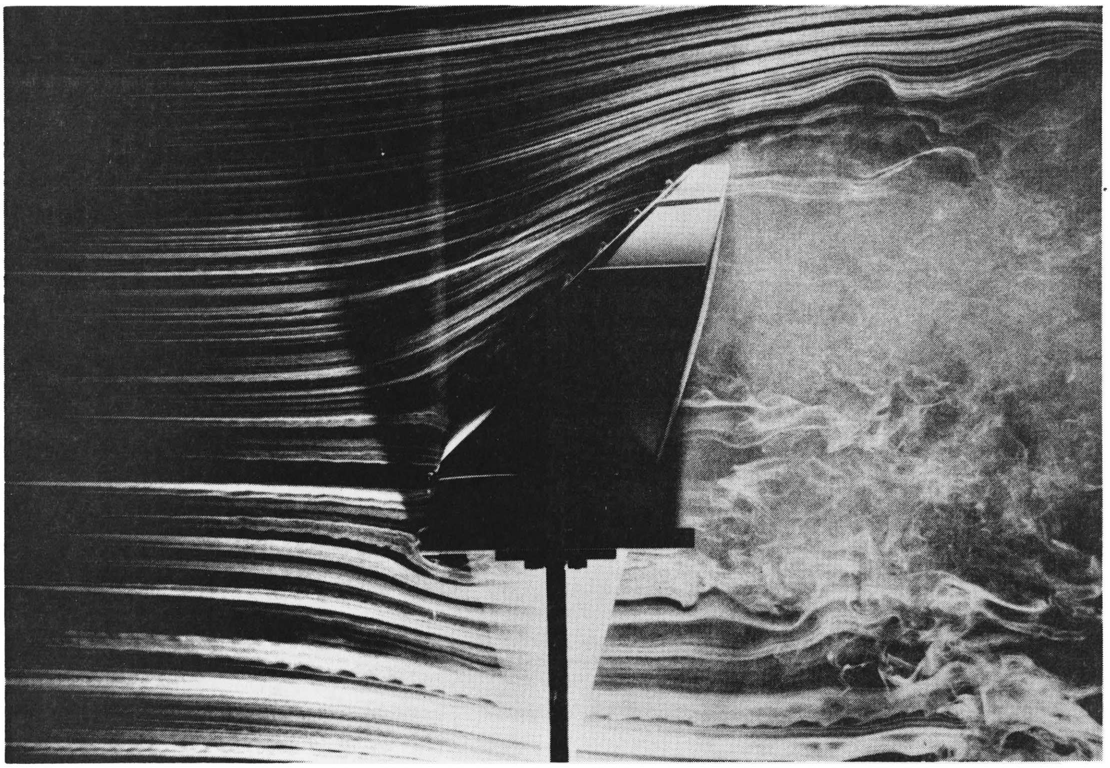

α=180°

Figure 44b. Flow Around the Conical Horn Antenna - GABRIEL UHR10 D

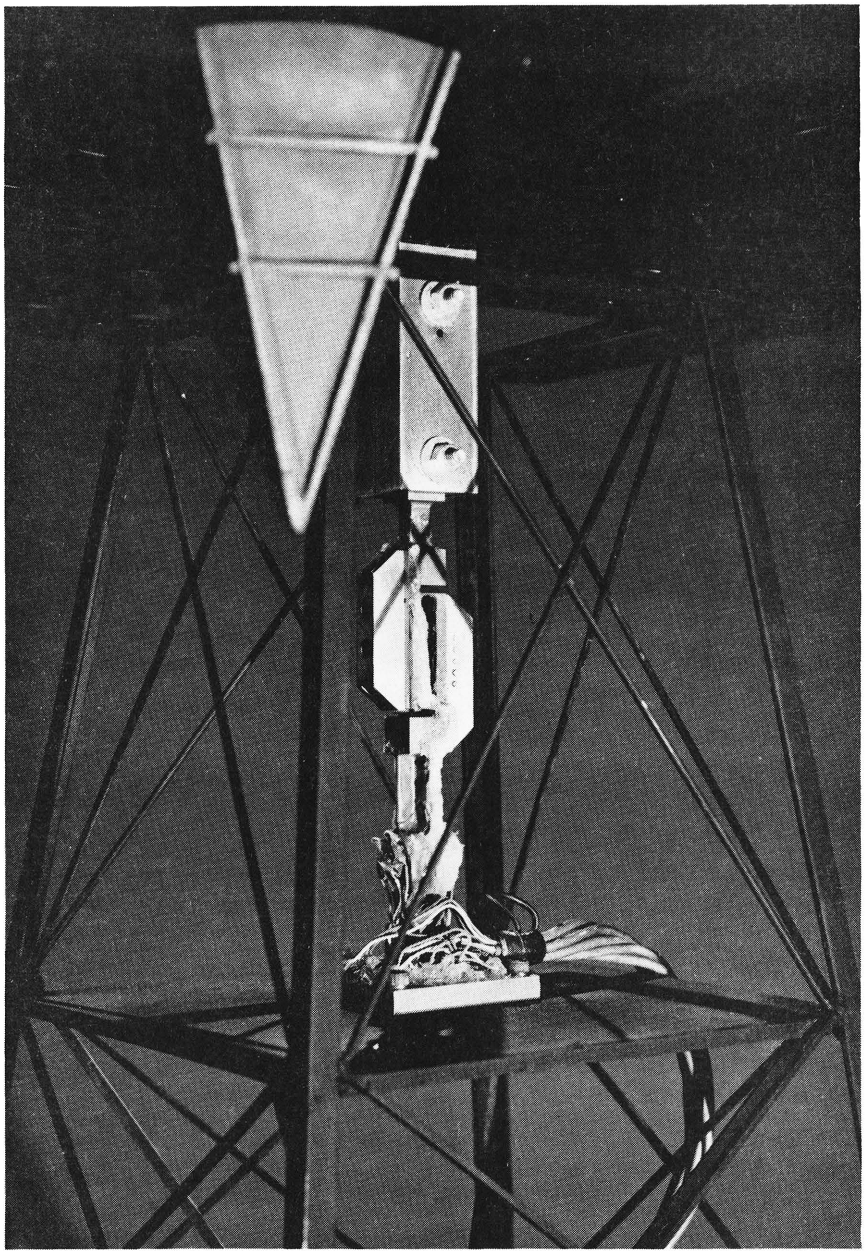

Figure 45. Force Balance Setup for Horn Antenna Tests

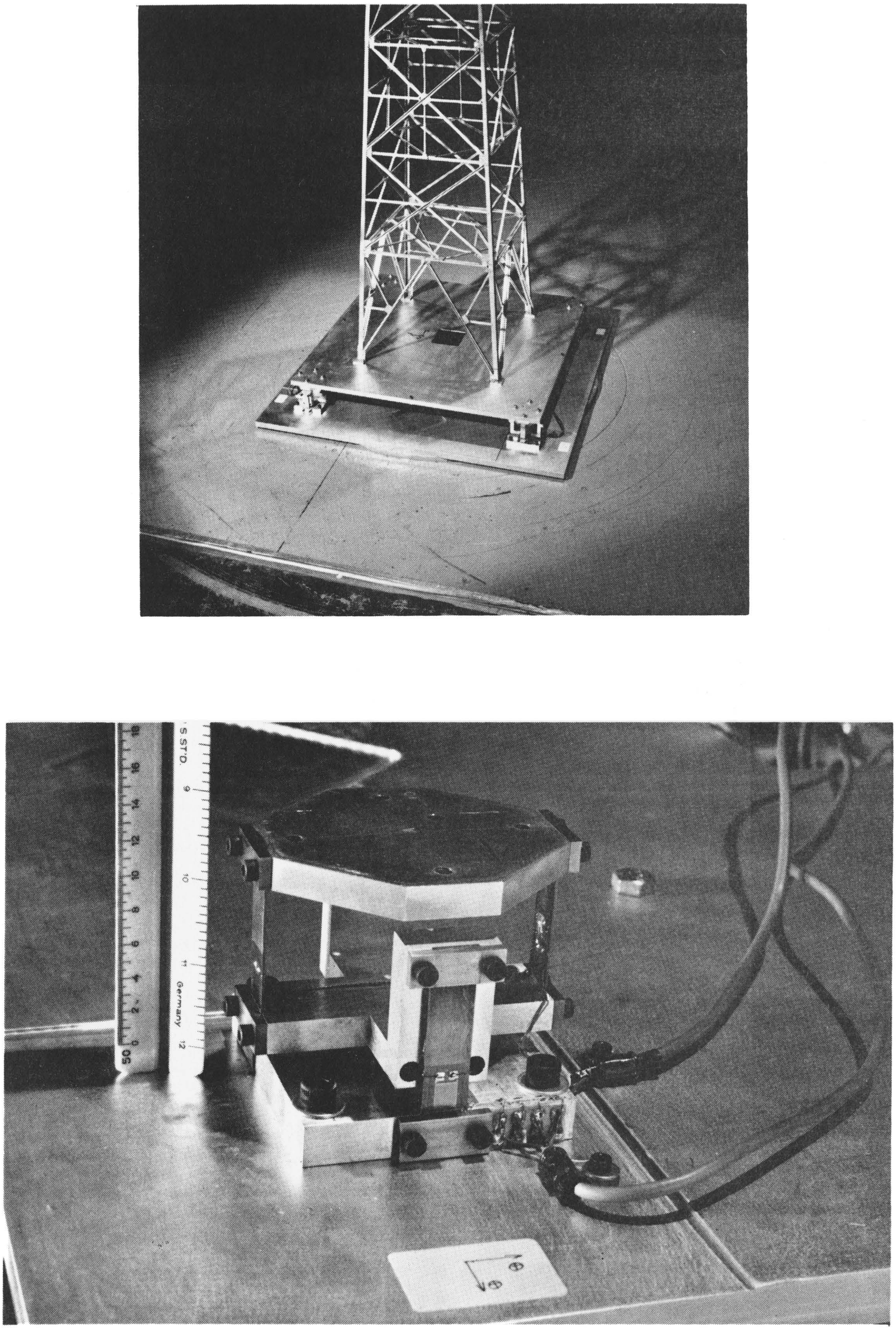

Figure 46. Force Balance Setup for Tower Section Tests

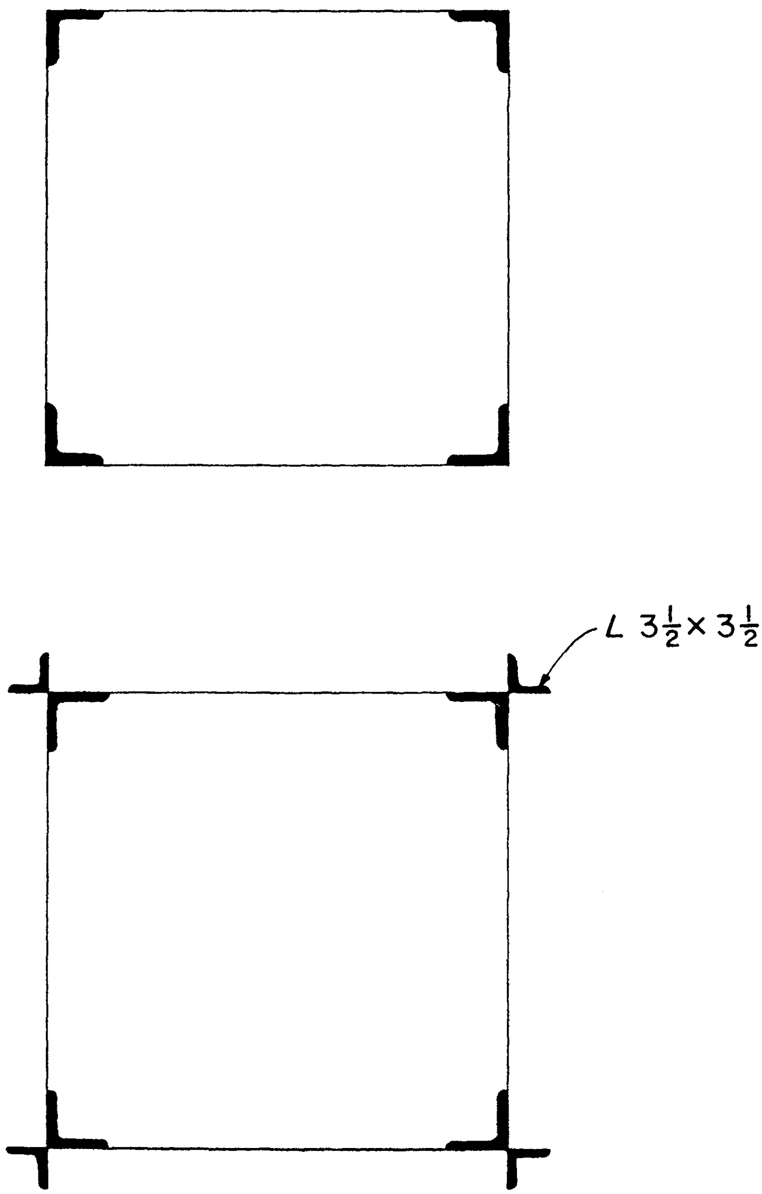

Figure 47. Tower Section Without and With Heel Angles

TABLES

Table 1. Wind Loads on the Two Pyramidal Horn Antennas

*** NORMALIZED FORCES AND MOMENTS ON THE AT&T MICROWAVE HORN ANTENNA ***

TWO PYRAMIDAL HORN ANTENNAS

WIND	CD	CL	CMR	CMP	CMY	AREA(SQ.FT)	YD(FT)
0.0	.951	.231	-.244	.678	-.793	170.6	7.1
10.0	.801	.117	-.235	.525	-.608	208.1	6.5
20.0	.821	-.010	-.321	.438	-.524	245.6	5.3
30.0	.797	-.170	-.345	.369	-.403	253.4	4.6
40.0	.873	-.158	-.324	.379	-.498	242.1	4.3
50.0	.832	-.039	-.313	.322	-.555	263.5	3.9
60.0	.835	-.022	-.203	.172	-.382	275.6	2.1
70.0	.845	-.048	-.073	.071	-.224	279.7	.8
80.0	.854	.061	.031	.063	-.116	275.5	.7
90.0	.888	.050	.117	.041	.005	263.2	.5
100.0	.898	-.013	.206	.094	.157	248.8	1.0
110.0	.891	.073	.250	.102	.188	246.1	1.1
120.0	.818	.007	.393	.212	.234	257.7	2.6
130.0	.934	-.076	.524	.429	.355	260.9	4.6
140.0	.940	-.018	.497	.573	.489	282.9	6.1
150.0	.916	-.010	.410	.599	.595	287.3	6.5
160.0	.976	.032	.348	.627	.805	254.8	6.4
170.0	.938	-.011	.257	.552	.993	206.2	5.9
180.0	.914	-.297	.150	.386	.941	170.6	4.2
190.0	.938	-.143	.129	.462	.646	208.1	4.9
200.0	.940	-.121	.072	.428	.446	245.6	4.6
210.0	.951	.040	-.019	.491	.478	253.4	5.2
220.0	1.029	.154	-.106	.595	.631	242.1	5.8
230.0	.976	.258	-.181	.612	.700	263.5	6.3
240.0	.962	.225	-.191	.636	.585	275.6	6.6
250.0	.999	.097	-.114	.645	.350	279.7	6.5
260.0	.999	-.069	.002	.580	.080	275.5	5.8
270.0	1.008	-.200	.157	.551	-.190	263.2	5.5
280.0	1.051	-.239	.172	.615	-.381	248.8	5.8
290.0	1.049	-.130	.067	.625	-.394	246.1	6.0
300.0	.959	-.007	-.085	.536	-.350	257.7	5.6
310.0	.922	.179	-.146	.519	-.387	260.9	5.6
320.0	.835	240	-.173	.468	-.398	282.9	5.6
330.0	.783	341	-.181	.431	-.433	287.3	5.5
340.0	712	337	-.204	.432	-.518	254.8	6.1
350.0	.773	.233	-.159	.542	-.706	206.2	7.0

Table 1. (Continued)

*** FULL SCALE WIND LOADS ON THE AT&T MICROWAVE HORN ANTENNA ***

TWO PYRAMIDAL HORN ANTENNAS

WIND	FD(LBS)	FL(LBS)	MR(FT-LBS)	MP(FT-LBS)	MY(FT-LBS)	AREA(SQ FT)	QREF(PSF)
0.0	423.2	102.8	-1084.9	3016.8	-3528.1	170.6	2.61
10.0	428.6	62.5	-1255.3	2805.6	-3252.5	208.1	2.57
20.0	531.3	-6.2	-2075.7	2832.4	-3390.0	245.6	2.63
30.0	546.3	-116.3	-2362.8	2527.9	-2761.3	253.4	2.70
40.0	554.4	-100.1	-2057.7	2407.7	-3161.1	242.1	2.62
50.0	586.7	-27.7	-2205.5	2268.7	-3913.9	263.5	2.68
60.0	625.5	-16.6	-1518.3	1285.0	-2859.1	275.6	2.72
70.0	632.1	-35.7	-544.9	527.5	-1675.5	279.7	2.67
80.0	607.2	43.2	221.0	445.6	-827.2	275.5	2.58
90.0	616.6	34.8	811.4	282.9	33.3	263.2	2.64
100.0	602.5	-8.5	1385.1	632.0	1050.6	248.8	2.70
110.0	580.4	47.9	1631.3	662.3	1226.7	246.1	2.65
120.0	558.6	5.0	2680.7	1446.2	1596.6	257.7	2.65
130.0	646.4	-52.9	3624.9	2965.2	2455.0	260.9	2.65
140.0	706.4	-13.9	3732.1	4306.8	3674.6	282.9	2.66
150.0	693.2	-7.8	3102.7	4535.2	4507.6	287.3	2.63
160.0	655.8	21.2	2341.3	4210.4	5412.1	254.8	2.64
170.0	514.2	-5.8	1407.3	3027.6	5446.3	206.2	2.66
180.0	415.6	-134.8	680.3	1751.9	4278.2	170.6	2.66
190.0	523.2	-79.7	718.3	2576.0	3604.2	208.1	2.68
200.0	620.9	-80.2	478.5	2831.0	2945.7	245.6	2.69
210.0	650.3	27.4	-132.1	3355.2	3270.6	253.4	2.70
220.0	673.9	101.1	-694.4	3894.2	4134.7	242.1	2.71
230.0	701.6	185.3	-1304.2	4403.4	5036.1	263.5	2.73
240.0	715.7	167.2	-1424.8	4729.8	4354.3	275.6	2.70
250.0	745.8	72.5	-849.6	4817.9	2612.0	279.7	2.67
260.0	746.9	-51.7	16.4	4339.5	600.3	275.5	2.71
270.0	714.1	-141.7	1111.4	3902.6	-1344.5	263.2	2.69
280.0	703.8	-160.0	1154.4	4114.7	-2547.8	248.8	2.69
290.0	697.4	-86.1	442.4	4153.1	-2616.4	246.1	2.70
300.0	668.4	-5.0	-589.8	3736.0	-2439.9	257.7	2.70
310.0	639.7	124.4	-1015.0	3599.7	-2684.8	260.9	2.66
320.0	628.1	180.7	-1299.7	3520.9	-2990.8	282.9	2.66
330.0	594.8	258.9	-1378.5	3276.4	-3286.9	287.3	2.64
340.0	478.7	226.1	-1372.1	2900.1	-3478.2	254.8	2.64
350.0	420.1	126.7	-864.8	2945.0	-3836.1	206.2	2.64

Table 2. Wind Loads on the Two Pyramidal Horn Antennas with Bottom Edge Blinders

*** NORMALIZED FORCES AND MOMENTS ON THE AT&T MICROWAVE HORN ANTENNA ***

TWO PYRAMIDAL HORN ANTENNAS WITH BOTTOM EDGE BLINDERS

WIND	CD	CL	CMR	CMP	CMY	AREA(SQ FT)	YD(FT)
0.0	.984	.222	-.266	.565	-.780	170.6	5.7
10.0	.828	.122	-.213	.389	-.549	208.1	4.7
20.0	.793	-.008	-.282	.349	-.439	245.6	4.4
30.0	.794	-.135	-.356	.351	-.380	253.4	4.4
40.0	.855	-.100	-.354	.385	-.506	242.1	4.5
50.0	.801	.029	-.348	.329	-.583	263.5	4.1
60.0	.829	.016	-.218	.161	-.413	275.6	1.9
70.0	.875	-.011	-.071	.050	-.231	279.7	.6
80.0	.873	.064	.041	.045	-.119	275.5	.5
90.0	.913	.040	.125	.019	.004	263.2	.2
100.0	.912	-.006	.225	.073	.155	248.8	.8
110.0	.930	.048	.273	.104	.165	246.1	1.1
120.0	.852	-.036	.397	.217	.208	257.7	2.6
130.0	.960	-.084	.506	.400	.327	260.9	4.2
140.0	.947	-.010	.482	.529	.468	282.9	5.6
150.0	.926	-.016	.423	.553	.576	287.3	6.0
160.0	.986	.026	.368	.573	.785	254.8	5.8
170.0	.951	-.018	.273	.482	.966	206.2	5.1
180.0	.960	-.220	.165	.359	.964	170.6	3.7
190.0	1.017	-.129	.094	.438	.687	208.1	4.3
200.0	1.017	-.110	.037	.411	.489	245.6	4.0
210.0	1.007	.020	-.017	.477	.526	253.4	4.7
220.0	1.106	.146	-.099	.541	.668	242.1	4.9
230.0	1.054	.239	-.163	.561	.741	263.5	5.3
240.0	1.030	.261	-.171	.611	.622	275.6	5.9
250.0	1.046	.137	-.092	.613	.380	279.7	5.9
260.0	1.053	-.041	.040	.571	.083	275.5	5.4
270.0	1.079	-.216	.174	.563	-.195	263.2	5.2
280.0	1.143	-.198	.185	.614	-.383	248.8	5.4
290.0	1.127	-.031	.080	.624	-.392	246.1	5.5
300.0	.980	.069	-.098	.517	-.348	257.7	5.3
310.0	.959	.212	-.169	.482	-.363	260.9	5.0
320.0	.859	.319	-.219	.416	-.397	282.9	4.8
330.0	.790	.363	-.211	.374	-.448	287.3	4.7
340.0	.737	.259	-.218	.325	-.551	254.8	4.4
350.0	.795	.273	-.193	.413	-.690	206.2	5.2

Table 2. (Continued)

*** FULL SCALE WIND LOADS ON THE AT&T MICROWAVE HORN ANTENNA ***

TWO PYRAMIDAL HORN ANTENNAS WITH BOTTOM EDGE BLINDERS

WIND	FD(LBS)	FL(LBS)	MR(FT-LBS)	MP(FT-LBS)	MY(FT-LBS)	AREA(SQ.FT)	QREF(PSF)
0.0	447.7	101.1	-1210.9	2571.1	-3545.6	170.6	2.67
10.0	449.6	66.5	-1158.9	2114.6	-2982.0	208.1	2.61
20.0	511.1	-4.9	-1820.2	2248.7	-2831.5	245.6	2.62
30.0	525.8	-89.2	-2358.5	2327.1	-2515.8	253.4	2.61
40.0	544.5	-63.8	-2253.6	2450.5	-3223.0	242.1	2.63
50.0	548.7	19.8	-2386.8	2256.0	-3997.9	263.5	2.60
60.0	589.5	11.1	-1549.6	1146.0	-2933.8	275.6	2.58
70.0	635.5	-7.8	-519.1	362.0	-1678.1	279.7	2.60
80.0	622.6	46.0	290.7	318.1	-850.6	275.5	2.59
90.0	628.9	27.4	862.9	133.9	26.0	263.2	2.62
100.0	599.0	-3.8	1476.1	481.2	1014.4	248.8	2.64
110.0	602.1	31.4	1764.7	675.2	1069.2	246.1	2.63
120.0	567.6	-24.1	2645.4	1448.9	1389.3	257.7	2.59
130.0	659.5	-57.5	3475.6	2746.7	2245.7	260.9	2.63
140.0	706.6	-7.7	3595.5	3949.3	3494.5	282.9	2.64
150.0	703.7	-12.5	3216.6	4204.1	4381.0	287.3	2.65
160.0	663.2	17.7	2472.6	3852.0	5280.8	254.8	2.64
170.0	519.9	-9.7	1494.7	2635.7	5279.3	206.2	2.65
180.0	437.7	-100.3	752.3	1633.9	4394.7	170.6	2.67
190.0	566.8	-72.1	526.3	2439.7	3832.4	208.1	2.68
200.0	673.6	-72.8	242.7	2720.8	3236.9	245.6	2.70
210.0	688.4	13.9	-91.4	3259.1	3594.2	253.4	2.70
220.0	723.4	95.2	-649.9	3538.3	4366.6	242.1	2.70
230.0	748.5	169.6	-1154.9	3985.7	5262.2	263.5	2.69
240.0	753.9	191.0	-1250.8	4471.4	4554.8	275.6	2.66
250.0	775.0	101.7	-681.4	4541.7	2815.4	279.7	2.65
260.0	768.7	-29.8	291.9	4167.0	607.3	275.5	2.65
270.0	752.3	-150.6	1214.9	3929.2	-1362.0	263.2	2.65
280.0	752.1	-130.0	1217.6	4038.6	-2522.0	248.8	2.64
290.0	733.0	-20.1	520.1	4057.1	-2545.6	246.1	2.64
300.0	660.8	46.2	-660.6	3485.6	-2344.8	257.7	2.62
310.0	648.3	143.1	-1141.3	3261.0	-2454.3	260.9	2.59
320.0	632.7	234.8	-1613.1	3063.6	-2926.5	282.9	2.60
330.0	588.5	270.7	-1570.2	2782.8	-3338.4	287.3	2.59
340.0	485.6	170.9	-1435.1	2142.4	-3629.8	254.8	2.59
350.0	423.9	145.3	-1030.4	2203.3	-3676.5	206.2	2.59

Table 3. Wind Loads on the Two Pyramidal Horn Antennas with Ice Protection Canopies

*** NORMALIZED FORCES AND MOMENTS ON THE AT&T MICROWAVE HORN ANTENNA ***

TWO PYRAMIDAL HORN ANTENNAS WITH ICE PROTECTION CANOPIES

WIND	CD	CL	CMR	CMP	CMY	AREA(SQ.FT)	YD(FT)
0.0	1.063	.177	-.197	1.063	-.994	170.6	10.0
10.0	.843	.091	-.174	.774	-.625	208.1	9.2
20.0	.817	.005	-.174	.556	-.576	245.6	6.8
30.0	.823	-.153	-.184	.506	-.468	253.4	6.2
40.0	.941	-.165	-.158	.491	-.550	242.1	5.2
50.0	.907	-.077	-.132	.415	-.547	263.5	4.6
60.0	.914	-.036	-.076	.334	-.408	275.6	3.7
70.0	.939	-.026	-.013	.289	-.263	279.7	3.1
80.0	.952	.053	.023	.282	-.140	275.5	3.0
90.0	.968	.042	-.006	.252	-.008	263.2	2.6
100.0	.952	.081	.001	.284	.127	248.8	3.0
110.0	.968	.112	.084	.288	.208	246.1	3.0
120.0	.919	.021	.296	.427	.284	257.7	4.6
130.0	1.021	-.046	.456	.677	.455	260.9	6.6
140.0	1.002	-.034	.430	.762	.603	282.9	7.6
150.0	.971	-.007	.336	.766	.722	287.3	7.9
160.0	.946	-.019	.252	.743	.880	254.8	7.8
170.0	.936	-.031	.217	.618	1.054	206.2	6.6
180.0	.889	-.233	.131	.513	.957	170.6	5.8
190.0	.922	-.169	.102	.566	.674	208.1	6.1
200.0	1.039	-.072	.027	.576	.538	245.6	5.5
210.0	1.063	.072	-.073	.601	.556	253.4	5.7
220.0	1.096	.207	-.183	.659	.669	242.1	6.0
230.0	1.057	.284	-.261	.612	.711	263.5	5.8
240.0	1.028	.272	-.207	.605	.575	275.6	5.9
250.0	1.045	.131	-.103	.605	.342	279.7	5.8
260.0	1.051	-.045	.009	.558	.058	275.5	5.3
270.0	1.091	-.250	.226	.556	-.237	263.2	5.1
280.0	1.170	-.339	.294	.674	-.474	248.8	5.8
290.0	1.166	-.226	.209	.757	-.507	246.1	6.5
300.0	1.040	-.032	.039	.698	-.434	257.7	6.7
310.0	1.008	.124	-.082	.634	-.439	260.9	6.3
320.0	.902	.235	-.134	.543	-.441	282.9	6.0
330.0	.849	.353	-.169	.484	-.483	287.3	5.7
340.0	.771	.357	-.170	.565	-.625	254.8	7.3
350.0	.890	.283	-.133	.869	-.896	206.2	9.8

Table 3. (Continued)

*** FULL SCALE WIND LOADS ON THE AT&T MICROWAVE HORN ANTENNA ***

TWO PYRAMIDAL HORN ANTENNAS WITH ICE PROTECTION CANOPIES

WIND	FD(LBS)	FL(LBS)	MR(FT-LBS)	MP(FT-LBS)	MY(FT-LBS)	AREA(SQ FT)	QREF(PSF)
0.0	432.8	71.9	-802.7	4327.8	-4047.5	170.6	2.39
10.0	422.4	45.7	-870.8	3877.1	-3130.2	208.1	2.41
20.0	485.5	3.0	-1034.8	3304.1	-3419.3	245.6	2.42
30.0	503.8	-93.6	-1126.5	3099.3	-2867.1	253.4	2.42
40.0	548.0	-96.4	-919.2	2861.2	-3204.9	242.1	2.41
50.0	573.8	-49.0	-834.7	2626.9	-3462.3	263.5	2.40
60.0	604.5	-23.7	-501.9	2209.6	-2696.0	275.6	2.40
70.0	629.1	-17.3	-89.4	1934.9	-1759.1	279.7	2.39
80.0	630.1	35.1	150.2	1869.0	-925.5	275.5	2.40
90.0	612.7	26.9	-39.1	1594.5	-51.3	263.2	2.41
100.0	571.7	48.4	7.8	1705.5	760.2	248.8	2.41
110.0	574.5	66.5	499.8	1710.2	1233.7	246.1	2.41
120.0	565.5	13.1	1822.1	2627.8	1747.7	257.7	2.39
130.0	635.2	-28.4	2838.8	4214.3	2831.5	260.9	2.38
140.0	679.5	-23.3	2915.1	5165.7	4087.0	282.9	2.40
150.0	665.9	-4.6	2304.0	5256.9	4951.3	287.3	2.39
160.0	576.8	-11.3	1533.6	4525.8	5362.2	254.8	2.39
170.0	460.6	-15.3	1069.2	3040.1	5183.7	206.2	2.39
180.0	366.5	-96.0	540.9	2114.7	3946.0	170.6	2.42
190.0	465.8	-85.6	516.1	2857.2	3406.0	208.1	2.43
200.0	622.0	-43.1	159.0	3447.2	3220.5	245.6	2.44
210.0	659.7	44.5	-451.0	3729.0	3451.1	253.4	2.45
220.0	648.9	122.5	-1084.3	3902.5	3957.9	242.1	2.44
230.0	680.9	183.2	-1678.8	3940.3	4583.4	263.5	2.45
240.0	693.2	183.1	-1393.5	4080.3	3874.1	275.6	2.45
250.0	710.0	89.0	-698.5	4108.2	2327.1	279.7	2.43
260.0	703.2	-30.0	56.9	3735.5	389.7	275.5	2.43
270.0	706.5	-162.1	1465.1	3603.2	-1537.9	263.2	2.46
280.0	713.0	-206.7	1793.8	4106.3	-2892.3	248.8	2.45
290.0	703.7	-136.4	1263.5	4571.3	-3062.6	246.1	2.45
300.0	645.8	-19.7	240.5	4336.1	-2697.9	257.7	2.41
310.0	633.7	78.2	-512.9	3983.7	-2758.9	260.9	2.41
320.0	613.4	159.7	-909.2	3689.9	-3000.5	282.9	2.40
330.0	577.5	240.5	-1147.1	3294.9	-3288.9	287.3	2.37
340.0	473.1	219.1	-1040.7	3464.8	-3834.6	254.8	2.41
350.0	441.3	140.3	-658.1	4304.2	-4442.7	206.2	2.40

Table 4. Wind Loads on the Conical Horn Antenna - AFC CH10

*** NORMALIZED FORCES AND MOMENTS ON THE AT&T MICROWAVE HORN ANTENNA ***

AFC CH10

WIND	CD	CL	CMR	CMP	CMY	AREA(SQ.FT)	YD(FT)
0.0	.935	.043	.135	.519	-.812	133.0	5.6
10.0	.820	.180	.028	.517	-.791	137.5	6.3
20.0	.815	.255	.011	.511	-.775	140.4	6.3
30.0	.740	.263	-.035	.508	-.694	141.8	6.9
40.0	.771	.255	-.016	.495	-.575	140.3	6.4
50.0	.738	.230	-.042	.473	-.437	135.8	6.4
60.0	.722	.084	-.062	.371	-.287	128.6	5.1
70.0	.647	.268	-.073	.431	-.217	119.2	6.7
80.0	.511	.394	-.159	.520	-.219	107.6	10.2
90.0	.435	.158	-.140	.379	.002	102.9	8.7
100.0	.557	.162	-.154	.298	.012	107.6	5.3
110.0	.514	.076	-.091	.179	.175	119.2	3.5
120.0	.691	.018	.012	.038	.347	128.6	.5
130.0	.716	.147	.075	.040	.435	135.8	.6
140.0	.633	.191	.051	.066	.480	140.3	1.0
150.0	.656	.174	.064	.042	.537	141.8	.6
160.0	.702	.209	.173	.036	.597	140.4	.5
170.0	.640	.119	.227	.070	.580	137.5	1.1
180.0	.764	-.021	.285	.039	.560	133.0	.5
190.0	.600	-.001	.308	.093	.466	137.5	1.6
200.0	.580	.053	.386	.183	.420	140.4	3.2
210.0	.526	-.079	.332	.225	.303	141.8	4.3
220.0	.684	-.004	.235	.263	.249	140.3	3.8
230.0	.658	-.026	.175	.247	.164	135.8	3.8
240.0	.734	-.107	.119	.181	.100	128.6	2.5
250.0	.498	-.266	.170	.082	-.098	119.2	1.6
260.0	.429	-.302	.170	-.051	-.172	107.6	-1.2
270.0	.422	-.344	.151	-.204	-.259	102.9	-4.8
280.0	.586	-.314	.021	.069	-.359	107.6	1.2
290.0	.642	-.277	.112	.091	-.431	119.2	1.4
300.0	.750	-.220	.125	.147	-.445	128.6	2.0
310.0	.789	-.175	.174	.193	-.524	135.8	2.4
320.0	.790	-.368	.068	.250	-.672	140.3	3.2
330.0	.782	-.286	.063	.315	-.704	141.8	4.0
340.0	.845	-.230	.101	.377	-.729	140.4	4.5
350.0	.856	-.100	.171	.465	-.768	137.5	5.4

Table 4. (Continued)

*** FULL SCALE WIND LOADS ON THE AT&T MICROWAVE HORN ANTENNA ***

AFC CH10

WIND	FD(LBS)	FL(LBS)	MR(FT-LBS)	MP(FT-LBS)	MY(FT-LBS)	AREA(SQ.FT)	QREF(PSF)
0.0	322.8	15.0	465.7	1794.2	-2806.3	133.0	2.60
10.0	291.0	63.9	99.8	1834.1	-2807.2	137.5	2.58
20.0	295.6	92.6	40.6	1851.8	-2810.2	140.4	2.58
30.0	269.3	95.9	-129.2	1850.9	-2527.0	141.9	2.57
40.0	262.9	87.1	-54.8	1686.8	-1958.7	140.3	2.43
50.0	239.5	74.6	-134.7	1534.9	-1418.8	135.8	2.39
60.0	225.3	26.2	-193.5	1157.1	-895.7	128.6	2.43
70.0	188.9	78.1	-212.0	1256.6	-633.6	119.2	2.45
80.0	134.5	103.6	-418.0	1368.3	-575.9	107.6	2.44
90.0	109.9	39.8	-354.9	958.6	4.1	102.9	2.46
100.0	150.7	43.9	-417.1	806.4	33.8	107.6	2.51
110.0	154.4	23.0	-272.1	538.8	524.5	119.2	2.52
120.0	223.0	5.8	37.3	121.1	1119.0	128.6	2.51
130.0	257.6	52.9	271.5	144.4	1563.5	135.8	2.65
140.0	235.1	71.1	189.5	245.2	1783.6	140.3	2.65
150.0	249.9	65.2	240.9	158.6	2012.6	141.8	2.64
160.0	238.1	71.0	585.5	123.7	2024.8	140.4	2.42
170.0	209.1	38.9	740.3	229.3	1894.7	137.5	2.38
180.0	243.9	-6.9	909.3	123.2	1786.2	133.0	2.40
190.0	206.4	-.4	1060.0	320.3	1603.6	137.5	2.50
200.0	205.4	18.7	1367.4	649.8	1489.3	140.4	2.52
210.0	189.7	-28.3	1198.2	809.6	1092.4	141.8	2.54
220.0	239.1	-1.4	822.1	919.9	869.9	140.3	2.49
230.0	214.4	-8.6	570.8	805.3	536.1	135.8	2.40
240.0	224.3	-32.8	363.1	554.5	307.0	128.6	2.38
250.0	142.8	-76.3	488.1	235.4	-281.7	119.2	2.41
260.0	109.9	-77.5	437.3	-131.5	-440.9	107.6	2.38
270.0	102.5	-83.6	367.5	-495.3	-629.2	102.9	2.36
280.0	161.0	-86.4	57.4	188.9	-986.6	107.6	2.55
290.0	199.2	-86.1	347.2	283.5	-1336.8	119.2	2.60
300.0	252.4	-74.0	420.0	493.5	-1495.9	128.6	2.62
310.0	276.2	-61.2	610.3	674.8	-1834.6	135.8	2.58
320.0	285.1	-132.9	246.4	904.0	-2426.1	140.3	2.57
330.0	284.6	-104.0	230.3	1147.5	-2562.7	141.8	2.57
340.0	303.9	-82.9	364.7	1357.5	-2623.1	140.4	2.56
350.0	297.9	-35.0	594.9	1617.2	-2674.8	137.5	2.53

Table 5. Wind Loads on the Conical Horn Antenna - ANDREW SHX10

*** NORMALIZED FORCES AND MOMENTS ON THE AT&T MICROWAVE HORN ANTENNA ***

ANDREW SHX10

WIND	CD	CL	CMR	CMP	CMY	AREA(SQ.FT)	YD(FT)
0.0	.900	.108	.076	.654	-.828	139.6	7.3
10.0	.783	.175	-.017	.655	-.790	146.8	8.4
20.0	.770	.210	-.121	.583	-.748	150.8	7.6
30.0	.743	.286	-.169	.574	-.755	150.3	7.7
40.0	.856	.366	-.168	.569	-.767	145.9	6.7
50.0	.790	.355	-.167	.640	-.655	140.6	8.1
60.0	.777	.276	-.210	.625	-.546	133.0	8.0
70.0	.749	.413	-.206	.641	-.432	123.0	8.6
80.0	.589	.406	-.228	.589	-.293	110.7	10.0
90.0	.495	.180	-.111	.470	-.046	111.3	9.5
100.0	.470	-.088	-.052	.398	.120	110.7	8.5
110.0	.559	-.063	.005	.253	.242	123.0	4.5
120.0	.629	-.032	.126	.123	.394	133.0	2.0
130.0	.762	.057	.216	.093	.438	140.6	1.2
140.0	.702	.128	.248	.096	.507	145.9	1.4
150.0	.712	.051	.283	.120	.564	150.3	1.7
160.0	.718	.074	.362	.150	.617	150.8	2.1
170.0	.743	.058	.415	.231	.641	146.8	3.1
180.0	.731	.046	.521	.294	.653	139.6	4.0
190.0	.638	-.017	.444	.321	.558	146.8	5.0
200.0	.629	-.043	.425	.381	.492	150.8	6.1
210.0	.618	-.112	.372	.448	.400	150.3	7.3
220.0	.739	-.036	.257	.487	.302	145.9	6.6
230.0	.705	-.009	.179	.442	.246	140.6	6.3
240.0	.763	-.185	.082	.362	.141	133.0	4.8
250.0	.654	-.208	.098	.271	.020	123.0	4.1
260.0	.651	-.161	.137	.127	-.068	110.7	2.0
270.0	.569	-.213	.131	-.029	-.191	111.3	-.5
280.0	.655	-.286	.192	.061	-.395	110.7	.9
290.0	.699	-.320	.271	.146	-.487	123.0	2.1
300.0	.806	-.371	.280	.199	-.581	133.0	2.5
310.0	.825	-.336	.265	.328	-.627	140.6	4.0
320.0	.837	-.332	.232	.397	-.658	145.9	4.7
330.0	.868	-.305	.206	.457	-.713	150.3	5.3
340.0	.868	-.235	.150	.507	-.716	150.8	5.8
350.0	.880	-.055	.138	.598	-.772	146.8	6.8

Table 5. (Continued)

*** FULL SCALE WIND LOADS ON THE AT&T MICROWAVE HORN ANTENNA ***

ANDREW SHX10

WIND	FD(LBS)	FL(LBS)	MR(FT-LBS)	MP(FT-LBS)	MY(FT-LBS)	AREA(SQ.FT)	QREF(PSF)
0.0	313.3	37.6	265.2	2276.2	-2882.6	139.6	2.49
10.0	285.0	63.7	-61.7	2383.3	-2875.7	146.8	2.48
20.0	288.3	78.7	-452.4	2184.6	-2800.1	150.8	2.48
30.0	275.9	106.2	-626.4	2132.1	-2805.6	150.3	2.47
40.0	310.1	132.7	-610.2	2062.4	-2778.0	145.9	2.48
50.0	282.2	126.7	-597.7	2286.7	-2339.1	140.6	2.54
60.0	263.5	93.6	-711.1	2119.1	-1851.5	133.0	2.55
70.0	221.6	122.1	-611.1	1897.2	-1278.5	123.0	2.41
80.0	156.2	107.7	-603.8	1560.4	-776.2	110.7	2.39
90.0	132.5	48.3	-296.1	1259.4	-123.7	111.3	2.41
100.0	125.5	-23.4	-137.8	1063.2	320.3	110.7	2.41
110.0	169.6	-19.3	15.9	768.4	732.9	123.0	2.47
120.0	207.4	-10.7	415.0	404.7	1298.1	133.0	2.48
130.0	264.7	20.0	752.2	322.4	1522.0	140.6	2.47
140.0	252.8	46.1	892.2	344.9	1827.7	145.9	2.47
150.0	265.7	19.2	1056.5	447.4	2104.4	150.3	2.48
160.0	254.4	26.3	1283.8	532.3	2186.6	150.8	2.35
170.0	252.1	19.7	1409.8	782.3	2176.9	146.8	2.31
180.0	236.4	14.9	1682.9	951.3	2109.6	139.6	2.32
190.0	220.0	-5.9	1532.7	1106.3	1924.7	146.8	2.35
200.0	220.5	-15.0	1489.6	1336.3	1723.0	150.8	2.32
210.0	216.5	-39.3	1303.0	1571.7	1400.7	150.3	2.33
220.0	266.4	-13.1	927.2	1756.4	1089.7	145.9	2.47
230.0	244.3	-3.0	620.6	1533.3	852.5	140.6	2.47
240.0	250.4	-60.9	268.7	1190.0	463.0	133.0	2.47
250.0	206.3	-65.7	308.0	856.1	63.3	123.0	2.56
260.0	184.9	-45.8	388.8	361.1	-192.3	110.7	2.57
270.0	162.0	-60.6	371.5	-81.8	-543.8	111.3	2.56
280.0	181.1	-79.1	530.4	169.7	-1093.0	110.7	2.50
290.0	203.9	-93.5	791.1	426.2	-1420.5	123.0	2.37
300.0	258.2	-118.9	897.2	635.5	-1860.6	133.0	2.41
310.0	288.7	-117.6	927.4	1147.1	-2193.6	140.6	2.49
320.0	306.0	-121.3	848.1	1449.9	-2404.9	145.9	2.51
330.0	327.8	-115.2	776.1	1724.6	-2691.2	150.3	2.51
340.0	316.9	-85.7	546.8	1848.5	-2612.0	150.8	2.42
350.0	311.7	-19.5	488.5	2117.1	-2732.9	146.8	2.41

Table 6. Wind Loads on the Conical Horn Antenna - GABRIEL UHR10 D

*** NORMALIZED FORCES AND MOMENTS ON THE AT&T MICROWAVE HORN ANTENNA ***

GABRIEL UHR10 D

WIND	CD	CL	CMR	CMP	CMY	AREA(SQ.FT)	YD(FT)
0.0	1.052	-.001	.081	.649	-.876	139.4	6.2
10.0	.943	.160	-.009	.632	-.842	147.3	6.7
20.0	.927	.235	-.106	.549	-.814	151.8	5.9
30.0	.890	.291	-.134	.521	-.782	154.1	5.9
40.0	.858	.216	-.103	.557	-.725	152.8	6.5
50.0	.854	.223	-.126	.514	-.617	149.4	6.0
60.0	.810	.124	-.130	.534	-.466	142.8	6.6
70.0	.791	.159	-.070	.463	-.231	133.3	5.8
80.0	.659	.141	-.029	.383	-.046	121.2	5.8
90.0	.671	.149	-.124	.549	-.036	106.5	8.2
100.0	.600	-.081	-.068	.360	.037	121.2	6.0
110.0	.628	-.080	.041	.210	.200	133.3	3.3
120.0	.712	-.196	.178	.132	.455	142.8	1.9
130.0	.814	-.156	.271	.092	.586	149.4	1.1
140.0	.838	-.072	.305	.108	.624	152.8	1.3
150.0	.852	.013	.323	.113	.639	154.1	1.3
160.0	.856	.019	.364	.173	.703	151.8	2.0
170.0	.867	-.070	.488	.243	.752	147.3	2.8
180.0	.933	-.010	.496	.313	.780	139.4	3.3
190.0	.879	.020	.441	.363	.695	147.3	4.1
200.0	.841	.072	.456	.418	.619	151.8	5.0
210.0	.785	.077	.368	.473	.562	154.1	6.0
220.0	.882	.038	.294	.523	.457	152.8	5.9
230.0	.847	.082	.190	.520	.364	149.4	6.1
240.0	.828	-.057	.075	.420	.254	142.8	5.1
250.0	.655	-.142	.068	.336	.096	133.3	5.1
260.0	.634	-.171	.104	.175	-.008	121.2	2.8
270.0	.574	-.243	.104	-.037	-.182	106.5	-.6
280.0	.730	-.033	-.051	.136	-.182	121.2	1.9
290.0	.705	-.080	.022	.223	-.270	133.3	3.2
300.0	.794	-.227	.088	.251	-.469	142.8	3.2
310.0	.919	-.207	.213	.304	-.577	149.4	3.3
320.0	.961	-.278	.190	.373	-.665	152.8	3.9
330.0	.954	-.339	.194	.441	-.728	154.1	4.6
340.0	.902	-.315	.126	.502	-.768	151.8	5.6
350.0	.916	-.209	.133	.593	-.804	147.3	6.5

Table 6. (Continued)

*** FULL SCALE WIND LOADS ON THE AT&T MICROWAVE HORN ANTENNA ***

GABRIEL UHR10 D

WIND	FD(LBS)	FL(LBS)	MR(FT-LBS)	MP(FT-LBS)	MY(FT-LBS)	AREA(SQ.FT)	QREF(PSF)
0.0	377.7	-.2	292.4	2330.2	-3145.0	139.4	2.58
10.0	357.2	60.5	-33.9	2394.5	-3188.4	147.3	2.57
20.0	359.6	91.4	-411.1	2129.1	-3158.3	151.8	2.56
30.0	347.2	113.4	-523.1	2031.2	-3051.1	154.1	2.53
40.0	320.0	80.5	-383.3	2078.5	-2702.4	152.8	2.44
50.0	309.9	81.0	-455.9	1863.5	-2237.9	149.4	2.43
60.0	283.3	43.3	-455.0	1865.7	-1630.9	142.8	2.45
70.0	251.2	50.4	-222.8	1468.7	-732.0	133.3	2.38
80.0	188.9	40.3	-83.3	1097.0	-132.2	121.2	2.36
90.0	175.5	39.1	-323.2	1434.4	-94.7	106.5	2.46
100.0	171.0	-23.2	-193.3	1027.0	104.3	121.2	2.35
110.0	207.8	-26.3	136.2	694.0	663.3	133.3	2.48
120.0	247.1	-68.1	618.7	459.4	1581.3	142.8	2.43
130.0	317.5	-60.9	1056.3	360.7	2284.9	149.4	2.61
140.0	335.8	-28.8	1224.0	432.7	2503.1	152.8	2.62
150.0	344.2	5.3	1303.3	458.3	2581.4	154.1	2.62
160.0	326.3	7.4	1386.6	661.0	2678.7	151.8	2.51
170.0	305.9	-24.7	1723.6	856.5	2653.4	147.3	2.40
180.0	311.2	-3.2	1652.3	1042.[illegible]	2599.5	139.4	2.39
190.0	339.2	7.6	1702.4	1398.8	2678.9	147.3	2.62
200.0	335.8	28.8	1821.8	1669.3	2472.7	151.8	2.63
210.0	317.9	31.1	1492.3	1914.5	2276.5	154.1	2.63
220.0	337.3	14.7	1124.1	1998.5	1748.3	152.8	2.50
230.0	316.3	30.6	710.8	1940.3	1361.1	149.4	2.50
240.0	298.3	-20.6	270.0	1514.0	914.5	142.8	2.52
250.0	223.3	-48.5	233.3	1145.0	328.3	133.3	2.56
260.0	195.5	-52.7	320.4	538.9	-26.1	121.2	2.54
270.0	155.4	-65.7	282.1	-100.0	-493.7	106.5	2.54
280.0	214.2	-9.7	-150.8	399.5	-534.2	121.2	2.42
290.0	224.7	-25.6	70.1	710.0	-859.5	133.3	2.39
300.0	268.8	-76.8	297.3	849.1	-1586.8	142.8	2.37
310.0	336.7	-75.9	778.8	1113.6	-2115.7	149.4	2.45
320.0	360.6	-104.4	712.3	1399.3	-2497.3	152.8	2.46
330.0	357.4	-127.1	727.3	1651.2	-2727.7	154.1	2.43
340.0	342.0	-119.3	478.5	1904.5	-2913.2	151.8	2.50
350.0	323.4	-73.8	468.7	2093.7	-2838.5	147.3	2.40

Table 7. Wind Loads on the Tower Section AA-DD

*** WIND LOADS ON THE AT&T MICROWAVE ANTENNA TOWER SECTION ***

TOWER SECTION AA-DD

WIND	CD	CL	AREA(SQ.FT)	FD(LBS)	FL(LBS)	QREF(PSF)
-10.0	2.545	-.255	143.8	569.8	-57.1	1.56
-5.0	2.440	-.100	143.8	542.5	-22.2	1.55
0.0	2.351	-.017	143.8	526.4	-3.8	1.56
5.0	2.387	.051	143.8	539.1	11.4	1.57
10.0	2.544	.168	143.8	573.7	37.8	1.57
15.0	2.631	.302	143.8	594.7	68.2	1.57
20.0	2.687	.363	143.8	602.3	81.4	1.56
25.0	2.740	.309	143.8	613.7	69.1	1.56
30.0	2.728	.240	143.8	616.1	54.2	1.57
35.0	2.734	.157	143.8	625.0	35.9	1.59
40.0	2.694	.090	143.8	617.3	20.7	1.59
45.0	2.666	.016	143.8	605.9	3.7	1.58
50.0	2.711	-.031	143.8	610.4	-7.0	1.57
55.0	2.744	-.095	143.8	618.7	-21.3	1.57

SOLIDITY(%) = 22.89 TILT = 0.0

Table 8. Wind Loads on the Tower Section FF-JJ

*** WIND LOADS ON THE AT&T MICROWAVE ANTENNA TOWER SECTION ***

TOWER SECTION FF-JJ

WIND	CD	CL	AREA(SQ.FT)	FD(LBS)	FL(LBS)	QREF(PSF)
-10.0	3.328	-.201	355.2	1844.3	-111.5	1.56
-5.0	3.125	-.072	355.2	1739.4	-40.0	1.57
0.0	2.960	.023	355.2	1652.0	12.7	1.57
5.0	3.048	.069	355.2	1696.8	38.6	1.57
10.0	3.263	.180	355.2	1806.3	99.5	1.56
15.0	3.364	.255	355.2	1876.2	142.0	1.57
20.0	3.508	.238	355.2	1942.9	131.6	1.56
25.0	3.593	.194	355.2	1998.0	107.8	1.57
30.0	3.636	.189	355.2	2015.2	104.9	1.56
35.0	3.548	.150	355.2	1982.1	83.7	1.57
40.0	3.442	.081	355.2	1901.2	44.8	1.55
45.0	3.287	.009	355.2	1811.8	5.0	1.55
50.0	3.397	-.023	355.2	1856.4	-12.4	1.54
55.0	3.581	-.097	355.2	1945.1	-52.9	1.53

SOLIDITY(%) = 12.61   TILT = 0.0

Table 9. Comparison of the Drag on the Tower Sections with Suggested Value in ANSI Standards

	Present Study		ANSI Standards	
Tower Section AA-DD	2.351	$\alpha = 0$;	2.944*	$\alpha = 0$
$\Psi = 0.2289$	2.666	$\alpha = 45$;	3.449**	$\alpha = 45$
Tower Section FF-JJ	2.960	$\alpha = 0$;	3.477	$\alpha = 0$
$\Psi = 0.1261$	3.287	$\alpha = 45$;	3.806	$\alpha = 45$

*$C_D = 4.13 - 5.18\ \Psi$

**$C_D = (4.13 - 5.18\ \Psi)(1 + 0.75\ \Psi)$

Table 10. Wind Loads on the Tower Section AA-DD at Tilt Angle of 5°

*** WIND LOADS ON THE AT&T MICROWAVE ANTENNA TOWER SECTION ***

TILTED TOWER SECTION AA-DD

WIND	CD	CL	AREA(SQ.FT)	FD(LBS)	FL(LBS)	QREF(PSF)
-10.0	2.617	-.255	143.8	584.1	-57.0	1.55
-5.0	2.493	-.094	143.8	560.6	-21.2	1.56
0.0	2.433	.016	143.8	544.7	3.6	1.56
5.0	2.483	.067	143.8	558.8	15.1	1.57
10.0	2.604	.157	143.8	583.5	35.2	1.56
15.0	2.684	.292	143.8	605.0	65.8	1.57
20.0	2.755	.356	143.8	623.8	80.6	1.57
25.0	2.775	.304	143.8	634.3	69.6	1.59
30.0	2.792	.247	143.8	634.4	56.0	1.58
35.0	2.809	.163	143.8	627.1	36.5	1.55
40.0	2.771	.081	143.8	620.7	18.0	1.56
45.0	2.703	.010	143.8	608.9	2.2	1.57
50.0	2.766	-.041	143.8	612.8	-9.0	1.54
55.0	2.808	-.128	143.8	622.5	-28.4	1.54

SOLIDITY(%) = 22.89 TILT = 5.0

Table 11. Wind Loads on the Tower Section AA-DD at Tilt Angle of 10°

*** WIND LOADS ON THE AT&T MICROWAVE ANTENNA TOWER SECTION ***

TILTED TOWER SECTION AA-DD

WIND	CD	CL	AREA(SQ.FT)	FD(LBS)	FL(LBS)	QREF(PSF)
-10.0	2.659	-.228	143.8	595.2	-50.9	1.56
-5.0	2.594	-.087	143.8	585.6	-19.6	1.57
0.0	2.557	.003	143.8	577.9	.7	1.57
5.0	2.571	.047	143.8	580.0	10.7	1.57
10.0	2.672	.124	143.8	600.6	27.9	1.56
15.0	2.739	.241	143.8	616.1	54.2	1.56
20.0	2.791	.316	143.8	634.9	71.8	1.58
25.0	2.807	.261	143.8	640.3	59.6	1.59
30.0	2.795	.189	143.8	642.5	43.5	1.60
35.0	2.822	.123	143.8	632.4	27.5	1.56
40.0	2.820	.039	143.8	630.5	8.7	1.55
45.0	2.768	-.043	143.8	623.4	-9.8	1.57
50.0	2.838	-.106	143.8	634.2	-23.7	1.55
55.0	2.843	-.204	143.8	641.7	-46.0	1.57

SOLIDITY(%) = 22.89 TILT = 10.0

Table 12. Wind Loads on the Tower Section AA-DD at Tilt Angle of 15°

*** WIND LOADS ON THE AT&T MICROWAVE ANTENNA TOWER SECTION ***

TILTED TOWER SECTION AA-DD

WIND	CD	CL	AREA(SQ.FT)	FD(LBS)	FL(LBS)	QREF(PSF)
-10.0	2.651	-.186	143.8	589.2	-41.4	1.55
-5.0	2.589	-.061	143.8	572.9	-13.5	1.54
0.0	2.527	.008	143.8	560.2	1.9	1.54
5.0	2.585	.023	143.8	565.3	5.0	1.52
10.0	2.638	.101	143.8	584.6	22.3	1.54
15.0	2.701	.211	143.8	595.4	46.6	1.53
20.0	2.727	.243	143.8	589.9	52.6	1.50
25.0	2.772	.185	143.8	621.9	41.5	1.56
30.0	2.796	.140	143.8	626.8	31.3	1.56
35.0	2.813	.054	143.8	615.7	11.9	1.52
40.0	2.815	-.024	143.8	619.3	-5.3	1.53
45.0	2.787	-.127	143.8	619.6	-28.1	1.55
50.0	2.877	-.212	143.8	642.4	-47.3	1.55
55.0	2.894	-.298	143.8	647.2	-66.7	1.56

SOLIDITY(%) = 22.89 TILT = 15.0

Table 13. Wind Loads on the Tower Section AA-DD with Heel Angles

*** WIND LOADS ON THE AT&T MICROWAVE ANTENNA TOWER SECTION ***

TOWER SECTION AA-DD WITH HEEL ANGLES

WIND	CD	CL	AREA(SQ.FT)	FD(LBS)	FL(LBS)	QREF(PSF)
-10.0	2.788	.144	150.1	645.2	33.4	1.54
-5.0	2.663	.122	150.1	619.6	28.5	1.55
0.0	2.563	.038	150.1	594.7	8.9	1.55
5.0	2.616	-.089	150.1	598.4	-20.4	1.52
10.0	2.764	-.173	150.1	620.8	-38.9	1.50
15.0	2.883	-.169	150.1	648.5	-38.0	1.50
20.0	2.924	-.126	150.1	682.2	-29.4	1.55
25.0	2.983	-.059	150.1	696.3	-13.9	1.55
30.0	3.019	-.011	150.1	705.6	-2.6	1.56
35.0	3.028	.030	150.1	697.4	6.9	1.53
40.0	2.960	.036	150.1	684.0	8.3	1.54
45.0	2.866	.029	150.1	667.5	6.8	1.55
50.0	2.921	.026	150.1	687.0	6.0	1.57
55.0	2.984	.058	150.1	697.4	13.5	1.56

SOLIDITY(%) = 23.66   TILT = 0.0

Table 14. Wind Loads on the Tower Section FF-JJ with Heel Angles

*** WIND LOADS ON THE AT&T MICROWAVE ANTENNA TOWER SECTION ***

TOWER SECTION FF-JJ WITH HEEL ANGLES

WIND	CD	CL	AREA(SQ.FT)	FD(LBS)	FL(LBS)	QREF(PSF)
-10.0	3.439	.163	375.3	2026.9	96.2	1.57
-5.0	3.217	.144	375.3	1874.6	84.0	1.55
0.0	2.982	.023	375.3	1731.7	13.3	1.55
5.0	3.075	-.134	375.3	1757.0	-76.7	1.52
10.0	3.335	-.197	375.3	1894.1	-111.8	1.51
15.0	3.480	-.205	375.3	1980.3	-116.5	1.52
20.0	3.627	-.120	375.3	2093.3	-69.2	1.54
25.0	3.744	-.066	375.3	2144.3	-37.6	1.53
30.0	3.762	.032	375.3	2163.2	18.3	1.53
35.0	3.713	.090	375.3	2092.4	50.8	1.50
40.0	3.625	.102	375.3	2024.5	56.9	1.49
45.0	3.501	.034	375.3	1954.6	19.0	1.49
50.0	3.543	-.044	375.3	2013.6	-24.9	1.51
55.0	3.670	-.029	375.3	2077.4	-16.5	1.51

SOLIDITY(%) = 13.22   TILT = 0.0

APPENDIX A

Supplementary Wind-Tunnel Tests of Conical Horn Antenna
GABRIEL UHR 10 D

Among three conical horn antennas tested, GABRIEL UHR10 D indicated the largest drag (Section 4.2.2). Attempts were made to reduce this drag. Details of the geometry of the antenna were modified and additional wind-tunnel tests were conducted. The geometry modifications included removal of the horizontal ribs (located on the back of the horn antenna) and changes of the antenna attachment (removal of one base ring).

A.1 Experimental Configuration

Figure A.1 is a definition sketch of the experimental configuration employed for the supplementary wind-tunnel tests. The experimental configuration differs from the one shown in Figure 1. Note that in the new configuration, the platform remains fixed with respect to the approach wind while the horn antenna is rotated to accomodate changes in the wind direction.

A.2 Effects of the Back Ribs

Variation of the drag force for the horn antenna with and without the back ribs is compared in Figure A.2. A small reduction in the drag, especially for wind directions less than 90°, is seen for the antenna without the back ribs. The measured wind loads are collected in Tables A.1 and A.2.

A.3 Modification of the Base

As shown in Figure 13, GABRIEL UHR10 D antenna is attached to the platform by means of two identical base rings. One of the rings was removed. As a result the clearance between the antenna and the platform was reduced. During wind-tunnel tests of this configuration, large oscillations of the antenna were observed at wind speeds exceeding 40 fps. The dominant component of the oscillations was about the lateral axis; that is, in the direction of the pitching moment.

Figure A.3 shows time series records of the pitching moment for the antenna at 0° wind direction with two base rings and with a single base ring. The data was recorded 65 seconds after the wind was turned on. It is clearly seen that removal of one base ring doubled the amplitude of the pitching moment fluctuations. Although neither the full scale stiffness nor damping were simulated for the wind-tunnel model, the data showed that a slight change in the geometry of the antenna mounting (removal of one base ring) resulted in signifcantly different dynamic loading. This high sensitivity to the geometrical details of the antenna and the supporting structure needs further investigation.

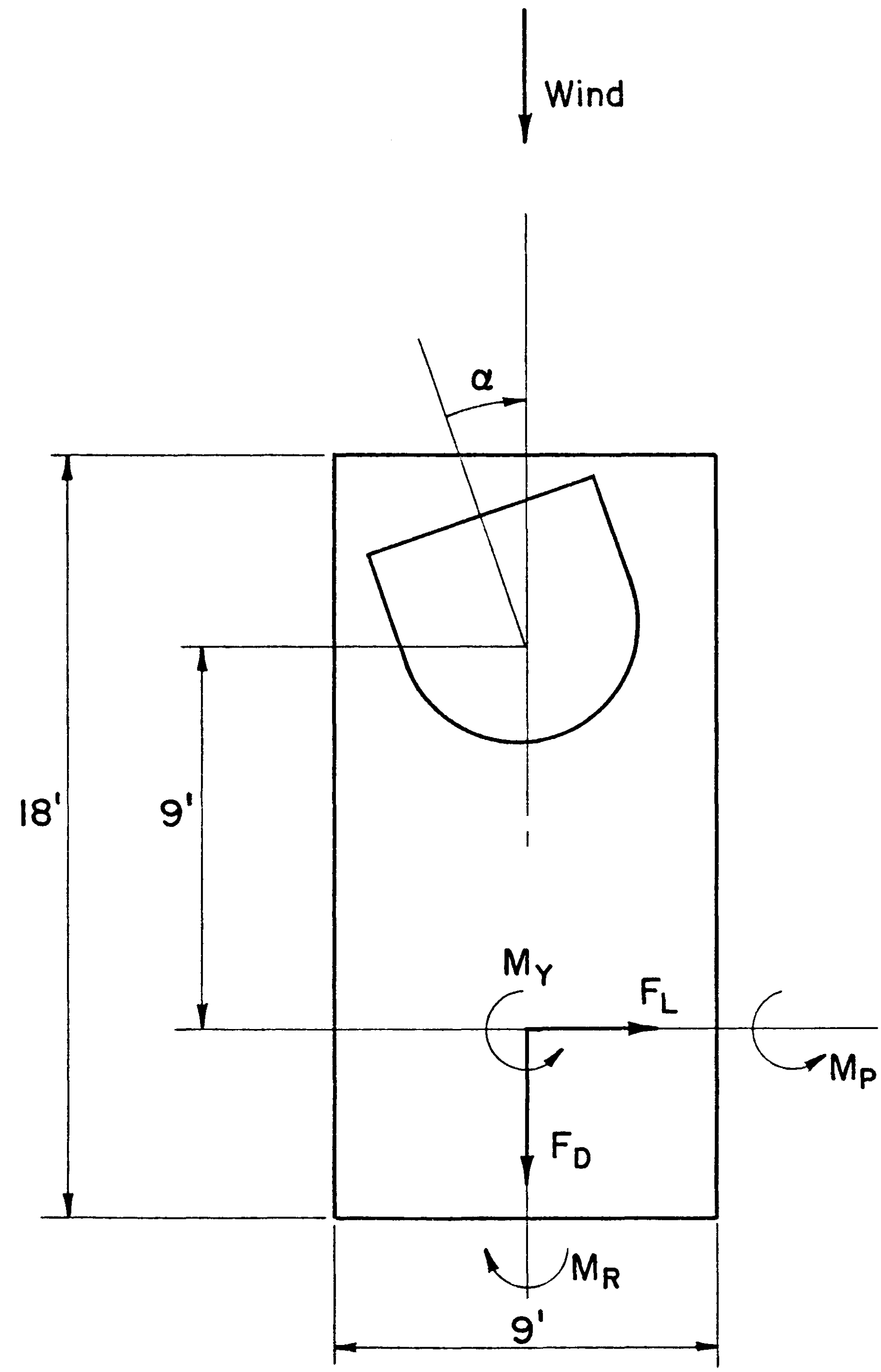

Figure A.1. Configuration for Supplementary Wind Tunnel Tests

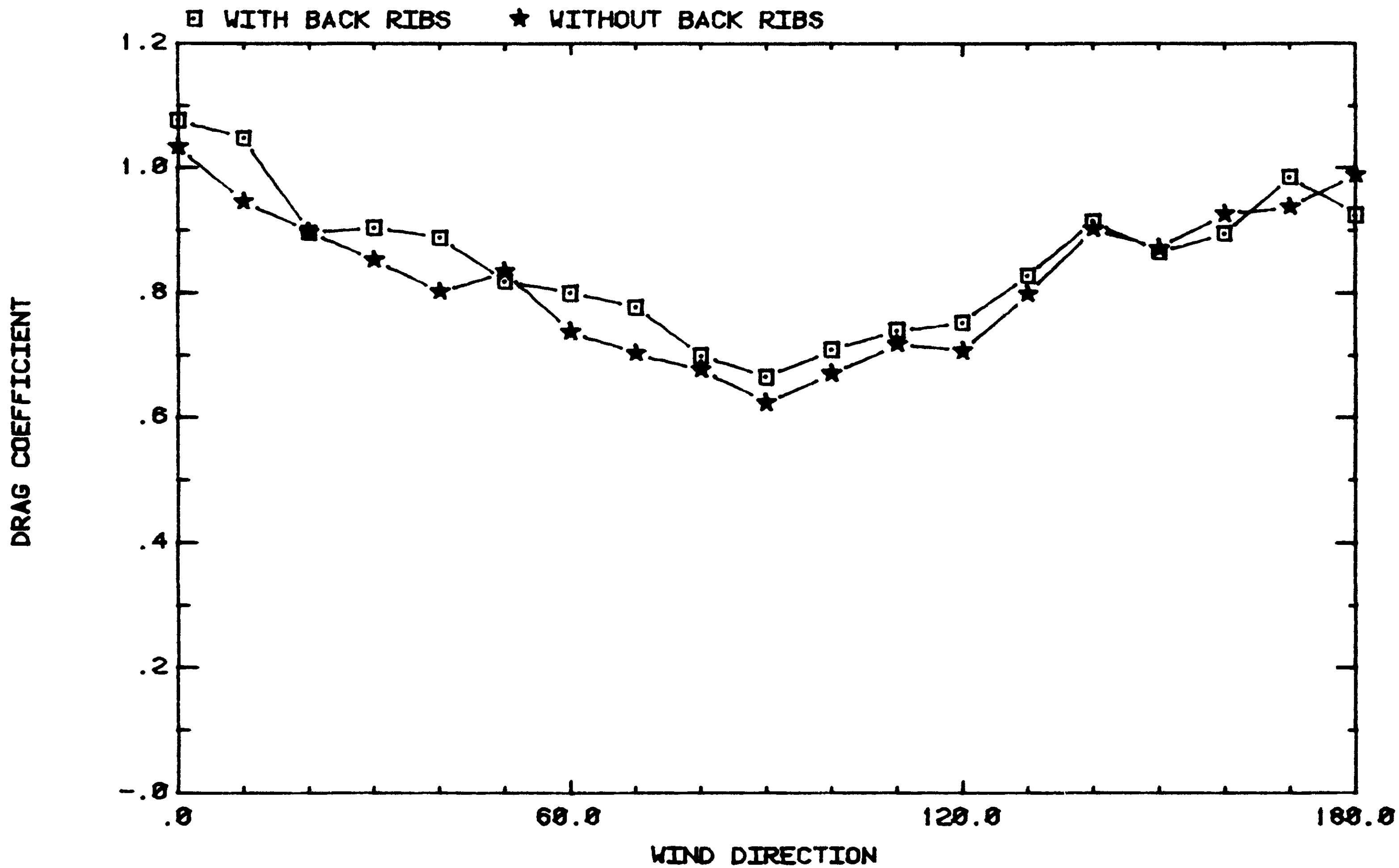

Figure A.2. Effects of Back Ribs on the Drag of GABRIEL UHR10 D

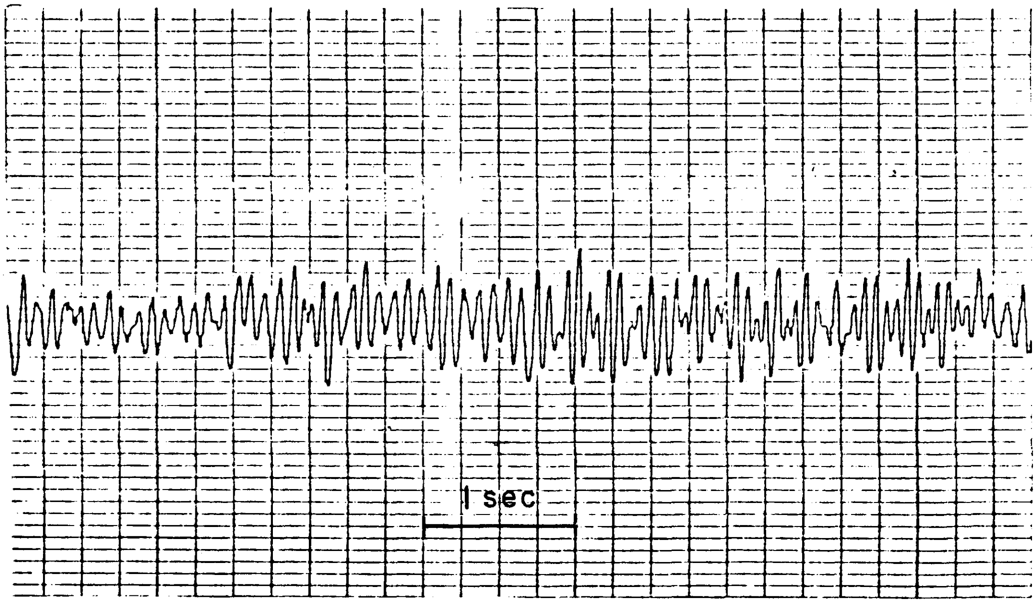

Two Base Rings

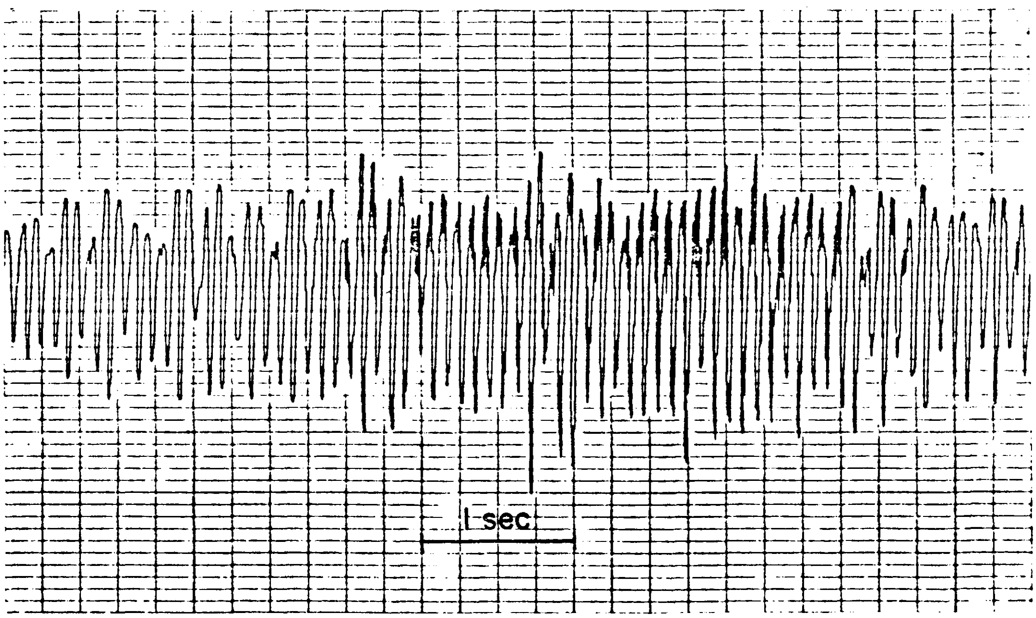

One Base Ring

Figure A.3. Effects of Base Rings on the Pitching Moment of GABRIEL UHR10 D

Table A.1a. Wind Loads on GABRIEL UHR10 D with Back Ribs

*** NORMALIZED FORCES AND MOMENTS ON THE AT&T MICROWAVE HORN ANTENNA ***

GABRIEL UHR10 D - APPENDIX

WIND	CD	CL	CMR	CMP	CMY	AREA(SQ FT)	YD(FT)
0.0	1.076	.030	.080	.880	.016	139.4	8.2
10.0	1.047	.197	-.036	.801	- 132	147.3	7.7
20.0	.897	.223	- 129	.741	- 207	151 8	8.3
30.0	.905	.233	-.150	.665	-.205	154.1	7.4
40.0	.888	.278	-.147	.722	-.177	152.8	8.1
50.0	.819	.262	-.128	.644	-.126	149.4	7.9
60.0	.800	141	-.093	.544	-.047	142.8	6.8
70.0	.777	.057	-.013	.437	.080	133.3	5.6
80.0	.699	.019	038	.451	.128	121.2	6.5
90 0	.665	.148	-.068	.626	-.033	106 5	9.4
100.0	.709	.021	.014	.409	-.007	121.2	5.8
110.0	.740	.103	.052	250	- 010	133.3	3.4
120.0	.752	.021	046	.137	035	142.8	1.8
130.0	.828	029	.085	091	078	149.4	1.1
140.0	.914	- 012	.100	022	.091	152.8	.2
150.0	865	-.001	.073	-.005	.064	154.1	-.1
160.0	.895	-.078	.056	-.055	.065	151.8	-.6
170.0	.986	-.077	.058	-.145	.050	147.3	-1.5
180.0	.924	-.038	.027	-.130	- 018	139.4	-1 4

Table A.1b. Wind Loads on GABRIEL UHR10 D with Back Ribs

*** FULL SCALE WIND LOADS ON THE AT&T MICROWAVE HORN ANTENNA ***

GABRIEL UHR10 D - APPENDIX

WIND	FD(LBS)	FL(LBS)	MR(FT-LBS)	MP(FT-LBS)	MY(FT-LBS)	AREA(SQ.FT)	QREF(PSF)
0.0	353.5	9.8	264.2	2890.3	51.8	139.4	2.36
10.0	363.7	68.5	-125.9	2783.1	-458.6	147.3	2.36
20.0	326.8	81.3	-470.7	2698.7	-753.0	151.8	2.40
30.0	328.8	84.7	-546.3	2417.3	-745.2	154.1	2.36
40.0	317.7	99.6	-524.8	2581.6	-633.4	152.8	2.34
50.0	290.0	92.8	-454.2	2282.7	-445.5	149.4	2.37
60.0	268.0	47.4	-312.6	1822.1	-156.7	142.8	2.35
70.0	247.6	18.2	-39.9	1392.2	255.1	133.3	2.39
80.0	201.5	5.6	109.4	1300.1	368.5	121.2	2.38
90.0	165.0	36.8	-169.7	1552.9	-81.5	106.5	2.33
100.0	205.1	6.2	40.7	1183.2	-20.2	121.2	2.39
110.0	234.0	32.6	164.9	790.3	-30.3	133.3	2.37
120.0	254.4	7.0	156.4	462.7	119.0	142.8	2.37
130.0	291.9	10.3	298.7	320.4	273.5	149.4	2.36
140.0	329.1	-4.4	360.6	77.5	326.6	152.8	2.36
150.0	313.1	-.5	264.1	-17.7	231.3	154.1	2.35
160.0	324.1	-28.4	203.3	-200.0	234.9	151.8	2.39
170.0	349.8	-27.4	205.7	-514.1	178.3	147.3	2.41
180.0	305.2	-12.4	89.6	-427.8	-58.3	139.4	2.37

Table A.2a. Wind Loads on GABRIEL UHR10 D without Back Ribs

*** NORMALIZED FORCES AND MOMENTS ON THE AT&T MICROWAVE HORN ANTENNA ***

GABRIEL UHR10 D WITHOUT BACK RIBS - APPENDIX

WIND	CD	CL	CMR	CMP	CMY	AREA(SQ.FT)	YD(FT)
0.0	1.033	.003	.043	.852	.010	139.4	8.2
10.0	.946	.110	-.075	.752	-.124	147.3	8.0
20.0	.898	.154	-.160	.708	-.201	151.8	7.9
30.0	.852	.199	-.164	.667	-.205	154.1	7.8
40.0	.801	.193	-.178	.673	-.187	152.8	8.4
50.0	.834	.160	-.174	.639	-.144	135.8	7.7
60.0	.737	.098	-.108	.525	-.045	142.8	7.1
70.0	.702	-.071	-.040	.438	.087	133.3	6.2
80.0	.676	-.100	-.011	.414	.126	121.2	6.1
90.0	.624	.095	-.132	.661	-.054	106.5	10.6
100.0	.671	.016	-.011	.386	-.029	121.2	5.8
110.0	.717	-.064	.037	.204	.028	133.3	2.8
120.0	.706	-.002	.043	.080	.022	142.8	1.1
130.0	.798	-.022	.084	.046	.072	149.4	.6
140.0	.902	-.046	.084	-.018	.083	152.8	-.2
150.0	.871	-.024	.082	-.025	.072	154.1	-.3
160.0	.926	-.104	.064	-.084	.082	151.8	-.9
170.0	.938	-.130	.043	-.105	.063	147.3	-1.1
180.0	.989	-.028	.040	-.135	.004	139.4	-1.4

Table A.2b. Wind Loads on GABRIEL UHR10 D without Back Ribs

*** FULL SCALE WIND LOADS ON THE AT&T MICROWAVE HORN ANTENNA ***

GABRIEL UHR10 D WITHOUT BACK RIBS - APPENDIX

WIND	FD(LBS)	FL(LBS)	MR(FT-LBS)	MP(FT-LBS)	MY(FT-LBS)	AREA(SQ.FT)	QREF(PSF)
0.0	338.4	1.0	140.3	2791.3	31.6	139.4	2.35
10.0	324.6	37.9	-258.2	2581.6	-424.3	147.3	2.33
20.0	323.8	55.6	-578.1	2552.8	-724.2	151.8	2.38
30.0	305.6	71.4	-588.7	2390.7	-735.7	154.1	2.33
40.0	279.5	67.5	-621.8	2347.5	-652.1	152.8	2.28
50.0	269.1	51.6	-560.5	2061.2	-464.0	135.8	2.38
60.0	248.0	33.1	-362.2	1766.4	-150.5	142.8	2.36
70.0	212.9	-21.5	-119.8	1327.1	263.8	133.3	2.27
80.0	197.1	-29.2	-31.9	1207.9	368.8	121.2	2.41
90.0	152.5	23.1	-322.0	1615.0	-131.1	106.5	2.29
100.0	188.9	4.5	-30.6	1087.9	-82.4	121.2	2.32
110.0	220.5	-19.6	114.3	627.5	84.8	133.3	2.31
120.0	241.0	-.7	148.2	273.1	75.2	142.8	2.39
130.0	278.3	-7.5	293.0	161.2	250.8	149.4	2.34
140.0	315.1	-16.2	294.2	-64.2	290.4	152.8	2.29
150.0	311.7	-8.6	294.6	-89.3	259.3	154.1	2.32
160.0	326.8	-36.8	225.9	-298.1	288.8	151.8	2.33
170.0	323.1	-45.0	148.7	-360.3	216.3	147.3	2.34
180.0	319.7	-9.2	128.2	-436.7	14.3	139.4	2.32

APPENDIX B

Technical Details of Tested Antennas and Equipment

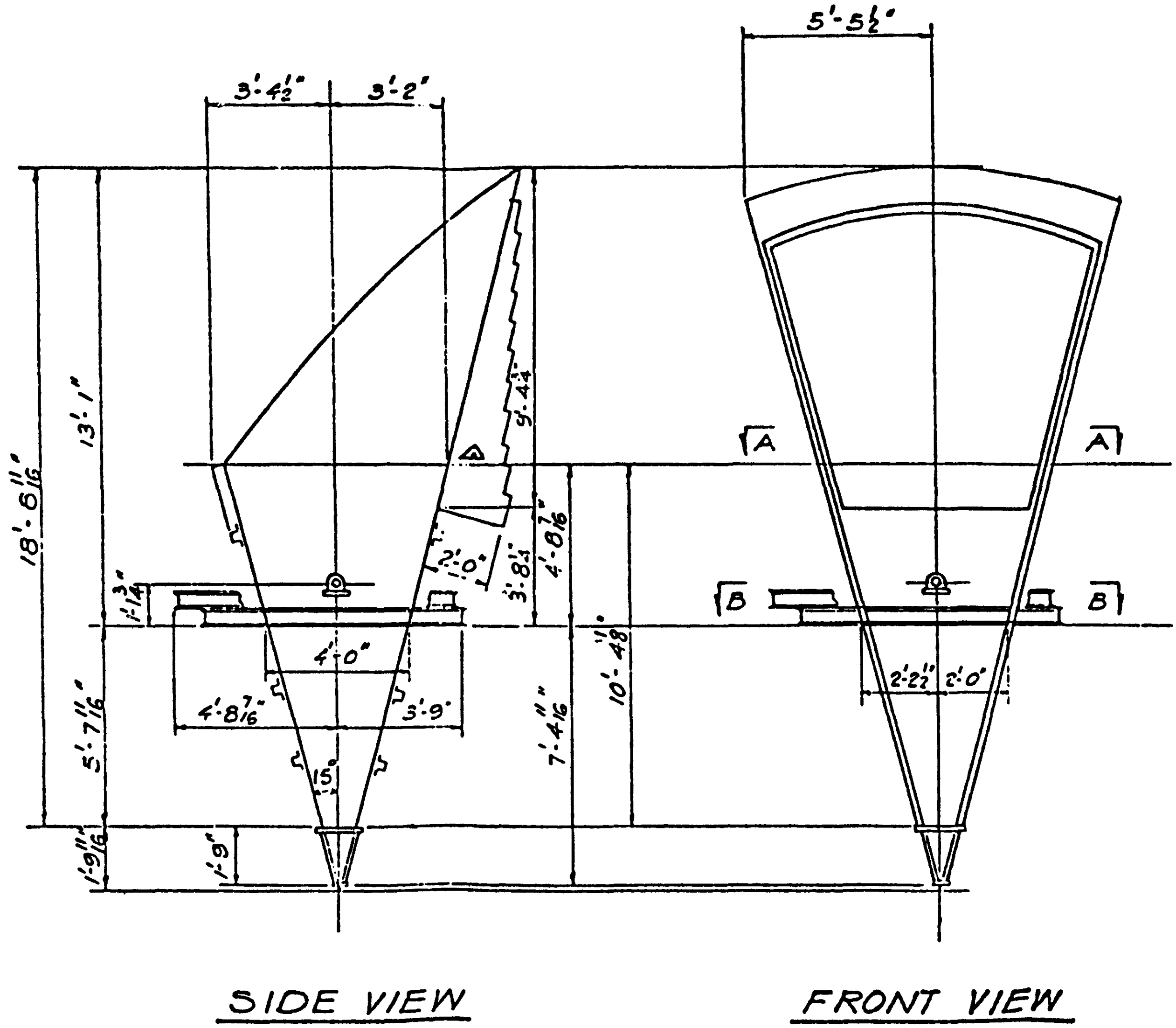

Figure B.1. Dimensions of the Pyramidal Horn

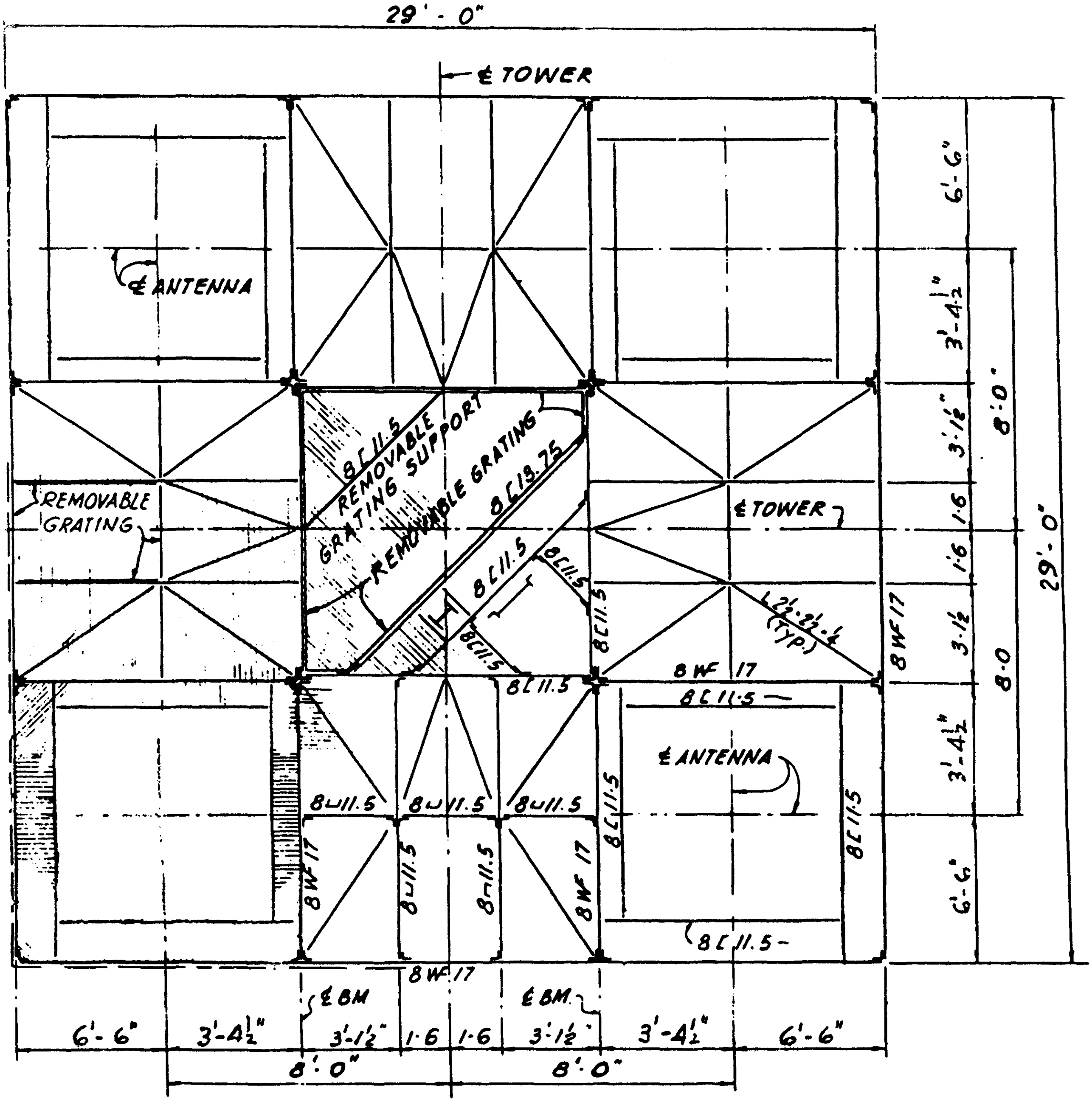

Figure B.2. Plan at A-A Level Antenna Platform

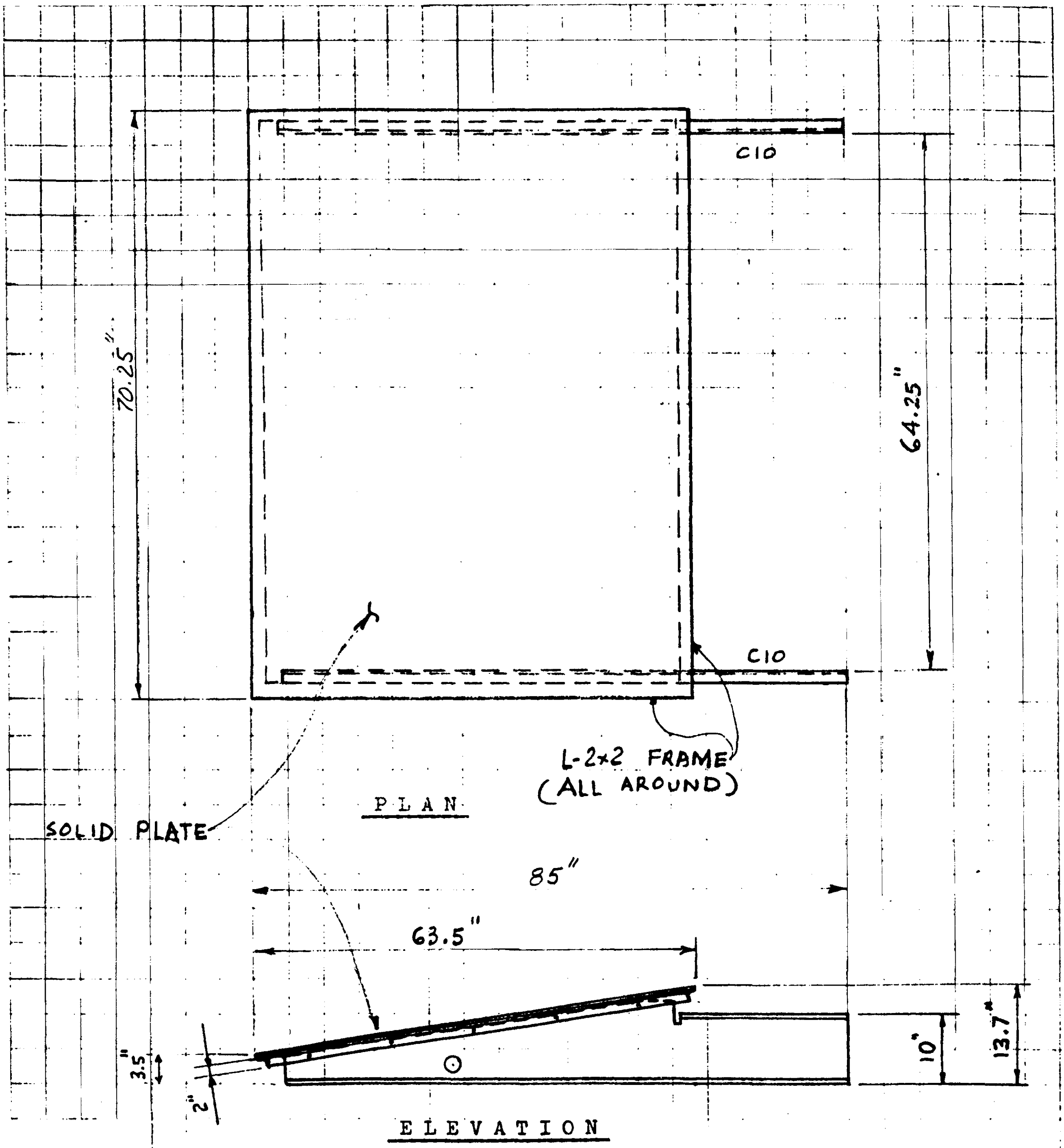

Figure B.3. Dimensions of the Bottom Edge Blinder

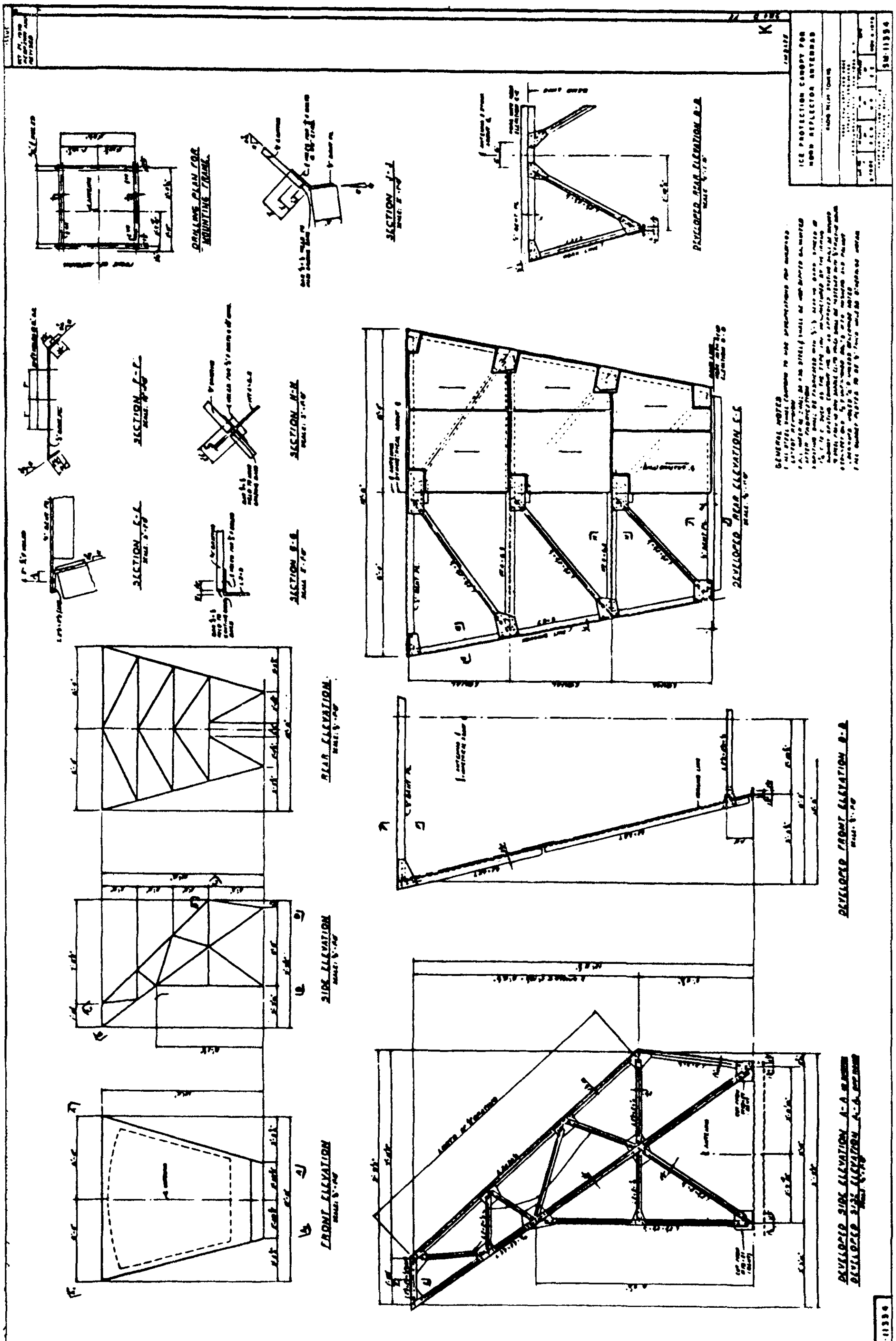

Figure B.4. Ice Protection Canopy